UNIVERSITEIT VAN PRETORIA
UNIVERSITY OF PRETORIA
YUNIBESITHI YA PRETORIA

Sequential injection analysis of selected components in liquid fertilizers

by

Thomas Arnoldus van der Merwe

Submitted in partial fulfilment of the requirements for the degree

MAGISTER SCIENTIAE

in the Faculty of Science

University of Pretoria

Pretoria

November 1999

© University of Pretoria

UNIVERSITEIT VAN PRETORIA
UNIVERSITY OF PRETORIA
YUNIBESITHI YA PRETORIA

Sequential injection analysis of selected components in liquid fertilizer

by

Thomas Arnoldus van der Merwe

Supervisor: Professor Jacobus F. van Staden

Department of Chemistry

University of Pretoria

Degree: Magister Scientiae

SYNOPSIS

Sequential injection has, over the past eight years, developed into a viable alternative to flow-injection, but its full potential has not yet been fully realized. It developed out of existing flow-injection methods when a need for mechanically simple and robust flow-injection methodology arose. In this study the development of this method is discussed with its numerous advantages and disadvantages over existing flow-injection methods.

The theoretical basis on which this technique is based is outlined as well as parameters that influence the design of the manifold. With the manifold design principles established, the manifold is evaluated using real sample analysis, with liquid fertilizer as the source of selected elements. Adjustments made to existing flow-injection methods, for the determination of nitrite with sequential injection analysis, are discussed, while a new method is proposed for nitrate determination. The viability of solid-phase reductors and *in situ* preparation of reagents, combined with sequential injection analysis, is also studied.

UNIVERSITEIT VAN PRETORIA
UNIVERSITY OF PRETORIA
YUNIBESITHI YA PRETORIA

Sekwensiële inspuit analise van geselekteerde komponente in vloeibare kunsmis

deur

Thomas Arnoldus van der Merwe

Leier: Professor Jacobus F. van Staden

Departement Chemie

Universiteit van Pretoria

Graad: Magister Scientiae

SAMEVATTING

Sekwensiële inspuit analise het die afgelope agt jaar ontwikkel in 'n lewensvatbare alternatief tot vloei-inspuit prosesanaliseerders, maar die volle potensiaal daarvan is nog nie besef nie. Sekwensiële inspuit analise het onstaan vanuit vloei-inspuit analise toe die vraag na meganies eenvoudig en robuuste vloei-inspuit metodologie onstaan het. In hierdie studie word die ontwikkeling van die metode bespreek tesame met die voor- en nadele daarvan bo bestaande vloei-inspuit metodes.

Die teorie waarop die tegniek gebaseer is, word kortliks bespreek sowel as die parameters wat die ontwerp van die sisteem beïnvloed. Met die sisteem parameters vasgestel, is die sisteem geëvalueer om die lewensvatbaarheid daarvan te bepaal. Vloeibare kunsmis het as bron van geselekteerde elemente gedien wat in die evaluasie gebruik is. Aanpassings gemaak aan bestaande vloei-inspuit metodes vir die bepaling van nitriet met behulp van sekwensiële inspuit analise, word bespreek. 'n Nuwe sekwensiële inspuit analise metode vir die bepaling van nitraat word voorgestel en die lewensvatbaarheid van *in situ* bereidings metodes vir reagense en vastetoestand reduksie toestelle in sekwensiële inspuit analiseerders word bestudeer.

Table of Contents

Synopsis iii

Samevatting v

Acknowledgements vii

Chapter 1 Sequential Injection Analysis 1

1.1 Introduction 1

1.2 Sequential injection 3

1.3 Sequential injection vs flow- and stopped-flow injection 6

1.4 Aim of this study 8

1.5 References 9

Chapter 2 Theoretical Background of Flow Systems 10

2.1 Introduction 10

2.2 Dispersion of injected zones 11

2.2.1 Transport 12

2.2.2 Dispersion 13

2.3 Theoretical models 17

2.3.1 Taylor's model 17

2.3.2 Tanks-in-series model 18

2.3.3 Mixing chamber model 19

2.3.4 General model 20

2.4 Practical definition of dispersion 21

2.4.1 Růžička's dispersion coefficient 21

2.5 Influence of geometric and hydrodynamic factors on dispersion 23
2.5.1 Hydrodynamic factors 24
2.5.1.1 Flow rate 24
2.5.1.2 Geometric factors 24
2.5.1.2.1 Straight tubes 25
2.5.1.2.2 Coils 25
2.5.1.2.3 Knitted reactors 26
2.5.1.2.4 Normal packed tubes 26
2.5.1.2.5 Single bead string reactors (SBSR) 27
2.5.2 Contribution of chemical kinetics to dispersion 27
2.6 From flow injection to sequential injection via the random walk model 27
2.7 References 33

Chapter 3 Design of the Sequential Injection System 34
3.1 Introduction 34
3.2 Components of the SIA system 34
3.2.1 Manifold 35
3.2.1.1 Propelling system 35
3.2.1.1.1 Pumps 35
3.2.1.1.2 Pump tubing 38
3.2.1.1.3 Flow rate 39
3.2.1.1.4 Sample and reagent volumes 40
3.2.1.2 Injection system 41
3.2.1.3 Detector 43
3.2.2 Computerized control and data accusation 45

3.2.2.1 Data output 45
3.2.2.2 Interface board 46
3.2.2.3 Distribution board 46
3.2.3 Manifold dimensions and geometry 47
3.2.3.1 Manifold tubing 47
3.2.3.2 Effect of tube diameter 47
3.2.3.3 Holding coil 48
3.2.3.4 Reaction coils 49
3.2.3.5 Order of injection 50
3.3 Conclusion 51
3.4 References 53

Chapter 4 Determination of Nitrite by Sequential Injection Analysis 54
4.1 Introduction 54
4.2 Uses of nitrite 55
4.3 Properties 56
4.4 Choice of analytical method 56
4.5 Reaction principles 57
4.6 Determination of nitrite with sequential injection analysis 58
4.6.1 Experimental 58
4.6.1.1 Reagents and solutions 58
4.6.1.2 Equipment 60
4.6.1.3 Procedure 61
4.7 Method optimisation 62
4.7.1 Physical parameters 62
4.7.1.1 Pump speed 63
4.7.1.2 Holding coil 67
4.7.1.2.1 Tube diameter 68
4.7.1.2.2 Holding coil length 69

4.7.1.2.3 Holding coil geometry 71
4.7.1.3 Reaction coil 1 71
4.7.1.3.1 Tube diameter 72
4.7.1.3.2 Coil length 73
4.7.1.3.3 Coil geometry 74
4.7.1.4 Reaction coil 2 75
4.7.1.4.1 Tube diameter 75
4.7.1.4.2 Coil length 77
4.7.1.4.3 Coil geometry 78
4.7.1.5 Up-take tubes 78
4.7.1.6 Order of injection 78
4.7.2 Chemical parameters 79
4.7.2.1 Carrier stream 79
4.7.2.2 Chromogenic reagent 80
4.7.2.3 Buffer solution 82
4.8 Evaluation of method 83
4.8.1 Linearity 83
4.8.2 Accuracy 84
4.8.3 Precision 85
4.8.4 Detection limit 85
4.8.5 Interferences 86
4.8.6 Sample frequency 87
4.9 Conclusion 87
4.10 References 89

Chapter 5 Determination of Nitrate in Water, Water Effluents, and Fertilizers by Reduction with Copperized-Cadmium and Sequential Injection Analysis 91

5.1 Introduction 91

5.2 Uses of nitrate 93
5.3 Properties 94
5.4 Choice of analytical method 95
5.5 Determination of nitrate with sequential injection analysis 96
5.5.1 Experimental 96
5.5.1.1 Reagents and solutions 96
5.5.1.2 Equipment 98
5.5.1.3 Procedure 100
5.6 Method optimisation 102
5.6.1 Physical parameters 102
5.6.1.1 Pump speed 102
5.6.1.2 Holding coil 105
5.6.1.2.1 Holding coil length 106
5.6.1.3 Reaction coil 1 107
5.6.1.3.1 Tube diameter 108
5.6.1.4 Reaction coil 2 109
5.6.1.4.1 Tube diameter 109
5.6.1.4.2 Coil length 110
5.6.1.4.3 Coil geometry 112
5.6.1.5 Uptake tubes 112
5.6.1.6 Order of injection 112
5.6.1.7 Reductor 113
5.6.1.7.1 Reductor diameter 113
5.6.1.7.2 Reductor length 115
5.6.1.7.3 Reductor position 116
5.6.2 Chemical parameters 118
5.6.2.1 Carrier stream 118
5.6.2.2 Chromogenic reagent 120
5.6.2.3 Sample volume 123

5.6.2.4 Reduction material 125
5.7 Evaluation of the method 129
5.7.1 Linearity 129
5.7.2 Accuracy 129
5.7.3 Precision 131
5.7.4 Detection limit 131
5.7.5 Interferences 132
5.7.6 Sample frequency 132
5.8 Conclusion 134
5.9 References 135

Chapter 6 Determination of Boron by Sequential Injection Analysis 137
6.1 Introduction 137
6.2 Uses of boron 138
6.3 Properties 139
6.4 Natural occurrence 140
6.5 Essentiality of boron in plants 141
6.6 Choice of analytical method 142
6.7 Choice of chromogenic reagent 143
6.8 Reaction principles 144
6.9 Determination of Boron by sequential injection analysis 145
6.9.1 Experimental 145
6.9.1.1 Reagents and solutions 145
6.9.1.2 Equipment 146
6.9.1.3 Procedure 148
6.10 Method optimisation 149
6.10.1 Physical parameters 149
6.10.1.1 Flow rate 149
6.10.1.2 Holding coil/RC 1 151

6.10.1.3 Reaction coil 2 153
6.10.1.3.1 Tube diameter 153
6.10.1.3.2 Coil length 154
6.10.1.3.3 Coil geometry 156
6.10.1.4 Uptake tubes 156
6.10.1.5 Order of injection 157
6.10.1.6 Temperature 158
6.10.1.7 Reaction kinetics 158
6.10.2 Chemical parameters 159
6.10.2.1 Carrier stream 160
6.10.2.2 Chromogenic reagent 160
6.10.2.2.1 Azomethine-H 160
6.10.2.2.2 Ascorbic acid 163
6.10.2.3 Buffer solution 163
6.10.2.4 Disodium EDTA 166
6.10.2.5 Sample 167
6.11 Evaluation of method 168
6.11.1 Linearity 168
6.11.2 Accuracy 169
6.11.3 Precision 170
6.11.4 Detection limit 171
6.11.5 Interferences 172
6.11.6 Sample frequency 173
6.12 Conclusion 173
6.13 References 174

Chapter 7 Automated *in situ* Preparation of Azomethine H and the Subsequent Determination of Boron in Fertilizers with Sequential Injection Analysis 177

7.1 Introduction 176

7.2 Reaction principles 177

7.3 *In situ* preparation of azomethine H and the determination of boron with sequential injection analysis 178

7.3.1 Experimental 178

7.3.1.1 Reagents and solutions 178

7.3.1.2 Equipment 179

7.3.1.3 Procedure 181

7.4 Method optimisation 181

7.4.1 Physical parameters 181

7.4.1.1 Flow rate 183

7.4.1.2 Order of injection 184

7.4.1.3 Mixing devices 185

7.4.2 Chemical parameters 189

7.4.2.1 Carrier stream 189

7.4.2.2 Salicylaldehyde 191

7.4.2.3 H-acid 191

7.4.2.4 Sample 194

7.4.2.5 Buffer solution 195

7.4.2.6 Disodium EDTA 197

7.5 Evaluation of method 197

7.5.1 Linearity 197

7.5.2 Accuracy 198

7.5.3 Precision 200

7.5.4 Detection limit 201

7.5.5 Interferences 201

7.5.6 Sample frequency 201

7.6 Conclusion 201

7.7 References 203

Addendum A Method development 204

Publications and Presentations 211

UNIVERSITEIT VAN PRETORIA
UNIVERSITY OF PRETORIA
YUNIBESITHI YA PRETORIA

CHAPTER 1

Sequential Injection Analysis

1.1 Introduction

Sequential injection analysis (SIA) was introduced in 1990 [1, 2] when the need for a simple and convenient process analyser occurred. At that stage flow-injection analysis (FIA) were successfully employed as a laboratory technique and versatile tool for the enhancement of instrumental analysis, but the manifold design of this technique proved to be too complex for the industrial environment. Stopped-flow injection was the next generation of methods that developed out of FIA but it still had several disadvantages. Since its introduction, sequential injection evolved into a reliable, robust and simple method with a low frequency of maintenance and numerous possible applications based on the same principles as FIA.

Flow-injection analysis was the first generation in a series of the continuous flow analysis (CFA) methods. The term 'flow-injection analysis', was coined by Růžička and Hansen [3] in 1975 and has since then gained widespread acceptance within the scientific community. For an analysis method to fall under the term flow-injection analysis, it should have certain essential features that distances itself from other automatic analysis methods. With FIA the flow is not segmented by air bubbles and the sample is injected directly into a continuous flowing stream, instead of being aspirated into it, as with earlier methods. The injected plug is carried along the system, partially

dispersing along the way. This partial dispersion, or dilution of the analyte, can then be manipulated by controlling the geometric and hydrodynamic characteristics of the system. A continuous sensing system yields a transient signal which is suitably recorded. The signal is detected with neither a physical nor a chemical equilibrium within the system. The operational timing must be highly reproducible since small variations might result in serious variations [4].

The FIA system consists of four parts (Fig. 1.1). The first is a propelling unit which produces the flow at a constant flow rate, for example, a peristaltic pump or syringe pump. Secondly, an injection system which allows the accurate and reproducible introduction of an accurately measured sample volume into the flow, for example, an injection valve. Thirdly, a reactor, along which the transport operation takes place, as well as additional processes, if necessary. This reactor can be a knotted, straight, or coiled tube containing solid reagents [5], ion exchangers [6], reductants [4], immobilized enzymes [7], or it can be played by a mixing chamber. The last part of the system is the flow-cell accommodated in a detector (e.g. spectrophotometer, fluorometer, potentiometer) which transduces some properties of the analyte into a continuous signal to a recorder or computer [4].

The next technique that was developed was that of stopped-flow injection. This method makes use of the same methodology as FIA, except that the unidirectional flow is stopped as soon as a suitable section of the dispersed sample zone is positioned in the observation field of the detector. This procedure enables reaction rate measurements to be made. Sequential injection is the third generation of injection systems and employs bidirectional flow with the sample and reagent zones stacked in a tubular conduit and transported to the detector. This method is thoroughly explained in the following section (Sec. 1.2).

UNIVERSITEIT VAN PRETORIA
UNIVERSITY OF PRETORIA
YUNIBESITHI YA PRETORIA

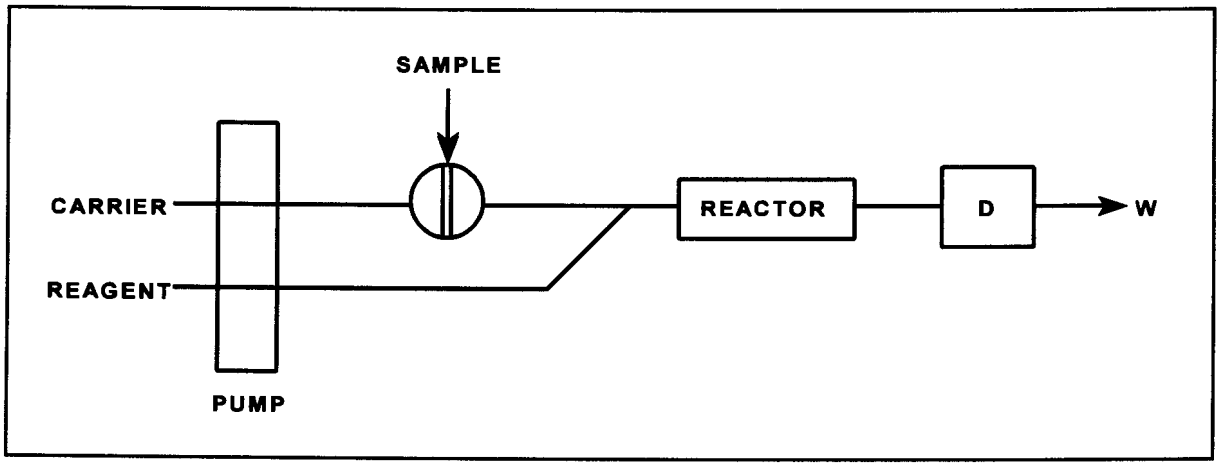

Fig. 1.1 General arrangement of an FIA system. D is the detector and W is the waste.

1.2 Sequential injection

In conventional flow-injection and stopped-flow injection the sample zone is injected into a flowing carrier stream by means of an injection valve (Fig. 1.1). This sample zone is then merged with auxiliary reagent streams on its way to the detector. In the case of sequential injection analysis (Fig. 1.2) a selector valve (SV) [8, 9] is used, rather than an injection valve, to aspirate the different solutions. Wash solution (port 1), sample zone (port 2), and reagent (port 3) are sequentially aspirated into a channel (RC 1) with a pump capable of three actions (stop, forward, reverse). The three zones are present as a stack of well-defined zones, which is then pumped through a reactor (RC 2) into the detector (D) and then towards waste.

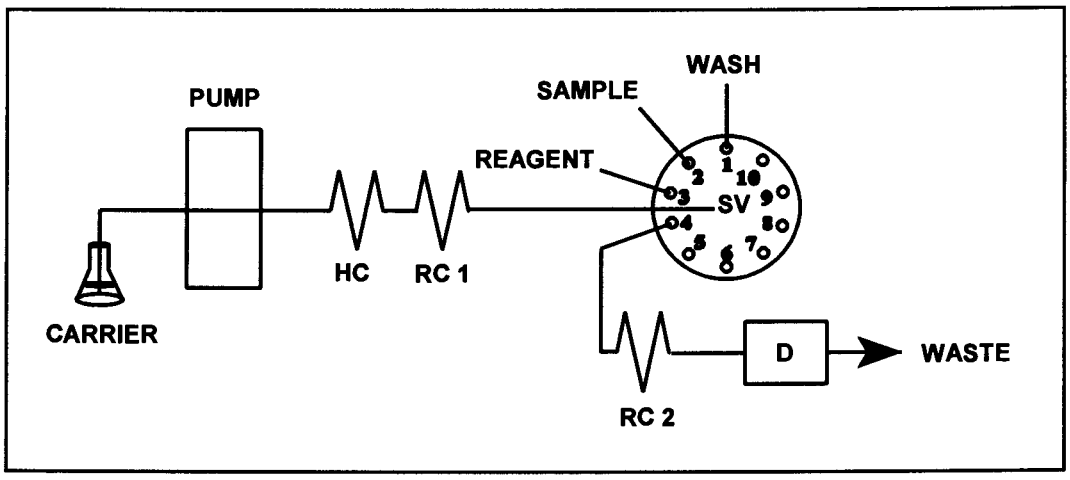

Fig. 1.2 General arrangement of the components of an SIA system. HC - holding coil, RC 1 -first reaction coil, RC 2 - second reaction coil, D - detector.

As soon as a zone is aspirated, merging of this zone with adjacent zones is observed due to the flow rate differences in a zone. The part of the zone nearest to the wall of the reactor moves slower than that nearer to the core of the zone which penetrates the core of the adjacent zone (Fig. 1.3, A). With flow reversal (Fig. 1.3, B) this effect is amplified with more penetration taking place as the zones are pumped towards the detector (Fig. 1.3, C).

The versatility of the sequential injection system depends on the amount of ports available on the selector valve used, whereas for FIA it depends on the channels available on the multichannel pump. In the case of SIA a mixing chamber is used to mix more than three zones at any one time [8] to ensure proper mixing, whereas, for FIA numerous reagents can be added along the line without the assistance of a mixing chamber. When the sequential injection sample zone moves through the detector without stopping, a peak similar to that obtained by first-order flow-injection (FI) is recorded (Fig. 1.4). This peak is narrower than the sum of the sample and reagent peaks as a complete overlap between the two zones is not possible.

UNIVERSITEIT VAN PRETORIA
UNIVERSITY OF PRETORIA
YUNIBESITHI YA PRETORIA

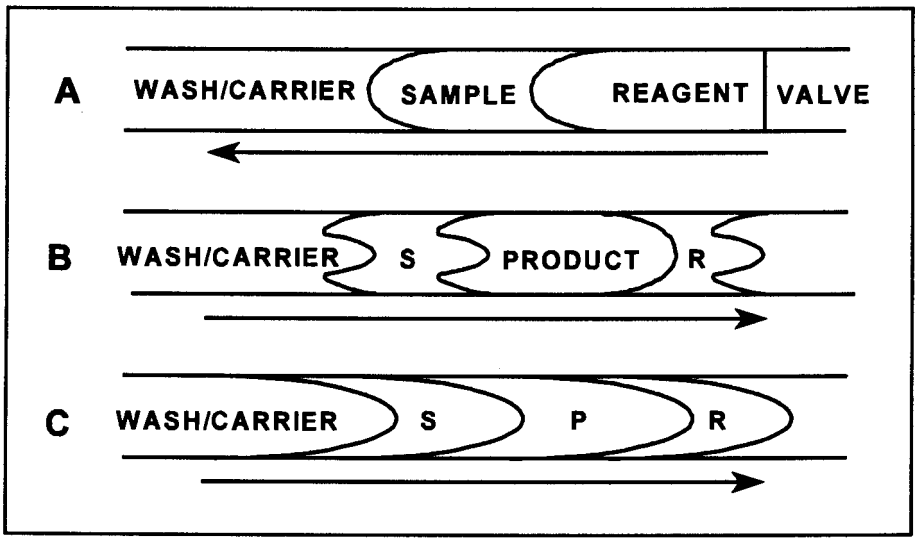

Fig. 1.3 The principle of sequential injection. (A) - Profile of zones after injection. (B) - immediately after flow reversal and (C) - in reaction-coil 2. S - sample, R - reagent, P - formed products

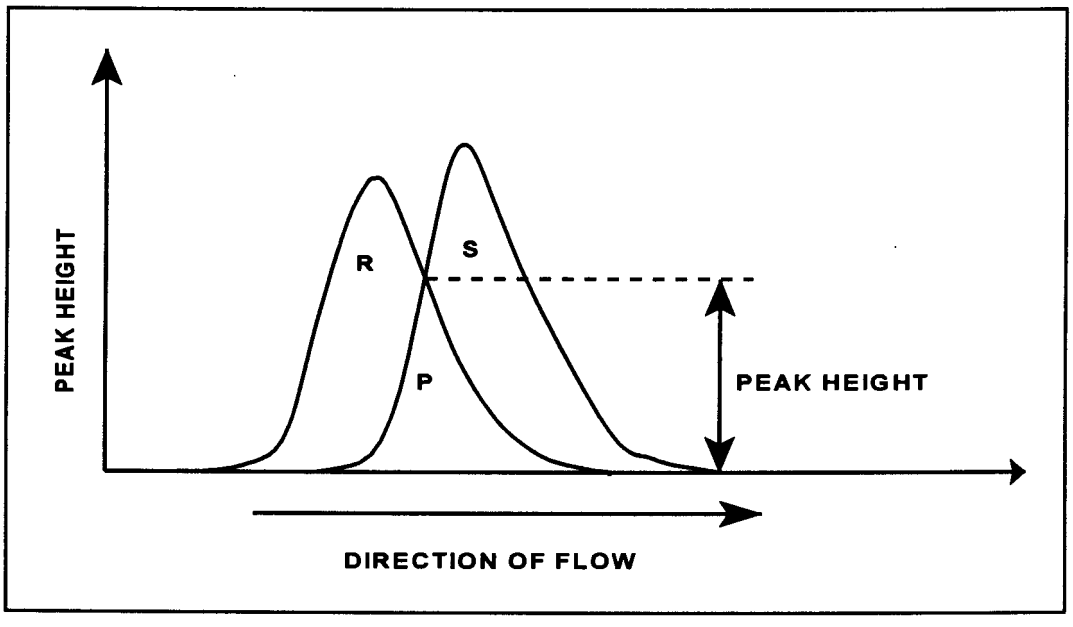

Fig. 1.4 Reagent, product and sample peaks as they arrive at the detector after flow reversal.

1.3 Sequential injection vs flow- and stopped-flow injection

One of the most important drawbacks of the first generation technique, flow-injection analysis (FIA), is that it uses reagents continuously [8,9,10]. Carrier solution and reagents are continuously pumped towards waste (Fig. 1.1), while the sample is injected into the stream with short intervals. Stopped-flow was an improvement on flow-injection, with the carrier stream pumped only when the assay is not in progress [10]. Sequential injection is more economical than both the above-mentioned techniques. Only small amounts (in the micro litre range) of reagent and sample are used during each assay while carrier solution is only used for the flushing of the stacked zone towards the detector.

With FIA a new manifold has to be designed for each new application [11], since the reaction time is controlled by the length of the reaction coil used and has to be adjusted every time the reaction rate changes. In the case of stopped-flow injection the reaction time is controlled by the length of the stopped-flow interval, making reaction rate measurements possible, and providing the method with an additional degree of information. The sequential injection manifold does not have to be physically altered in any way once it is optimised, since volume and time are controlled totally by the action of the pump used in the analysis. One manifold can thus be used for the determination of several elements with only a change in the solutions used and volumes aspirated.

The complexity of the manifolds is another important drawback of the earlier techniques [11]. Both FIA and stopped-flow injection analysis require separate lines for the carrier and for each of the reagents added to the main stream. This adds up to a lot of lines when complex reactions are employed. It was this disadvantage that eventually led to the development of sequential injection. Sequential injection makes use of a pump with a single channel, a multi-position selector valve, detector and a reaction coil. There is only one channel that is being pumped, while the valve selects the different solutions needed for the reaction. In the case of FIA the flow rate of each one of the separate channels being pumped, has to be optimised separately, whereas for SIA only the volumes of the reagents aspirated have to be optimised.

FIA does, however, possess several advantages that is not improved upon by SIA. The sampling rate of FIA is in some cases twice the rate obtainable with SIA, making it ideally suited for industrial use. Better reproducibility is obtainable and the FIA system does not have to be computer controlled, although it could be computer controlled if the need for a totally automated system arrises. SIA on the other hand is fully computer controlled making it possible to optimise the system (volumes injected, reaction times and dilution) without any physical changes [12]. The SIA system is also robust, reliable, has a long term stability and a low frequency of maintenance [9], which is fundamental in terms of cost and manpower in the process environment.

1.4 Aim of this study

'Liquid' or 'fluid' fertilizers have developed alongside the solid fertilizers which at present dominates markets in countries like Great Britain [13]. They consist of solutions, and more recently of suspensions, of fertilizer salts in water, most of which are also used in solid fertilizers [14]. Both single and multinutrient fertilizers are commercially available with a wide range of applications with added advantages, for example, more uniform distribution, immediate absorption, possibility of incorporating pesticides and fungicides and lower manual labour. With South Africa's economic dependence on agriculture, large amounts of fertilizer are produced every year. In this study methods are proposed for the monitoring of selected elements present in liquid fertilizer as well as other water-based samples.

Nitrate is one of the main sources of nitrogen in liquid and solid fertilizers [13, 14] and it is also present in a number of meat products as an additive, and therefore the need for a nitrate analyser exists. A FIA method, utilising a cadmium reductor [15], was recently developed to determine nitrate, but a reductor of this type has not been used in SIA previously. In this study the feasibility of such a reductor is described as well as the problems surrounding the use of a solid phase reductor in conjunction with SIA.

The ability to make use of highly reactive or sensitive reagents, which can be generated *in situ,* sometimes make FIA the automatic choice under difficult conditions, where a high amount of sensitivity is required. The final aim of this study was to develop a method for the *in situ* preparation of azomethine H, the reagent used in the determination of boron, from an existing FIA method [16] to investigate SIA's adaptability to the *in situ* preparation of sensitive reagents.

1.5 References

1. J. Růžička and G. D. Marshall, G.D., **Anal. Chim. Acta**, **237** (1990) 329.
2. J. Růžička, G. D. Marshall and G. D. Christian, **Anal. Chem.**, **62** (1990) 1861.
3. J. Růžička and E. H. Hansen, **Anal. Chim. Acta**, **78** (1975) 145.
4. J. Růžička and E. H. Hansen, **Flow Injection Analysis**, 2nd ed., Wiley, New York, 1988.
5. A. M. Almuaibed and A. Townsend, **Anal. Chim. Acta, 245** (1991) 115.
6. S. Olsen, L. C. R. Pessenda, J. Růžička and E. H. Hansen, **Analyst, 108** (1983) 905.
7. L. Gordon and L. Orgen, **Anal. Chim. Acta, 130** (1981) 45.
8. J. Růžička and T. Gübeli, **Anal. Chim. Acta, 63** (1991) 1680.
9. T. Gübeli, **Anal. Chem.**, **63** (1991) 2407.
10. A. Ivaska and J. Růžička, **Analyst, 118** (1993) 1885.
11. G. D. Marshall and J. F. van Staden, **Process control and quality, 3** (1993) 251.
12. J. Růžička, **Analyst, 119** (1994) 1925.
13. K. Simpson, **Fertilizers and manures**, Longman Inc., New York, 1986.
14. U. S. Jones, **Fertilizers and soil fertility**, Reston Publishing, Inc., Virginia, 1982.
15. J. F. van Staden and M. A. Makhafola, **Fresenius J. Anal. Chem., 354 (1996)** 70.
16. W.D. Basson, R. G. Bohmer and D.A. Stanton, **Analyst, 94** (1969) 1135.

UNIVERSITEIT VAN PRETORIA
UNIVERSITY OF PRETORIA
YUNIBESITHI YA PRETORIA

CHAPTER 2

Theoretical Background of Flow Systems

2.1 Introduction

Sequential injection is based on the mixing of a sample with a reagent, to yield a product that is measured by a detector of some sort. The manifold must be designed in such a way that the reagent is in sufficient access at the maximum of the profile to ensure the greatest degree of reaction [1]. To achieve this, numerous physical and chemical factors have to be optimised to obtain the ideal environment for repeatable and accurate determinations.

The key operations of sequential injection are the mutual dispersion of the zones and zone sequencing. Both these operations have to be carried out in such a way that the desired degree of penetration of sample and reagent zones will be achieved within an adequate resident time, while yielding a satisfactory sampling rate [2]. In comparison to conventional FIA [3] the dispersion of the sample zone has to be adjusted to suit the requirement. The major factors influencing the dispersion are (a) laminar flow, producing the parabolic distortion of the initial zone boundaries, (b) axial diffusion, (c) radial diffusion, (d) radial mixing of confluent points and (e) secondary flow processes. Included in the secondary flow processes are the radial circulation induced by coiling of the flow conduits, vortex shedding caused by step changes in tube

diameter, small regions of turbulent flow, produced by sharp angle bends (in the valve for instance) and surge in flow when the selection valve is switched. Flow reversal is another major factor governing the penetration not present in FIA. A good understanding of the fundamentals and theory behind flow injection is therefore essential in the design of an effective sequential injection manifold.

2.2 Dispersion of injected zones

Reproducibility of zone dispersion is a central issue in FIA and is equally important in SIA [4]. Dispersion was defined by Růžička and Hansen as: *the ratio of the concentrations before and after the dispersion process has taken place in those elements of fluid that correspond to the maximum on the dispersion curve* (Fig. 2.1) [5].

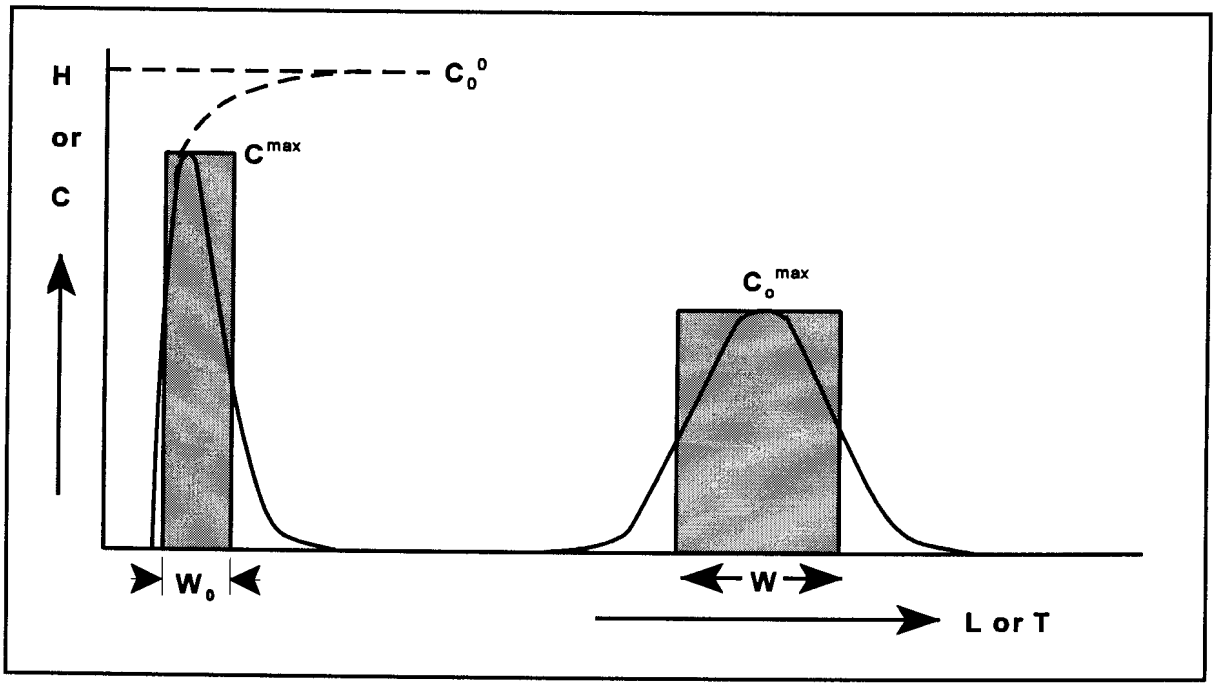

Fig. 2.1 The key parameters for defining dispersion. $C = C_0^0$ and $D_t = 1$

By denoting C_0^0 as the original concentration of the injected sample solution and C^{max} as the concentration in the element of fluid corresponding to the peak maximum, then the dispersion will be defined as:

$$D = \frac{C_0^0}{C^{max}} \quad (1)$$

where D - dispersion and C - concentration.

2.2.1 Transport

There are two factors contributing to the dispersion of the injected sample.

(a) **Convective transport,** that occurs under laminar flow conditions. This yields a parabolic velocity profile with sample molecules at the tube walls having zero linear velocity and those at the centre of the tube having twice the average velocity.

(b) **Diffusional transport**, due to the presence of concentration gradients in the convective transport regime, gives rise to *axial* and *radial* diffusion (Fig. 2.2). Axial diffusion is the result of horizontal concentration gradients at the leading and trailing edges of the injected sample zone, but it contributes insignificantly to the overall dispersion. Radial dispersion, however, makes an important contribution to the overall dispersion and is the result of concentration differences perpendicular to the direction of flow.

A third type of transport exists, originating from density gradients, but its contribution to the final dispersion is small since density differences between the fluid and the sample zone are generally negligible.

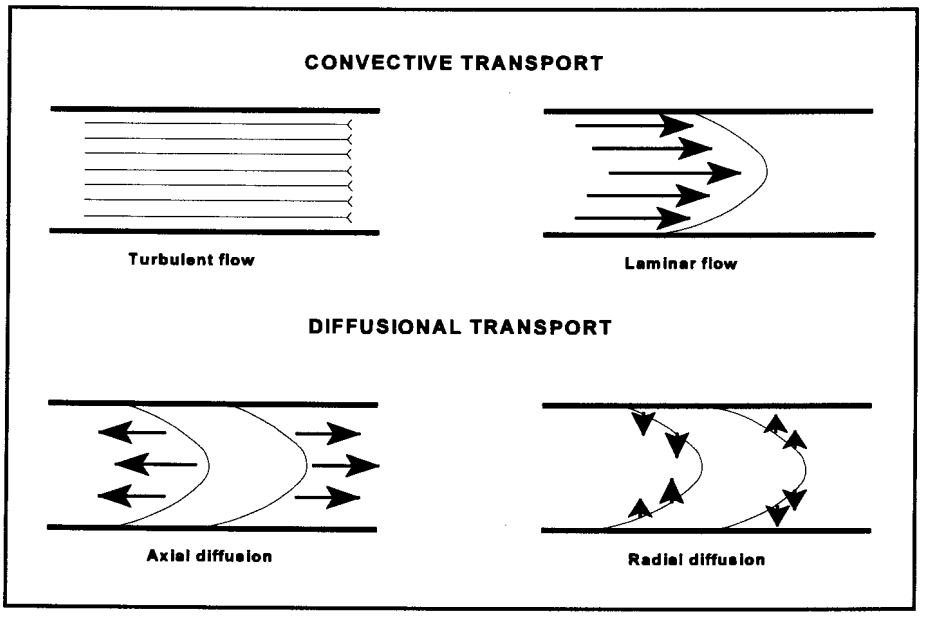

Fig. 2.2 General types of transport in closed tubes.

2.2.2 Dispersion

The concentration profile of the sample zone in a flowing stream is time-dependent, producing four situations as the sample travels towards the detector.

(i) No dispersion occurs when the sample is inserted into the carrier stream. The peak profile corresponding to zero dispersion, would be rectangular in shape. This situation occurs in neither FIA nor SIA.

(ii) Convective transport sets in immediately after injection. The zone profile is parabolic with an initial vertical portion corresponding to the emergence of the molecules at the head of the parabola and a 'tail' corresponding to the retarded portion of the sample. This situation occurs when t_a, the travel time is short and coincides with the residence time T of the maximum (t' is zero).

$$t_a = \frac{L}{2\bar{u}} \quad \textbf{(2)}$$

where t_a = travel time (sec)

L = overall tube length (cm)

$\bar{u}$ = mean linear velocity (cm/sec)

(iii) During the third stage the contribution made by the diffusion, especially the radial type, becomes significant and competes with convective transport. The progress of the centre of the injected zone is slowed down relative to the trailing portion changing the peak into a more slanted position, with a longer peak time (t') and a longer "tail" portion.

(iv) During the fourth stage the profile of the injected zone is much more compact and symmetrical. The travel should, however, be long enough to obtain these Gaussian peaks.

$$t' = T - t = \frac{\Delta t}{2} \quad \textbf{(3)}$$

where t' = peak time (sec)

T = residence time (sec)

t_a = travel time (sec)

Δt = baseline-to-baseline time (sec)

and the residence time (T) being

$$T = \frac{L}{\bar{u}} \tag{4}$$

where L = reactor length (cm)

$\bar{u}$ = mean linear velocity (cm/sec).

If the residence time is expressed in terms of the (theoretical) volume of the system and the volumetric flow-rate then

$$\bar{t}_r = \frac{reactor\ volume}{flow\text{-}rate} = \frac{\pi R^2 L}{q} \tag{5}$$

where $\bar{t}_r$ = reduced mean residence time (sec)

R = tube radius (cm)

q = flow rate (ml/min).

The total dispersion (D) is the sum of the contributions of the four different parts of the system: injection, transport, detector, and connectors.

$$D = D_{injection} + D_{transport} + D_{detector} + D_{connector} \tag{6}$$

2.3 Theoretical models

Various attempts have been made to derive a general expression, C = F(t), accounting the signal profile and relating its characteristics (travel, residence and baseline-to baseline times, and peak height or area) to the experimental parameters of the flow system (e.g. flow-rate and reactor length). Some of the models that have been developed to derive the mathematical expression will be described here. Table 1 gives a list of symbols that will be used in the discussions.

Table 1 List of symbols

Sample/reagent		**Reactor geometry**	
C	= concentration (mol.ℓ^{-1})	L	= overall tube length (cm)
C^o	= initial concentration	l	= partial tube length (cm)
C^{max}	= concentration at signal maximum	R	= tube radius (mm)
		r	= partial tube radius (cm)
V_i	= injected volume ($\mu\ell$)	d	= tube diameter (mm)
		Vi	= volume of reactor/system (mℓ)
Hydrodynamic aspects		**FIA/SIA signal**	
q	= flow rate (mℓ.min^{-1})	D	= dispersion coefficient
u	= linear velocity (cm.sec^{-1})	t_a	= travel time (sec)
u_0	= maximum linear velocity (cm.sec^{-1})	Δt	= baseline-to-baseline time (sec)
$\bar{t}_r$	= mean residence time (sec)	T	= residence time (sec)

2.3.1 Taylor's model

This model is applicable to a Gaussian distribution defined by C = f(t) in a form that depends on the chosen parameters, namely

$$C = \frac{m}{r^2}\frac{1}{4\pi Dt}\exp\left[\frac{-(x-L)^2}{4Dt}\right] \quad (7)$$

and

$$C = \frac{C_0 V_i}{q\ \sigma(2\pi)^{1/2}}\exp\left[\frac{(t-\bar{t}_r)^2}{2\sigma^2}\right] \quad (8)$$

where m = injected solute mass ($m = C_0V_i$)

σ = parameter corresponding to the standard deviation characteristic of a Gaussian distribution

x = axial distance from the injection point.

This model is only applicable if the injected volume is negligible compared to the reactor volume ($V_i << V_r$). As this is not the case for SIA where the zone volumes are of the same order as the reactor volumes, this model is not applicable to the sequential injection technique.

2.3.2 Tanks-in-series model

This model is analogous to the description of liquid chromatography in terms of theoretical plates [5,6]. It relies on the assumption that fluid flow passes sequentially through a large number (N) of minichambers in which stirring is perfect (instantaneous mixing). The mathematical expression derived from this model is [5]

$$C = \frac{1}{(\bar{t}_r)_N}\left[\frac{t}{(\bar{t}_r)_N}\right]^{N-1} \frac{1}{(N-1)!} \exp\left[\frac{-t}{(t_r)_N}\right] \quad \textbf{(9)}$$

where $(\bar{t}_r)_N$ = the mean residence time of an element of fluid in a given tank [5,6].

The larger the value of N the more Gaussian the profile of the C = f (t) curves become. Under these conditions the variance is given by

$$\sigma^2 = N(\bar{t}_r)_N^2 = \frac{\bar{t}_r^2}{N} \quad \textbf{(10)}$$

since the overall mean residence time is $\bar{t}_r = N(\bar{t}_r)_N$. The Random walk model (Sec. 2.6) uses a similar approach to explain mixing in SIA.

2.3.3 Mixing chamber model

This model is based on the model developed by Pardue and Fields [7], which in turn was inspired by the tanks-in-series model. In 1979, Pungor *et al* [8] developed a mathematical model to describe the dispersion when there is a mini-mixing chamber positioned close to or in the reactor. The concentration of a substance in the mixing chamber can be described as a function of time by

$$\frac{d\Delta C_t}{dt} = \frac{V}{W}\left[\Delta(C_s)_t - \Delta C_t\right] \quad \textbf{(11)}$$

where t = time(sec) from the time of injection

$\Delta c_t = C_t - C_o$, C_t is the actual analyte concentration in the carrier stream on entry to the mixing chamber and C_0 is the analyte concentration before injection

V = flow rate ($m\ell.min^{-1}$)

W = volume of the mixing chamber ($m\ell$).

2.3.4 General model

The general model describes the overall dispersion phenomena the best, taking into account both the convective and diffusional transport.

$$D\left(\frac{\delta^2 C}{\delta l^2} + \frac{\delta^2 C}{\delta r^2} + \frac{1}{r}\frac{\delta C}{\delta r}\right) = \frac{\delta C}{\delta t} + u_0\left(1 - \frac{r^2}{R^2}\right)\frac{\delta C}{\delta l} \qquad \textbf{(12)}$$

This is derived by applying a mass balance to a differential element of volume in the fluid and takes into account axial and radial concentration gradients, as well as flow-profiles under a laminar flow regime. The left hand side corresponds to diffusional transport, the first term within the brackets accounting for axial diffusion (dependence of C on l) and the other two for radial diffusion (dependence of C on r). The first term on the left hand side corresponds to matter build-up. And the second term accounts for the contribution from convective transport for which the velocity profile is parabolic in shape and given by

$$u = u_0\left(1 - \frac{r^2}{R^2}\right) \qquad \textbf{(13)}$$

The molecules at the tube walls (r = R) have zero velocity (u = 0) whereas, those in the centre

($r = 0$), have the maximum velocity ($u = u_0$).

2.4 Practical definition of dispersion

The dilution or dispersion at the detector, of a sample injected into the carrier stream, is given by the position and shape of the analyte signal band. Therefore, it is the parameters characterising the transient signal which are chosen to define the dispersion. An FIA peak is characterized by

(a) its position, as defined by the travel time, t_a

(b) the bandwidth, characterized by the baseline-to-baseline time, Δt, and

(c) the coordinates of the band maximum (T, C^{max}).

Bearing in mind the general theoretical considerations and the description of the different models used to define dispersion, it is easy to understand the difficulty involved in relating them to the experimental observations in a straightforward way. One of the various approaches, Růžička's dispersion coefficient, is discussed below.

2.4.1 Růžička's dispersion coefficient

This coefficient was proposed by Růžička and Hansen in 1977 [9] and it is also known as the 'practical dispersion' or simply dispersion coefficient. The dispersion is defined as the ratio of concentration before dispersion begins (C^0) and after dispersion has taken place (C) in a given

11461734(
b1433911

FIA system, i.e.

$$D = \frac{C^0}{C} \qquad \textbf{(14)}$$

Thus each point on the signal record has a corresponding dispersion coefficient. At the signal maximum,

$$D^{max} = \frac{C^0}{C^{max}} \qquad \textbf{(15)}$$

The dispersion coefficient can now be determined from the ratio of the height of the signal found in the absence of dispersion (i.e. for continuous flow of undiluted sample) to that of the FIA or SIA signal. Thus

$$D^{max} = \frac{k_0 h^0}{k_1 h^{max}} = \frac{h^0}{h^{max}} \qquad \textbf{(16)}$$

where k_0 = proportionality constant

k_1 = proportionality constant (equal to k_0 if height and concentration are linearly related)

h^0 = magnitude of the response (potential, pH, absorbance or fluorescence intensity) recorded when the sample solution is used as the carrier.

Hence the dispersion coefficient can often be taken as the signal height ratio. From its definition it follows that dispersion always exceeds unity with greater dispersion resulting in a flatter curve.

2.5 Influence of geometric and hydrodynamic factors on dispersion

Ramsing *et al.* [10] proposed the following expression for the dispersion coefficient of an elementary FIA system, which relates it to the geometric characteristics of the reactor (L, R), some hydrodynamic aspects (u, $\bar{t}_r$) and the injected volume (V_i):

$$D = \frac{2\pi^{3/2}R^2(Lu\delta\bar{t}_r)^{1/2}}{V_i} \qquad \textbf{(17)}$$

where δ = longitudinal dispersion number

defined by Levenspiel and Smith [11] for a non-Gaussian curve as

$$\sigma^2 = 8\delta^2 + 2\delta \qquad \textbf{(18)}$$

or

$$\delta = \frac{1}{8}[8(\sigma^2 + 1)^{1/2} - 1] \qquad \textbf{(19)}$$

where σ^2 = variance of dispersion in a flow system

According to this equation there is a relationship between D^{max}, which describes the peak height and σ, which provides a measure of the peak width.

2.5.1 Hydrodynamic factors

2.5.1.1 Flow rate

According to Vanderslice's expression, the flow rate, q, can be related to the travel and baseline-to-baseline times through

$$t_a = \frac{k}{q^{0.125}} \qquad \textbf{(20)}$$

and

$$\Delta t_a = \frac{k'}{q^{0.64}} \qquad \textbf{(21)}$$

where k, k' = constants.

This equation derived for FIA is also applicable to SIA systems [1]. The dispersion coefficient, D, will therefore decrease with increasing flow rate, resulting in better sensitivity of the method.

2.5.1.2 Geometric factors

This section deals with the influence of the reactor shape (open, coiled, packed) and dimensions on dispersion.

2.5.1.2.1 Straight tubes

Straight tubes represents the simplest situation. It can be seen from the following two equations that t_a and Δt increase with reactor length according to Vanderslices's predictions [12]

$$t_a = kL^{1.025} \quad \textbf{(22)}$$

and

$$\Delta t = k'L^{0.64} \quad \textbf{(23)}$$

It is also clear that t_a and Δt are directly related to the diameter (R = d/2), in agreement with Vanderslice's predictions [12]

$$t_a = kd^2 \quad \textbf{(24)}$$

and

$$\Delta t = k'd^2 \quad \textbf{(25)}$$

the residence time and the dispersion coefficient therefore increase linearly with the tube diameter.

2.5.1.2.2 Coils

When the reactor tube is coiled helically, the centrifugal force originating from the circulation of the fluid through the tube, results in a radial type flow. At low flow rates, the centrifugal

forces are low and the velocity profile is practically parabolic. At high flow rates, the profile is completely different since the molecules at the tube walls travel at a higher velocity than those at the centre of the tube. Both situations result in a split circulation, symmetrical with respect to the central plane of the tube. This circulation has been termed 'secondary flow' by Tijssen [13]. Coiling is qualitatively defined by the relation

$$\lambda = \frac{coil\ \ diameter}{tube\ \ diameter} \qquad \textbf{(26)}$$

For $\lambda = 10$, the dispersion is one-fourth of that for the uncoiled tube [12]. It can therefore be observed that smaller coil diameter leads to smaller dispersion.

2.5.1.2.3 Knitted reactors

In knitted reactors, dispersion is dramatically reduced. This may be due to the intensifying of the dispersion-reducing effect introduced by coiling, since in effect the knots are very small coils.

2.5.1.2.4 Normal packed tubes

To describe the effect of a packed tube on dispersion the following equation is helpful,

$$\tau = \frac{tube\ \ diameter}{particle\ \ diameter}$$

For $5 < \tau < 50$ the axial dispersion is directly related to the particle size, with a smaller particle diameter leading to less dispersion.

2.5.1.2.5 Single bead string reactors (SBSR)

Single bead string reactors are normally tubes of variable length packed with tiny glass beads, 60 to 80 % that of the tube. Its main purpose is that of increasing radial dispersion, which reduces the dilution and therefore decreases dispersion. In FIA and SIA it lead to less dispersion than with open tubes (one-tenth), and peak heights are nearly independent of the flow rate. Other advantages offered by a SBSR are greater residence times and a smoother baseline [14].

2.5.2 Contribution of chemical kinetics to dispersion

Dispersion can not be considered as a purely physical phenomenon when a chemical reaction takes place in the system. Reaction rates should also be taken into account since the measurements are made under non-equilibrium conditions. When some property of a reaction product in the flow is measured, the chemical contribution results in a decrease in the practical dispersion. With a higher reaction rate constant the dispersion gets smaller, and dispersion increases when the reaction rate constant, k, is higher where a property of a reactant is measured.

2.6 From flow injection to sequential injection via the random walk model [4]

In 1990 Růžička *et al.* [15] used the random walk model to postulate that no net flow was needed for the successful operation of a flow-injection system. This model will be described in this section and its application in SIA.

Flow-injection analysis, in comparison with chromatography, relies on the injection of a well-defined sample zone into a moving carrier stream and the subsequent detection of the signal which has been modulated by a combination of physical and chemical interactions between the analyte and reactive surfaces or reagents [16]. Until recently both these techniques shared the common feature of a monotonous constant flow rate. This mode of operation is not an indispensable condition for FIA. A dramatic decrease in reagent consumption and the design of more effective flow-injection systems has resulted from the introduction of flow programming, first as stopped-flow then flow reversal [17] and finally sinusoidal flow [15]. As miniaturization and reduction of reagent consumption are also ultimate goals in chemical sensing, it is useful to review the use of combined injection. Programmed flow was a central issue in designing chemical sensors and structurally simplified chemical analysers.

The successful operation of any chemical analyser requires that the reactant and sample are brought together, mixed and allowed to react in a perfectly reproducible manner. To obviate the need for frequent recalibration, it is necessary to maintain reproducible flow rates for extended periods of operation. This has led to the practice of using unidirectional monotonous flow, because as long as a constant flow rate is maintained the sample may be injected into the system at any time. This ensures that what happens to one sample happens to all the other samples as well. Obviously to fulfill these criteria, strict control of the flow rate must be maintained throughout the entire analysis period.

A theoretical description of the zone dispersion process in the analyser channel is a central issue in chromatography as well as FIA and as it is a random process, it can be described by the random walk model. Whereas Giddings [18] used this model to describe the dynamics of

chromatographic processes, it was Betteridge [6] who, considering monotonous flow, applied it to the description of zone dispersion in FIA.

The random walk model allows one to view the element of fluid as being displaced during the dispersion process in any direction by a step of fixed length. The direction of the step is determined completely by chance. If the chance of moving in any direction is equal, then the random walk is symmetrical. As all molecules in a said element of fluid cannot be expected to move through the same step of fixed length (their movement is erratic), the length must be taken as the average length of the actual displacement. Thus, if a large number of particles start together on a random walk of many steps, the standard deviation, σ, of the resulting (Gaussian) concentration profile is

$$\sigma = \ell n^{1/2} \qquad \textbf{(28)}$$

where ℓ is the fixed step length and n is the number of steps taken. It is noteworthy that the spread of the zone and resultant degree of mixing with the surrounding carrier stream are proportional to the individual step length, ℓ, which is easy to understand as the final displacement of the molecule from the origin depends on step length in any one direction. The final zone displacement increases only with the square root of the number of steps, n, taken. This is to be expected as a cancellation effect must be considered in which the molecule is equally likely to move in the opposite direction to the original displacement. If several random walks occur simultaneously, as they do in chromatography and FIA, the final displacement of any molecule is determined by the sum of the displacements in all directions.

Therefore,

$$\sigma^2 = l^2 n_1 + l^2 n_2 + \ldots = \sigma_1^2 + \sigma_2^2 + \ldots \qquad \textbf{(29)}$$

so that the components of the process (variances, σ) are additive.

There are two driving forces which cause the molecules to move and the zone to spread: an internal one that is symmetrical and caused by molecular diffusion, and an external one caused by the flow imposed on the liquid which transports the zone through the system. If the flow is unidirectional and if the molecular diffusion and/or radial transfer (caused by coiling or packing the tubing) does not compensate for the asymmetry resulting from Poiseuille flow, the resulting concentration profile is asymmetric. Consequently, the result of such a random process is asymmetric. The accumulated distance of migration, L, imposed by the flow can be transversed in many ways, each of which constitutes a different number of random steps depending on the flow geometry. This relationship has been expressed in chromatography by means of the height equivalent to a theoretical plate, $H = \sigma^2/L$, which in fact is a measure of the generation of variance per unit length of a column travelled by the dispersing zone. Clearly, the zone spreading increases with the square root of the distance travelled (L), while separation of the components increases with the number of theoretical plates unidirectional traversed, and therefore linearly with the distance travelled (as $NH = L$ for the uniform plate dimension).

Resolution which is the key issue in chromatography, is satisfactory only when the distance between component zone centres become outdistanced by the spreading. This situation happens sooner for lower H values and higher L values. Giddings [17] showed in this elegant way why

no chromatographic separation will be achieved without forward motion, and why the use of unidirectional monotonous flow rate is an absolute condition for chromatographic separation.

The use of a unidirectional monotonous flow rate has been the prevailing practice in FIA, which, unlike chromatography, does not aim at the separation of the analyte components, but rather at their effective chemical conversion into detectable species. Therefore the key issue in FIA is reproducible dispersion into the carrier stream and timing of the arrival of the reacted zone at the detector.

The random walk model is useful for the visualisation of the degree of mixing, since the transition of the original square input, through skewed peaks, and finally to Gaussian-shaped peaks is indicative of the degree of mixing of the reagents. As it is well known that the skewness of the peak is a result of the initial acceleration and is further amplified by Poiseuille flow, the value of the symmetrical random walk is that it leads to the conclusion that efficient mixing of the reacting components can be achieved without actually travelling any net distance, L. By moving the injected zone forward and back in several steps (n) of sufficient length (ℓ) an efficient mixing of sample zone and carrier stream components may be achieved through a combination of external and internal forces. By selecting the step length and the number of flow reversals, any degree of mixing and any length of reaction time can conveniently be obtained by flow reversal. The need to travel the length of the channel in one direction in classical flow-injection systems is only necessary because the sample zone has to be transported from the injector, past a mixing point, through the reaction coil towards the detector and waste. Hence it is the physical size of the system and the configuration of its components (pump, injector, confluence point, reactor, detector, waste) which require a net flow of the carrier stream larger than the minimum

volume required by the reacting species. As forward flow is mainly used to achieve mutual dispersion of the reacting species, the fluid consumption is mainly determined by the flow channels and flow rates. The required volume is therefore much larger than if a net zero forward flow took place. On the other hand, as flow reversal yields zero net flow, a very high linear flow velocity can be imposed on the selected elements of fluid and thus a turbulent flow may be achieved if necessary.

Use of a flow pattern rather than constant monotonous flow, requires synchronisation of sample zone injection with the start of each flow cycle. Therefore, a system configuration must be conceived which will allow sample zone injection, reagent addition, mixing, measurement, and ejection of reacted mixture by a combination of forward and reverse flow steps. It follow from the foregoing that these steps may have different lengths, duration, and speed, provided that they always follow the same pattern. There are clearly many possible combinations of the step length (ℓ) and step number (n) and also of the resulting net flow, yet if the pattern is strictly repeatable in each measuring cycle, the sample zone dispersion, being composed of individual variances, will always be the same and so will be the reaction time. To achieve an absolute zero net flow is, of course not practical, but sample and reagent consumption can drastically be reduced and the flow system can dramatically streamlined if mutual dispersion of the sample and reagent zones, their reaction to yield detectable species and detection of these species occur within the same section of flow conduit.

2.7 References

1. E. R. Taljaard, **Application of sequential injection analysis as process analysers**, MSc, UP, 1996.
2. T. Gübeli, **Anal. Chem.**, **63** (1991) 2407.
3. J. Růžička, **Anal. Chem.**, **63** (1991) 2413.
4. J. Růžička and G. D. Marshall, **Anal. Chim. Acta**, **237** (1990) 237.
5. J. Růžička and E. H. Hansen, **Anal. Chim. Acta**, **99** (1978) 37.
6. D. Beteridge, **Anal. Chem.**, **50** (1978) 832A.
7. H. L. Pardue and B. Fields, **Anal. Chim. Acta**, **124** (1981) 39.
8. E. Pungor, Z. Fehêr, G. Nagy, K. Töth, G. Horvai and M. Gratzl, **Anal. Chim. Acta**, **B** (1979) 1.
9. J. Růžička, E. H. Hansen and E. A. Zagatto, **Anal. Chim. Acta**, **88** (1977) 1.
10. A. H. Ramsing, J. Růžička and E. H. Hansen, **Anal. Chim. Acta**, **129** (1981) 1.
11. O. Levenspiel and W. H. Smith, **Eng. Sci.**, **6** (1957) 227.
12. J. T. Vanderslice, K. K. Steward, A. G. Rosenfeld and D. J. Higgs, **Talanta**, **28** (1981) 11.
13. A. Tijssen, **Anal. Chim. Acta**, **88** (1980) 71.
14. J. Růžička and E. H. Hansen, **Flow Injection Analysis**, 2nd ed., Wiley, New York, 1988.
15. J. Růžička and G. D. Marshall, **Anal. Chim. Acta**, **237** (1990) 329.
16. J. Růžička and G. D Christian, **Analyst**, **115** (1990) 475.
17. G. D. Clark, **PhD Dissertation**, University of Washington, Seattle, 1989.
18. J. C. Giddings, **Dynamics of Chromatography**, Dekker, New York, 1965.

UNIVERSITEIT VAN PRETORIA
UNIVERSITY OF PRETORIA
YUNIBESITHI YA PRETORIA

CHAPTER 3

Design of the Sequential Injection System

3.1 Introduction

In the previous chapter the parameters that influence dispersion of the injected samples and reagents, and eventually the performance of a sequential injection system, were discussed. In order to obtain the optimal dispersion for the particular chemical reaction, or detector used, the sequential injection system must be carefully designed. Since both FIA and SIA make use of the same methodology, the design of the SIA system follow the same rules, established by Růžička and Valcarcel [1, 2], for FIA in providing limited, medium and high dispersion of the injected sample and reagent zones.

3.2 Components of the SIA system

A complete SIA system (Fig. 3.1), as used in this work, consist of a manifold (pump, selector valve and detector, interconnected with narrow-bore tubing), a control system (e.g. computer with interface for signal conversion) and data collector/processor (e.g. computer).

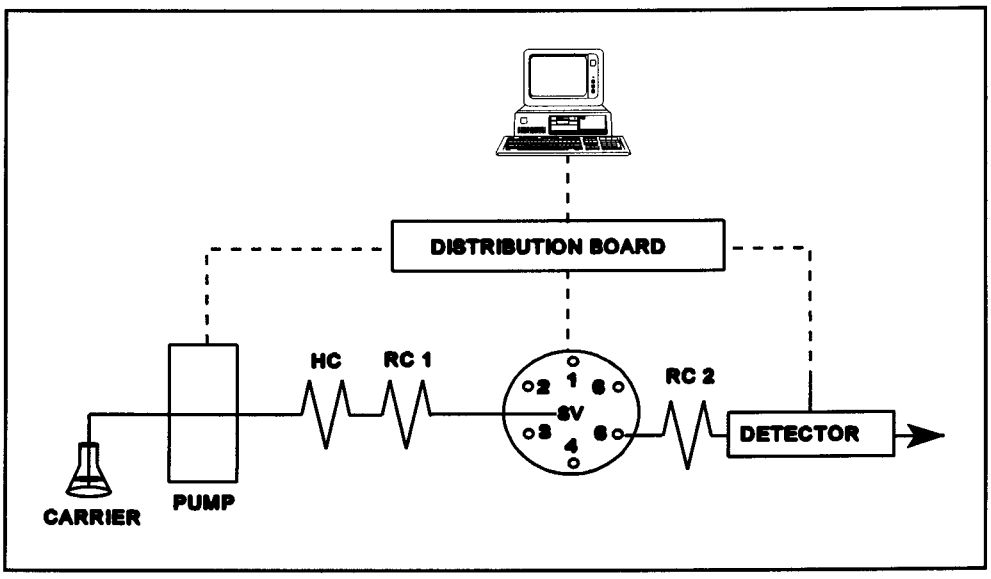

Fig. 3.1 Typical setup for a sequential injection system with a computer, interface, pump, selector valve (SV) and detector all interconnected with narrow-bore tubing. HC - holding coil, RC - reaction coil.

3.2.1 Manifold

3.2.1.1 Propelling system

3.2.1.1.1 Pumps

For a SIA system to be industrially viable, the results obtained must be accurate and highly reproducible. For this reason a propelling system of high quality, capable of delivering constant flow rates over long periods, is needed to deliver these highly reproducible results. The following design criteria was set by Marshall [3].

- The flow rate must be highly reproducible and reliable.
- Remote controlled to enable immediate stop, start, forward, and reverse pump actions with negligible pump inertia.
- Flow rate range of between 0.5 and 15 $m\ell.min^{-1.}$
- Pump pulsing should be negligible.
- Parts exposed to fluids must be resistant to a wide range of solvents and acids.
- Power requirements should be low enabling the pump to be incorporated into portable systems.
- Physical size of the pump should be kept to a minimum.
- Robust, able to withstand continuous use for extended periods.
- Not prone to blockage.
- Able to withstand pressures up to 700 kPa

Peristaltic pumps comply with most of the above mentioned requirements and offer additional advantages such as, low price, long service intervals and simplicity.

The peristaltic pump consist of a drum, powered by a electric motor, with bearing rollers on its edge (Fig. 3.2). Flexible tubing of some kind (Table 3.1) is pressed against a circular support (pressure band), with larger diameter than that of the drum, and as a result of the rotation of the drum, the fluid is forced in the same direction as pump head rotation. Peristaltic pumps does not deliver a totally pulse-free flow, such as obtained with a syringe pump, but if the amount of rollers is increased pulsation could be decreased to an acceptable level. Another property of the peristaltic pump is the fact that reproducibility increase with the angle through which the drum is rotated [4]. Small sample volumes are therefore best achieved by smaller diameter pump

tubing, and more revolutions of the pump head per volume unit.

One of the disadvantages of the peristaltic pump is its performance over long periods. The main problem is the pumping tube material which stretches and looses its flexibility with prolonged use. The initial flow rate would be a little higher than the flow rate obtained when the tube reaches the end of its useful lifespan. With regular replacement of the pump tubing this disadvantage can be obviated.

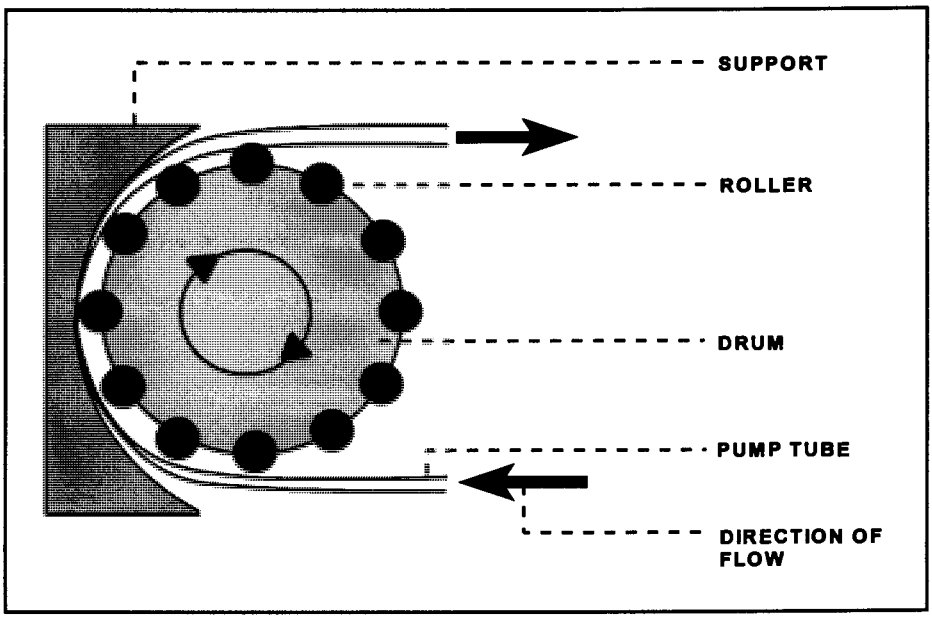

Fig. 3.2 Representation of a peristaltic pump and how it works.

3.2.1.1.2 Pump tubing

The pump tubing is just as important as the quality of the pump used in the sequential injection system. The wrong choice of pump tube material could lead to premature failure of the pump tube, while old tubes, or tubes of inferior material, lead to inconsistent flow rates. Table 1 lists a few solutions with the correct tubing for each of the solutions.

Table 3.1 Available tubing material with solutions for which they could be applied

Type of solution	Tubing material (trade names)
aqueous solution	PVC, Tygon
dilute ethanol solutions	PVC, Tygon
dilute acids and bases	PVC, Tygon
concentrated acids and bases	fluoroplast, ("Acidflex" from Technicon)
alcohols	modified PVC ("Solvaflex" from Technicon)
lower aclcohols	silicone rubber
formaldehyde and acetaldehyde	PVC, Tygon
acetone	silicone rubber
acetic acid and anhydride	silicone rubber
aliphatic hydrocarbons	fluoroplast ("Acidflex", from Technicon)
aromatic hydrocarbons	fluoroplast ("Acidflex" from Technicon)
chloroform	fluoroplast ("Acidflex" from Technicon)
carbon tetrachloride	modified PVC ("Solvaflex" from Technicon)

The pump tubing should be checked regularly for any decline in its flexibility to ensure a constant flow rate. As soon as the tube starts loosing its flexibility, or a drop in flow rate is observed, the pump tube should be replaced.

3.2.1.1.3 Flow rate

Flow rate can be varied in two ways. The first is to increase the speed at which the pump drum rotates keeping the pump tube diameter constant and the second is to keep the speed at which the pump drum rotates constant while changing the pump tube inside diameter. If low flow rates are required it is preferable to use smaller tubing rather than decreasing the speed of the pump which could lead to a decrease in reproducibility. In the case of high flow rates, larger tubing would be advantageous, as high pump speeds would lead to excessive wear of the pump tube and its premature failure.

According to Vanderslice's expression, $D = k'q^{1/2}$, where q is the flow rate in $m\ell.min^{-1}$, the dispersion coefficient, D, should increase with an increase in the flow rate. Exactly the opposite is observed experimentally with the dispersion decreasing with an increase in the flow rate. At the same time, an increase in peak height is observed as a result of the dispersion decrease.

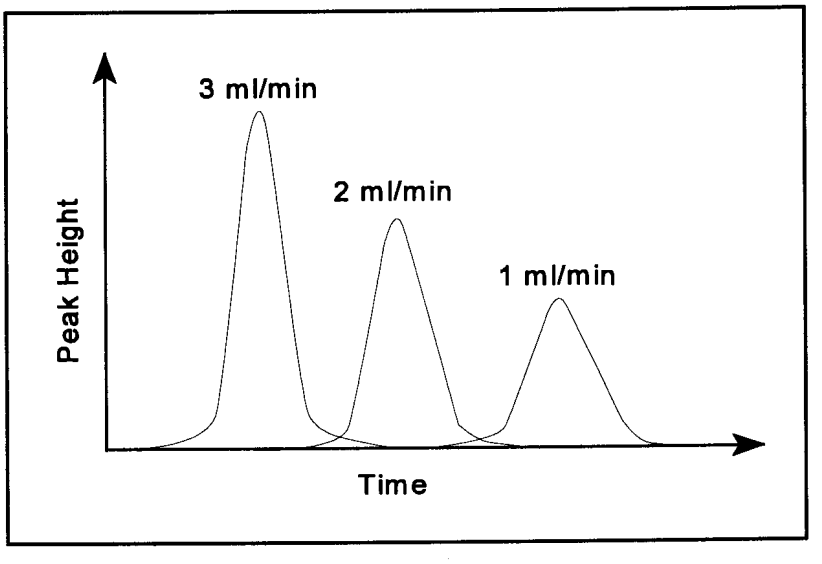

Fig 3.3 Influence of flow rate ($m\ell.min^{-1}$) variation on sensitivity (peak height) and dispersion (peak width).

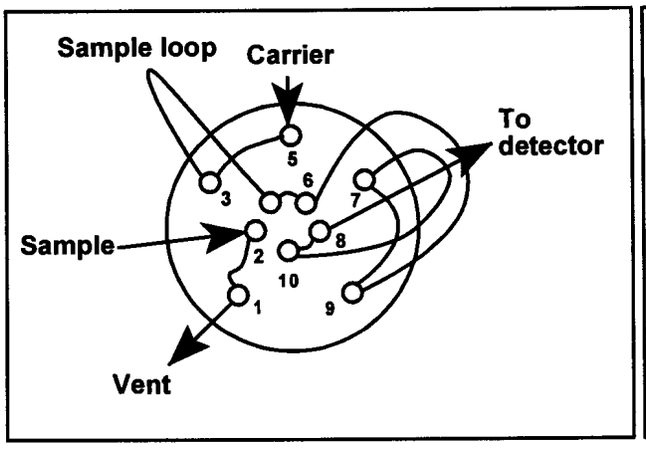

Fig.3.4 Schematic diagram of a 10-port flow-injection valve head

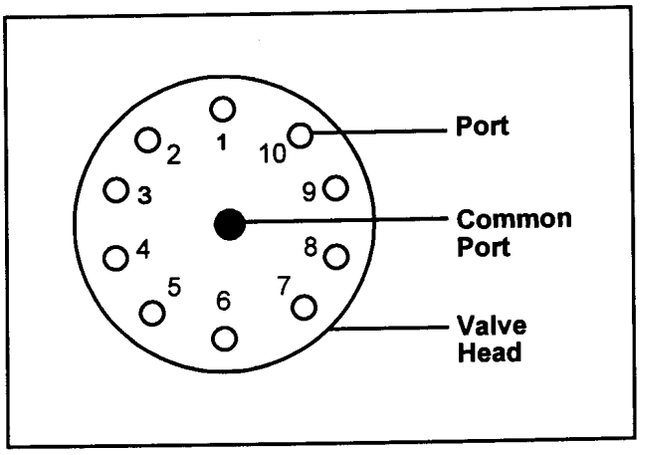

Fig. 3.5 10-port selector valve head as used in sequential injection analysis.

The flow rate should therefore be carefully optimised in order to obtain the correct dispersion for the specific reaction.

3.2.1.1.4 Sample and reagent volumes

Sample and reagent volumes are determined by the flow rate (pump speed) and the time period for which the sample and reagent solutions are pumped. Gübeli *et al.* [5] studied the effect of sample and reagent volumes on zone penetration and sensitivity and established the following rules:

(i) Changing the injected sample volume is an effective way of changing the measurement. Dilution of overly concentrated injected sample material is best achieved by reducing the injected sample volume.

(ii) Injecting at least twice as large a reagent zone volume as the sample zone volume, while keeping the sample zone less than or equal to 0.5 $S_{1/2}$, allows the optimum

conditions for single reagent based chemistries to be met. $S_{1/2}$ is defined as the sample volume that yields a dispersion of 2 in the manifold.

(iii) Two reagent chemistries can be accommodated provided that the sample volume is kept below the $S_{1/2}$ value, that the sample zone is surrounded by the reagent zones and that the concentrations of the injected samples are sufficiently high, to prevent sub-stoichiometric mixtures.

3.2.1.2 Injection system

The term 'injection' has its origin in early FIA systems where the sample was manually injected into the continuous flowing carrier stream. More recent FIA systems make use of flow injection valves with sample loops (Fig. 3.4) where the sample is introduced into the system by rinsing the sample loop with the carrier, but although the method of injection changed, the term 'injection' was carried over and the technique is still called "flow-injection analysis".

For sequential injection on the other hand, selector valves with 4 to 10 ports are used (Fig. 3.5) arranged around a central common port and the valve is able to connect any one of the ports to the common port in the middle, enabling 10 different solutions to be aspirated sequentially, at any time.

The flow-injection valve, on the other hand, connects a number of ports simultaneously in each one of its specific actions (inject or load) with only one solution injected. A valve should have certain properties to enable it to be incorporated into the SIA system and the following requirements [3] were set for a selection valve:

(i) Continuous, maintenance free operation for periods of weeks is necessary for process applications.

(ii) Flow paths should have minimal effect on dispersion

(iii) Various flow path options should be available including dead stop, flow through individually and flow through to common.

(iv) All wetted parts should be resistant to a broad range of solvents and acids.

(v) Valve ports should match the dimensions of the flow manifold and should not include torturous paths.

(vi) Remote control via Transistor-Transistor-Logic (TTL) or switch contacts should enable random selection of ports using 4 bit digital control. The ability to sequentially step through ports should also be available. Some means of feedback is required to indicate valve position at that specific time.

(vii) Power requirements of the valve should be low to enable the valve to be incorporated in portable systems. A 12 V apart from the usual power supply should be available.

(viii) Back pressures up to 700 kPa must be accommodated. For some applications 2000 kPa would be desirable.

(ix) Connection to various sizes of tubing should be by means of standard fittings.

(x) An intrinsically safe option would be required for certain applications.

(xi) Physical size should be kept as small as possible.

The solutions to be aspirated are arranged around the selector valve in such a way that the solution to be aspirated first is at the number one port of the valve (Fig. 3.5), while ports not in use are simply blanked off to avoid any air from getting into the manifold. The valve used in this

work is a 10-port Valco valve (Model ESCD10P, Valco Instruments, Houston, TX, USA). This valve is actuated by means of a computer signal which is converted by a distribution board to suit the signal input of the valve. This valve is only able to move in one direction (counter clockwise) and therefore the solutions should be arranged in the order in which they are going to be injected around the valve. The valve has an additional function, that of moving from any selected port of the valve to the first port of the valve (called the 'home' position) in one single step. Single step selection is possible with the 'STEP' command of the FlowTEK [6] program while the home position is selected by the single command 'HOME'.

3.2.1.3 Detector

A suitable sequential injection detector, and FIA detector, should possess a series of clear-cut attributes: small volume, low noise level, fast and linear response over a wide concentration range, and high sensitivity. The detection systems used in both FIA and SIA comprise the most frequently used types of detectors of which optical (spectrophotometric and non-spectrophotometric) and electrical detectors (amperometric, potensiometric, conductimetric, coulometric) are the most important.

Among the optical methods photometry is undoubtedly the most widely used technique thanks to the large number of species that may be monitored, either because of their intrinsic optimal properties or because of optical properties induced by reaction with a suitable substance. This technique is also employed in this work since a large number of selective colour forming reactions are available for the analysis of elements present in fertilizers.

The flow cell is one of the most important components of any flow-injection detector, and a sound flow cell design is therefore indispensable. The following guidelines were set for a flow cell design [6]:

(I) minimise dead volume,

(ii) simplify flow paths,

(iii) avoid bubble traps, and

(iv) ensure convenient maintenance schedule.

The detector may be placed between the valve and the pump (Fig. 3.6, A) [7] or down stream from the valve (Fig. 3.6, B) [6]. With the detector between the valve and the pump a double peak is formed, as the detectable compound moves through the detector twice, once when aspirated

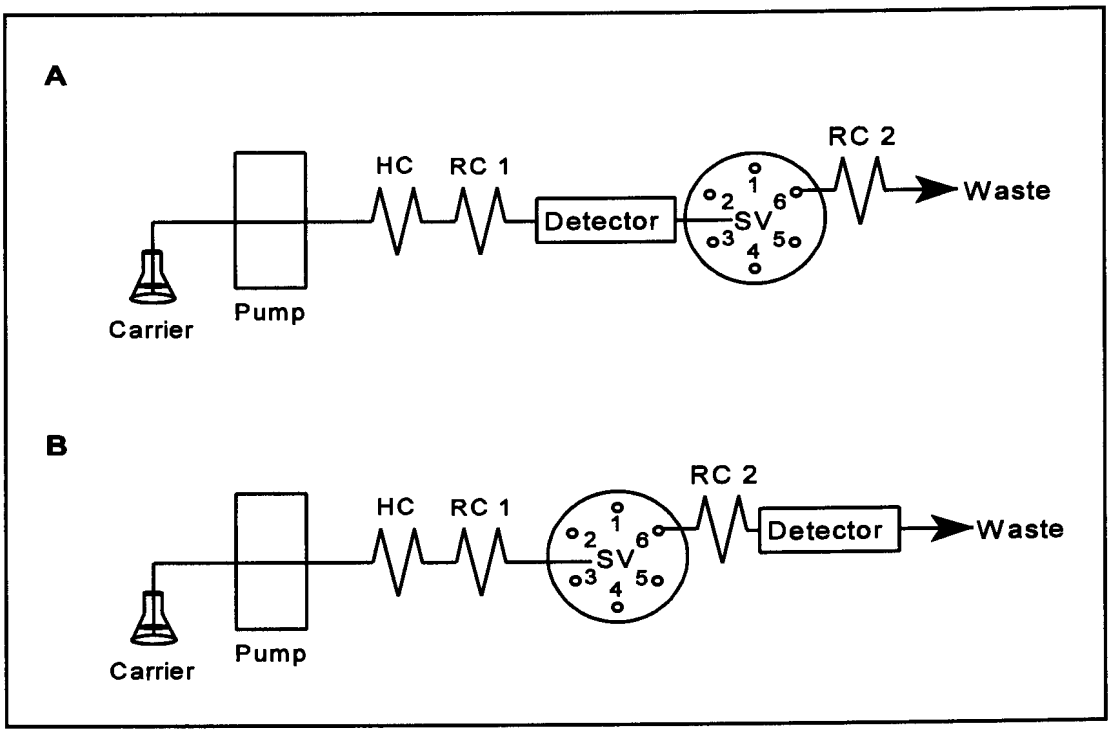

Fig. 3.6 Possible positions for the detector in a sequential injection system. SV - selector valve, HC - holding coil, RC - reaction coil.

and once when pumped towards the waste. The second position, downstream from the valve, is the most widely used, resulting in the familiar FIA response curves.

3.2.2 Computerized control and data accusation

Automated control of FIA systems is not mandatory, since manual systems have been developed and used successfully in a wide variety of applications. This is not the case for SIA. Switching of the pump (forward, reverse, stop), and selector valve (step, home) with simultaneous data acquisition make it impossible to operate SIA systems without microprocessor control. With FIA systems, reagents are continuously added to the flowing stream while sample volume is determined by the sample loop of the injection valve. In SIA's case reagent and sample volumes are accurately determined by the aspirating times of the individual solutions, requiring accurate instrumentation (pumps, valves) and control systems (microprocessor, software). Integration of this hardware and software must be such as to offer maximum flexibility and user-selectable configuration. This level of flexibility is often absent in commercial systems where the requirement for simplicity places constraints on flexibility.

3.2.2.1 Data output

Device control and data acquisition is best achieved with the use of a single software package capable of carrying out all calculations at the process analyser itself before releasing final concentration data. Such a package is the FlowTEK [6] package used to control the peristaltic pump and selector valve while receiving data from the detector. Data from the detector is obtained as peak height, peak width, peak time and concentration. This data is saved and stored

on a suitable medium.

3.2.2.2 Interface board

A general-purpose analog and digital input/output interface board (PC-30B, Eagle Electric, Cape Town, South Africa) was used to interface the computer to the analytical instrumentation. The minimum specifications of this board is set out in Table 3.2.

Table 3. 2 Minimum specifications for FlowTEK interface board

Property	Minimum specification
Analog input channels	4 single ended 12-bit resolution Input range (0 to 10V) Input impedance (> 100 kΩ/100 p) Acquisition rate ($3x10^4$ sec^{-1} variable)
Digital I/O	24 in 3 ports [programmable as Input or Output] TTL compatible
Required power	100 mA at ± 5V
PC connection	Uses a fully bussed full length 8-bit slot of an 80 x 86 computer

3.2.2.3 Distribution board

A distribution board was used between the computer and the instrumental components (Fig. 3.1). This distribution board allows the connection of devices and detectors to the interface board. A variable gain amplifier (0 to 10mV signals amplifiable up to 1000 times) is usually included into the board to enable connections to analog devices with an output range different to that available

on the interface board. The distribution board also allow different levels of electronic filtering with time constants of 0.01, 0.1, and 1 second with no additional signal smoothing necessary.

3.2.3 Manifold dimensions and geometry

3.2.3.1 Manifold tubing

The different components of the sequential injection manifold are connected by transport conduits of which PTFE (polytetrafluoroethylene) tubing is the most commonly used. PTFE tubing provides excellent resistance to a number of solutions, including most diluted acids and organic solutions, and is non-wettable preventing undue carry-over between successive analysis. Tubes with a range of internal diameters are commercially available, but a minimum tube wall diameter of 0.5 mm is required to provide sufficient mechanical strength. Tubes with small internal diameters produce lower dispersion, but they are prone to blocking when suspended particles are present in the solutions. If connections between tubing have to be made, connectors of the same internal diameter should be used in order to prevent dead volumes within the connectors. Care should also be taken in avoiding leaks, and possible introduction of air bubbles [2].

3.2.3.2 Effect of tube diameter

Tube length together with the tube diameter is used to obtain a certain amount of dispersion in the SIA system. The diameter should be very carefully considered as the wrong diameter could lead to the development of back pressure, result in blockages and limit the radial dispersion.

Smaller diameter tubing gives rise to higher back-pressures. When the pressure in the reverse stroke drop below the partial pressure of the dissolved gasses, bubbles form in the tubing, which results in poor reproducibility of the flow pattern and can lead to spurious signals from the detector. The back-pressure is also directly related to the pump speed, and therefore a reduced pump speed may be necessary for smaller diameter tubing,. When the pump is forced to work under conditions of high back pressure, it starts to labour with poor precision as the result.

The radial dispersion is also effected by the ratio of tube inner diameter to inner tubing surface. The frictional effect of the tubing walls decreases with increasing inner diameter, as the ratio of molecules next to the wall to those not touching the tube wall decrease. This helps to reduce axial dispersion, and narrow peaks are obtained.

The tubing connecting the selection valve to the reagents, the uptake tubes, should be as large as possible, in order to minimise back-pressure. The diameter and the length of the sample line should be kept to a minimum to reduce problems associated with carry-over. Holding coil diameters can also be larger, as long as the reaction products do not enter this coil.

3.2.3.3 Holding coil

A holding coil is incorporated into the system between the selector valve and the peristaltic pump (Fig. 3.1). The holding coil should be large enough to prevent the sample and reagents from entering the peristaltic pump tubing [8]. This precaution is necessary because, when the stacked zones enter the pump tubing, deformation of the zones take place and this results in a decrease in zone penetration, and therefore sensitivity and precision. Růžička and Gübeli [7] stated that

a large holding coil was necessary, since even prior to flow reversal the stacked reagent and sample zones, might occupy twice the volume of the originally injected zones. This is due to the parabolic profile of the injected zones (Chapter 2, Fig. 2.2).

In an experiment to study the influence of the holding coil on precision and sensitivity, the length and diameter of the coil was changed and its effect recorded. Longer coil lengths resulted in a precision increase but it had no effect on the sensitivity. This proves that deformation of the injected zones takes place if the reagent and/or sample zone enters the pump tubing resulting in a decrease in precision. The same results were obtained when the coil length were changed. It can therefore be concluded that larger diameter tubing must be used in the construction of the holding coil

3.2.3.4 Reaction coils

Reaction coils are incorporated into SIA manifolds to obtain the correct mixing or penetration of the sample and reagent zones. Two reaction coils are normally incorporated into the SIA system, the one between the holding coil and the valve and the other down stream from the valve. The reaction coil between the holding coil and the valve is sometimes incorporated into the holding coil, with a long holding coil as the result [3, 5, 7]. This reaction coil (RC 1, Fig. 3.1) should not exceed one-third of the wash solution, thereby ensuring that the manifold is adequately flushed during each experiment. RC 1 should be designed to accommodate the entire reagent zone and the non-cross-contaminated sample zone [7]. Earlier experiments [7, 9] showed that wider tubing is favoured, but it does not always influence the result to a great extend. In some cases [9] however it was found that short narrow bore reaction coils gave better results.

Reaction coil geometry is the third parameter that has to be optimised when it comes to reaction coils. The three types of reaction coil geometries most widely used are, straight, coiled and knitted reactors. Marshall [3] found that straight tubes resulted in greater axial dispersion. Coiled reactors gave less axial dispersion and knitted reactors the least axial dispersion of the three. Whereas with FIA it was desirable to minimize axial dispersion in order to minimize dilution, in SIA axial dispersion promotes zone penetration and therefore straight reactor tubes are more desirable as was mentioned earlier.

Most of the zone penetration takes place in the first section (holding coil, RC 1) of the SIA manifold, and once this has happened it is desirable to promote radial mixing in order for the reaction to take place. For this reason, a short length of knitted coil just prior to detection is usually incorporated in the manifold, RC 2. It is also feasible to use narrow tubing for this reaction coil, to prevent axial dispersion and therefore dilution of the product.

3.2.3.5 Order of injection

In double-injection FIA, the order in which the sample and reagent zones are introduced has a minimal effect, as the volume of the injection loops is usually much less than the system volume. The second zone, therefore, has a similar distance to travel than the first zone. In SIA, where at least one flow reversal takes place and zone volumes are of the same order as reactor volumes, this is not the case. The dispersion of the first zone introduced is greater than that of the second zone, since the total distance travelled by the first zone is further than that of the second zone, and dispersion is dependent on the distance travelled by the zone. One must therefore decide which zone has to be introduced first.

The order of injection is dictated by the kind of application and the following must be considered. When sensitivity is important, the reagent, at a sufficiently high concentration to ensure an excess, should be introduced first and allowed to penetrate the sample zone. The sample zone will experience less dispersion due to the shorter distance travelled. If buffering of the sample by a wash solution is required, the order must be reversed. If solubility considerations prevent the reagent concentration from being increased, an alternative is to sandwich the sample zone by two reagent zones, resulting in better sensitivity.

3.3 Conclusion

In this chapter the importance of tube dimension used in the SIA manifold, were realized. Decreasing the tube diameter resulted in either increased back-pressure or a blockage possibility that prevents the miniaturization of flow conduits beyond certain limits. Larger tube diameter improved precision without an excessive decrease in zone penetration.

In SIA straight reactors are preferred as they allow greater zone penetration through an axial dispersion increase. The same principle will hold for FIA when double injection is used as a means of introducing fixed volumes of sample and reagent in a stacked zone configuration analogous to SIA. The optimum arrangement for the chemical reaction to occur is obtained by enhancing mixing of the penetrated zone just prior to detection using one or other mechanical means. Pump speed has a definite effect on zone penetration, as well as the viability of the SIA method as process analyser. Faster pump speeds are desirable when analysis times are to be minimized, whereas slower pump speeds are preferred when maximum zone penetration is required.

The order of injection is dictated by the application of the system. The longer path length and therefore greater dispersion observed in the zone injected first must be considered in the design of procedure. Optimum use of the two dispersion patterns will ensure sensitive and reproducible measurements.

3.4 References

1. J. Růžička and E. H. Hansen, **Flow Injection Analysis**, 2 nd ed., Wiley, New York, 1988.
2. M. Valcarcel and M. D. Luque de Castro, **Flow Injection Analysis, Principles and Application**, Horwood, Chicester, 1978.
3. G. D. Marshall, **Sequential Injection Analysis**, PhD Dissertation, University of Pretoria, Pretoria, 1994.
4. A. Ivaska and J. Růžička, **Analyst, 118** (1993) 885.
5. T. Gübeli G. D. Christian and J. Růžička, **Anal. Chem.**, **63** (1991) 2407.
6. G. D. Marshall and J. F. van Staden, **Anal. Instrum.**, **20** (1992) 79.
7. J. Růžička and T. Gübeli, **Anal. Chem.**, **63** (1991) 1680.
8. J. F. van Staden and G. D. Marshall, **Process Control and Quality**, **3** (1992) 251.
9. E. R. Taljaard, **MSc Dissertation**, University of Pretoria, Pretoria, 1994.

CHAPTER 4

Determination of Nitrite by Sequential Injection Analysis

4.1 Introduction

Nitrite does not occur in large amounts in nature but the concentrations are frequently monitored because of its environmental application. Nitrite is deemed to be potentially hazardous to health if its maximum admissible concentration (MAC) of 0.1 $mg.\ell^{-1}$ is exceeded [1]. Nitrites are intermediate products of the oxidation of ammonia and the reduction of nitrates [1], processes that occur in fertilizer streams, wastewater treatment plants, effluent streams, water distribution systems and natural waters.

If the MAC value of nitrite is exceeded, it could have numerous negative effects on the individuals consuming the product with the high nitrite content. Infant meta-haemoglobin-anemia or the "blue baby" syndrome [2] can occur when microbes present in the stomach convert nitrate into nitrite. When the nitrite reaches the bloodstream it reacts with the haemoglobin, the agent that transports oxygen around the body. Normal oxyhaemoglobin, which contains blood in the ferrous form, becomes meta-haemoglobin with iron in the ferric form. As a result the oxygen-carrying capacity of the blood is diminished. Foetal haemoglobin has a greater affinity for nitrite than normal haemoglobin, nitrite persists for a while in the blood stream, and foetal stomachs are not acid enough to inhibit the microbes that convert nitrate to nitrite.

Stomach cancer has also been associated with high nitrite content in food and water. Nitrite can react with an organic compound called a secondary amine, a product formed by the breakdown of meat, in the stomach to form an N-nitroso compound in the following way:

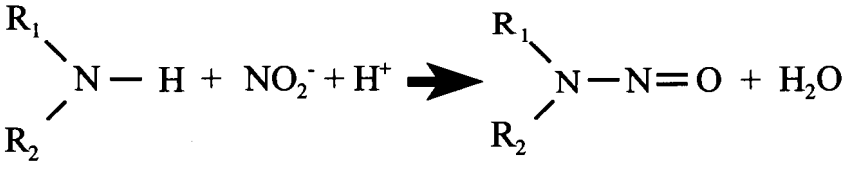

This N-nitroso compound is capable of modifying certain components of DNA that lead to cancer [2]. Thus the online monitoring of nitrite in process streams, natural and waste waters and other biological systems are of the utmost importance.

4.2 Uses of nitrite

One important application of nitrite is in the food industry where it is used in the curing of meat such as sausages, polony, ham, and bacon to prevent food poisoning from *Clostridium botulinum* [2] and to give the characteristic pink colour and organoleptic properties to the product. Since nitrite is an important precursor in the formation of nitrosamines, many of which have been shown to be potent carcinogens, its presence in products is mostly unwanted and it therefore has limited application.

4.3 Properties

When fertilizers are considered then nitrite's most important property is its high solubility and the fact that it doesn't accumulate in well aerated soil. High concentrations may, however, accumulate when N-fertilizers, that form alkaline solutions upon hydrolysis, are band applied to soils [3]. In such a fertilizer band the soil pH may reach values as high as 10. The activity of the nitrite oxidizer *Nitrobacter* is greatly inhibited by such high pH values. Thus, in fertilizer bands, nitrite can accumulate up to several hundred μg nitrogen per gram of soil.

Nitrite is also particularly reactive under acidic conditions, which may occur around the periphery of fertilizer granules where nitrification of the fertilizer is complete [3]. Both these extreme conditions should be avoided as far as possible to prevent the accumulation of toxic nitrite in soils.

4.4 Choice of analytical method

Numerous colorimetric methods have been proposed for the determination of micro-amounts of nitrite. The most widely used spectrophotometric method is the diazotisation of an aromatic amine and the subsequent coupling to form an azo dye which is then measured [4]. Other methods include amperometric determination with a glassy carbon working electrode [5], ultraviolet absorption [6] and potentiometric measurements with a nitrite ion-selective electrode [7].

The most promising method for the determination of nitrite with SIA is based on the diazotisation of nitrite. This reaction is a modified version [8, 9] of the Shinn [10] reaction which is based on the well-known Griess reaction. This is the reaction of nitrite with a primary aromatic amine to form a diazonium salt, which is then coupled with another aromatic compound to form an azo dye of which the absorbance is measured. A number of flow injection systems [11, 12, 13] have been developed using these modifications.

4.5 Reaction principles

Shinn's method [10] for the determination of nitrite, follows the technique of Bratton and his co-workers [14] in using sulphanilamide as the diazotising reagent and N-(1-naphthyl)-ethylenediamine dihydrochloride as the coupling reagent. The development of the red azo dye takes place according to the following reaction:

diazotisation:

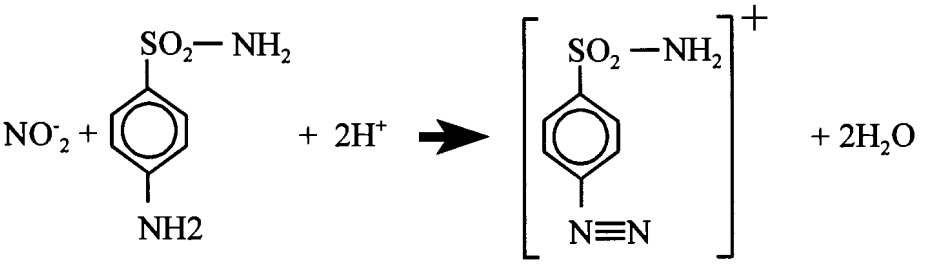

Sulphanilamide (Diazonium ion)

followed by coupling:

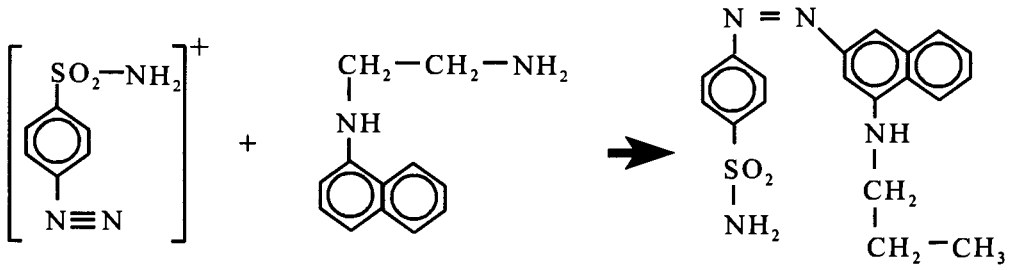

(Diazonium ion) N-(1-Naphtyl)ethylen diamine Azo-dye

According to these reactions an increase in the hydrogen concentration will lead to an increase in the rate of diazotisation (Eq 2), but to a decrease in the coupling rate (Eq 3). In the Wattenberg method [15] a pH of 3.27 was too high for rapid diazotisation to take place, not allowing enough time for diazotisation of the sulphanilic acid before the coupling reagent is added. The conditions for this reaction should therefore be carefully optimised to obtain maximum sensitivity.

4.6 Determination of nitrite with sequential injection analysis

4.6.1 Experimental

4.6.1.1 Reagents and solutions

Only analitical reagent grade reagents were used unless specified otherwise. ared. Deionised water, supplied by a Modulab system (Continental Water Systems, San Antonio, TX, USA) was used to prepare aqueous solutions. The solutions were degassed, by boiling in a microwave oven,

before introduction into the system and it was stored in an oxygen free environment when not in use.

Standard nitrite solution: A stock nitrite solution was prepared by dissolving 0.2463 g of oven dried sodium nitrite in deionised water and diluting it to 1 litre. Approximately 5 drops of chloroform were added to the stock solution and it was stored in a cool place. Working standard nitrite solutions were prepared by appropriate dilutions of the stock solution.

Buffer solution: The buffer solution was prepared by dissolving 30 g of ammonium chloride and 2 g of EDTA disodium salt [16] in 500 mℓ deionised water. The pH of this solution was adjusted to pH 6.6 [17] using a 25% (v/v) ammonia solution.

Carrier: The carrier solution was prepared by dissolving 10 g of ammonium chloride in 1 litre of deionised water. This solution had a pH of 4.56 and it was stored in a cool place when not in use.

Chromogenic reagent: The chromogenic reagent was prepared by dissolving 40 g sulphanil-amide and 2 g of N-(1-naphthyl)ethylenediamine dihydrochloride, obtained from Merck, in 200 mℓ of 80% (v/v) phosphoric acid, and quantitatively diluted it to 1 litre with deionised water. The pH of the solution was 1.07 and it was stored in a cool place when not in use.

Liquid fertilizer: Since the levels of nitrite in fertilizers are low a 1:1 fertilizer to deionised water ratio was used. The solution was filtered to get rid of any solid particles that formed during the dilution.

4.6.1.2 Equipment

The sequential injection manifold used, is shown in Fig. 4.1. The system consisted of a Gilson Minipulse peristaltic pump (Gilson Medical Electronics, Villiers-le-Bel, France) with a pumping tube of inside diameter 1.85 mm operating at a speed of 17 rpm. The pump was connected to a holding coil (HC) consisting of Tygon tubing with 0.76 mm i.d. wound around a perspex tube with an outside diameter (o.d.) of 10 mm.

The holding coil was connected to the first reaction coil (RC 1) via Tygon tubing with an i.d. of 0.76 mm wound around a perspex tube with o.d. 10 mm. RC 1 was connected to a 10 port electrically actuated selection valve (Model ECSD10P, Valco Instruments, Houston, TX, USA) using Tygon tubing with i.d. 0.76 mm. The second reaction coil (RC 2) connects the selection

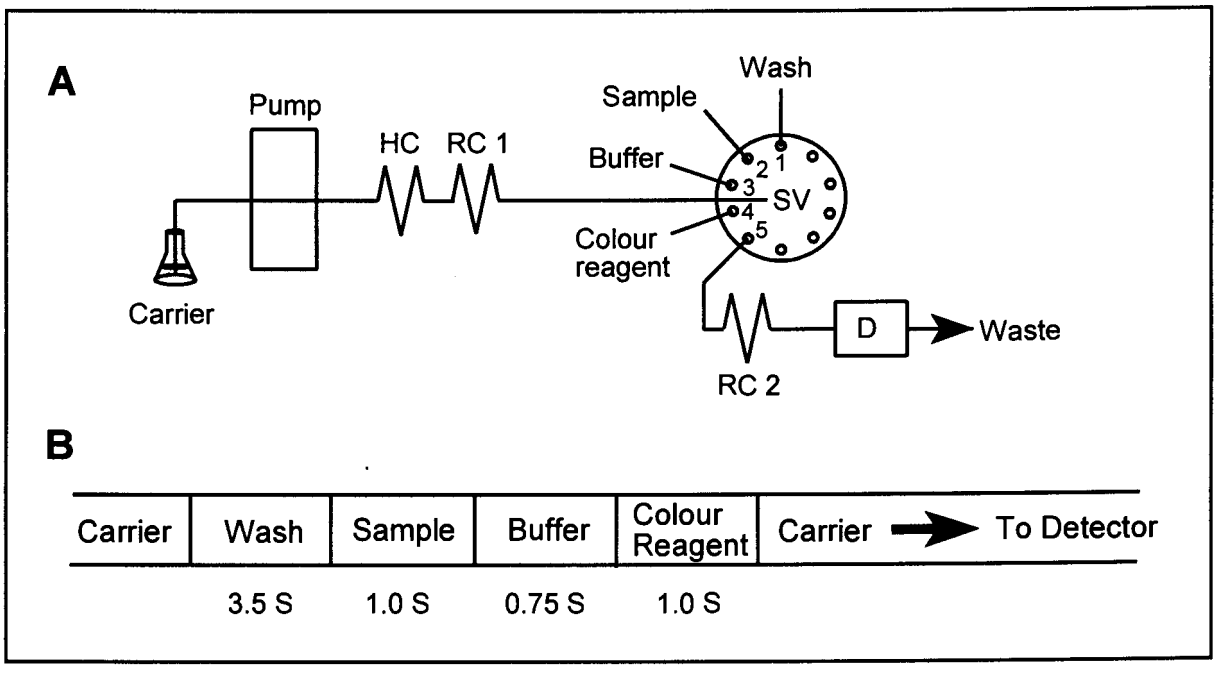

Fig. 4.1 A - Schematic diagram of the SIA manifold used in the determination of nitrite. B - Sequence of wash, sample, buffer and colour reagent as they are aspirated into the manifold

valve and the spectrophotometer via 0.76 mm i.d. Tygon tubing wound around a tube with o.d. 12.5 mm.

A Unicam 8625 UV-Visible spectrophotometer equipped with a Hellma type flow through cell (volume 80 $\mu\ell$) was used as detector and the absorbance was measured at 525 nm. Data acquisition and device control were achieved using a PC30-B interface board (Eagle Electric, Cape Town, South Africa) and an assembled distribution board (MINTEK, Randburg, South Africa). The FlowTEK [18] software package (MINTEK, Randburg, South Africa) for computer-aided flow-analysis was used throughout for device control and data acquisition.

4.6.1.3 Procedure

The device sequence for the determination of nitrite by sequential injection is given in Table 4.1. As seen from the sequential injection system depicted in Fig. 4.1 the cycle (wash, sample, buffer, chromogenic reagent, wash and flush to the detector) involved ports 1 to 6 of the selection valve.

The wash solution used had the same composition as the carrier solution and its purpose was that of preventing any carryover between the previous sample and the sample of the newly aspirated sequence.

Table 4.1 Device sequence for a full cycle of the sequential injection system.

Time (s)	Pump	Valve`	Description
0.00	Reverse	Wash	Draw up wash solution
3.50	Off		Pump stop
4.00		Sample	Valve selects sample solution
5.50	Reverse		Draw up sample solution
6.50	Off		Pump stop
6.75		Buffer	Valve selects buffer solution
8.25	Reverse		Draw up buffer solution
9.00	Off		Pump stop
10.00		Colour reagent	Valve selects colour reagent
13.50	Reverse		Draw up colour reagent
14.50	Off		Pump stop
16.00		Detector	Valve selects detector position
16.50	Forward		Pump stacked zones to detector
72.0	Off		Pump stop
72.5		Home	Return valve to starting position

4.7 Method optimisation

4.7.1 Physical parameters

The physical parameters were evaluated by comparing the sensitivity (degree of zone penetration) and precision (reproducibility of zone penetration) obtained for different parameter changes. The following physical parameters were optimised: pump speed (pump tube inside diameter, pump head rotation), holding coil (tube inside diameter, tube length and coil configuration), reaction

coil 1 (tube inside diameter, tube length and coil configuration) and reaction coil 2 (tube inside diameter, tube length and coil configuration). All the physical parameters were optimised with the actual reagents used in the determination of nitrite.

4.7.1.1 Pump speed

According to Valcárcel and Luque de Castro [19] the prerequisites for a propelling system are that the flow should be perfectly reproducible, pulse free, constant and it should deliver a constant flow. The peristaltic pump used in this experiment is not completely pulse free but, with pumping tube and flow rate optimised, the pulsations are small and reproducible enough, delivering a constant flow, provided that the pumping tube is in good condition.

The experimental conditions were of such a nature that standard Tygon tubing (Gradco, Manchester, England) could be used. Pumping tube inside diameter was optimised by choosing a constant pump head rotation, for example 10 rpm, and then varying the pump tube diameters. Pump tubes with inside diameters between 0.127 mm and 2.794 mm were evaluated. Table 4.2 contains the results obtained for the tube inside diameter optimisation and the results are graphicly depicted in Fig. 4.2. For Table 4.2 one peak height unit is equal to an absorbance of approximately 0.1.

Table 4.2 Influence of inside diameter on peak height and % RSD.

Tube diameter (mm)	Peak height	% RSD
1.14	5.18	0.85
1.30	5.90	1.03
1.52	6.31	0.70
1.65	6.79	0.93
1.85	7.15	0.43
2.06	7.97	1.10
2.29	8.06	0.80
2.54	8.61	1.30

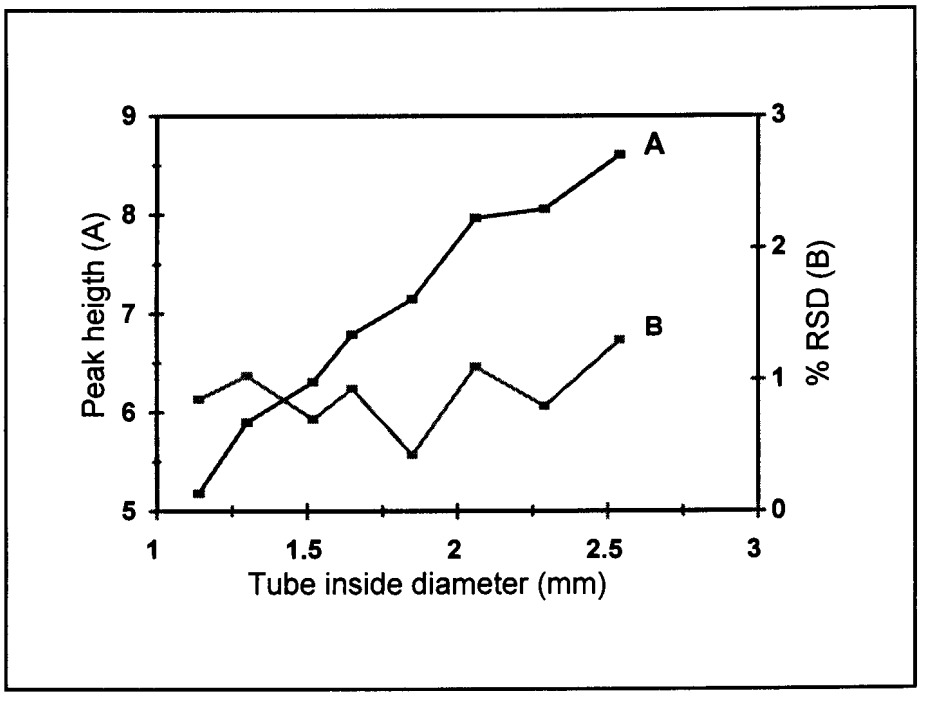

Fig. 4.2 Influence of inside diameter on peak height (A) and % RSD (B).

The flow rate was further optimised by keeping the optimum i.d. (1.85 mm) constant and changing the speed at which the pump head rotates (variable between 0 and 30 rpm). Table 4.3 shows the results obtained for the pump speed optimisation, and it is graphically depicted in Fig. 4.3.

Table 4.3 Influence of pump speed on peak height (sensitivity) and % RSD (precision)

Pump speed	Peak height	% RSD
10	5.867	1.04
11	5.987	1.10
12	6.123	0.71
13	6.219	2.12
14	6.343	0.52
15	6.543	1.25
16	6.674	1.45
17	6.898	0.96
18	7.142	1.23
19	7.297	1.14
20	7.403	1.35

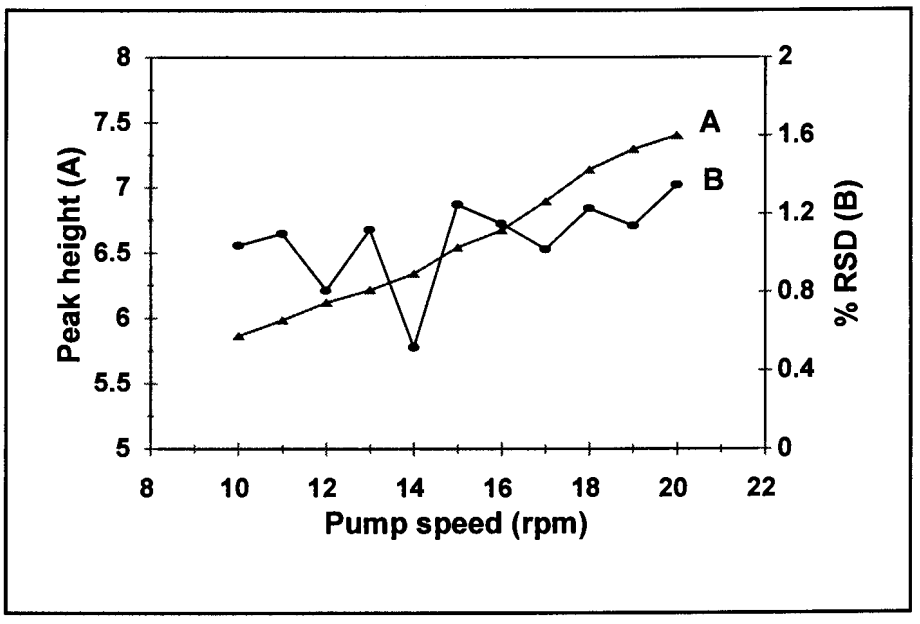

Fig. 4.3 Influence of pump speed (rpm) on sensitivity (peak height) and precision (% RSD).

Both Fig. 4.2 and Fig 4.3 show the expected upward trend of the peak height with an increase in the pump tube i.d. and pump speed. The best precision (0.52 %) was obtained with a tube inside diameter of 1.85 mm at a pump speed of 14 rpm. Vanderslice [19] related the flow rate, q, to the travel (t_a) and baseline-to-baseline times (Δt) through

$$t_a = \frac{k}{q^{0.125}} \qquad \textbf{(4)}$$

and

$$\Delta t = \frac{k'}{q^{0.64}} \qquad \textbf{(2)}$$

where k and k' are constants independent of the flow-rate [4].

According to these equations t_a, Δt and dispersion, should decrease with an increase in flow-rate. This trend is visible in Fig. 4.2 and Fig. 4.3 where the peak heights increase as the dispersion decrease with higher flow-rates. Fig. 4.4 shows the increase in the peak height (sensitivity) with a decrease in dispersion, confirming the trend described by Vanderslice.

UNIVERSITEIT VAN PRETORIA
UNIVERSITY OF PRETORIA
YUNIBESITHI YA PRETORIA

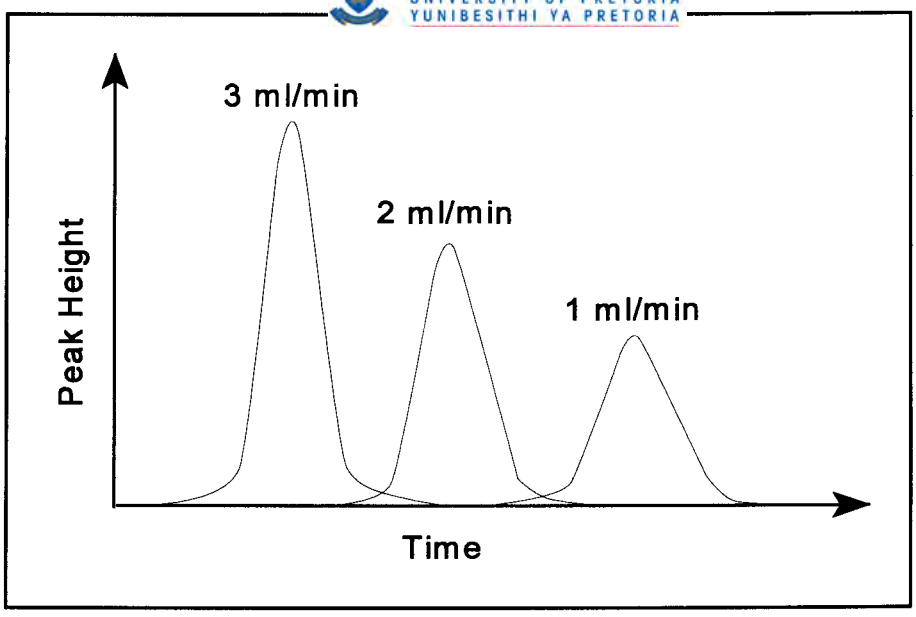

Fig. 4.4 Influence of an increase in the flow rate (mℓ/min) on the peak height and dispersion.

4.7.1.2 Holding coil

A holding coil is normally introduced between the peristaltic pump and the valve in a sequential injection system, to act as a buffer, or reservoir [20, 21] for the aspirated zones. This is necessary to prevent zone distortion of the sample and reagent zones when it enters the pump, resulting in high RSD values. When considering the holding coil's volume dispersion of the aspirated zones, as a result of the parabolic profiles of the zones, should also be taken into account. This dispersion can effectively double the volume occupied by the sample and reagent zones [22]. Three physical holding coil parameters have to be optimised *viz*: the tube diameter, tube length and the coil geometry.

4.7.1.2.1 Tube diameter

Tube diameters can influence results in two ways, firstly, too small tube diameters could cause high back pressure and therefore lower the precision, secondly, too large diameters increase the dead volume of the manifold and as a result the dispersion increase. Increasing the tube diameter should therefore have a positive influence on results up to a certain point.

In this particular case the tube diameters did not have an influential effect on the sensitivity and only a marginal effect on the precision (Fig. 4.5) although the expected trend was observed. It was found that a tube diameter of 0.76 mm gave the best precision (0.65 %) and this diameter was used in the optimisation of the other parameters.

Table 4.4 Effect of holding coil tube diameter on sensitivity (peak height) and precision (% RSD)

Tube diameter (mm)	Peak height	% RSD
0.64	3.08	0.86
0.76	3.12	0.65
0.89	3.20	0.78
1.02	3.15	0.95
1.14	3.11	0.94
1.60	3.12	0.97

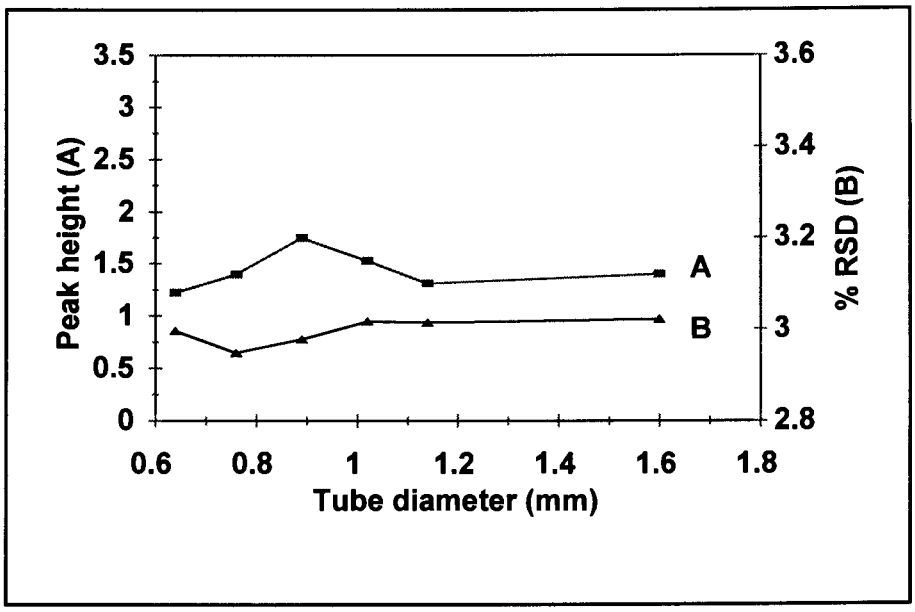

Fig. 4.5 Effect of holding coil diameter on sensitivity (peak height) and precision (% RSD)

4.7.1.2.2 Holding coil length

The holding coil length was optimised employing the optimum tube diameter (0.76 mm) arrived at in the previous section (Sec. 4.7.1.2.1). The total volume of the stacked zones was 0.50 mℓ (calculated by using the flow rate and aspiration times), which required a holding coil length of at least 0.50 mℓ in volume (246 cm) without taking dispersion into consideration, but the manifold in Fig 4.1 employed a 120 cm x 0.076 cm (0.272 mℓ) reaction coil between the peristaltic pump and the sequential valve, and therefore the holding coil had to be longer than 100 cm (454 mℓ). Table 4.5 shows the results obtained for the optimisation of the holding coil length with the results graphically depicted in Fig. 4.6.

Table 4.5 Influence of holding coil length on peak height and % RSD.

Coil length (cm)	Volume (mℓ)	Peak height	% RSD
100	0.454	2.88	2.23
120	0.544	3.76	1.24
140	0.635	3.95	0.92
160	0.726	2.86	2.38

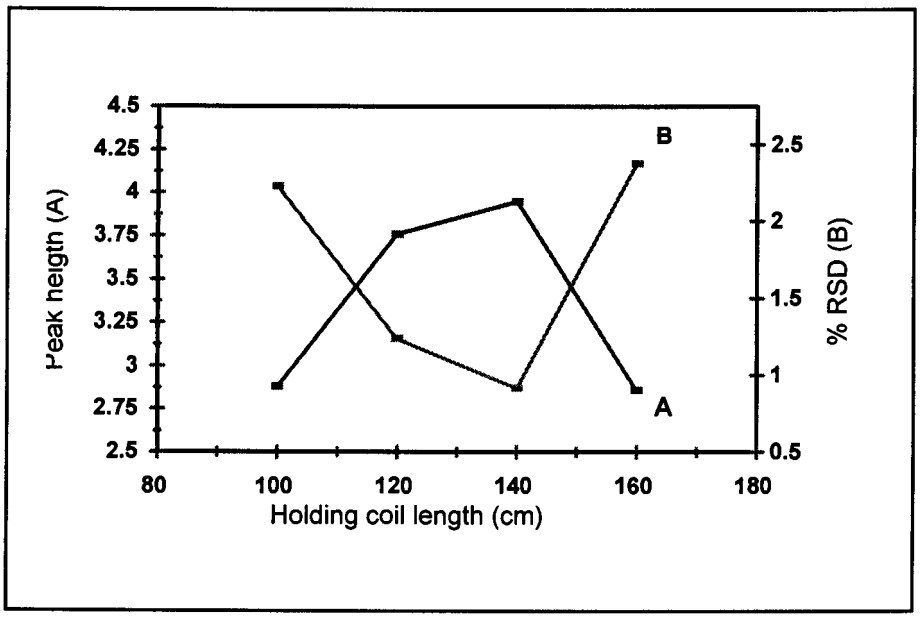

Fig. 4.6 Influence of holding coil length (cm) on peak height (A) and % RSD (B).

According to Fig. 4.6 an increase in holding coil length improved the precision and sensitivity while a coil length of 160 cm had a negative influence on these parameters. The best results (peak height = 3.95, %RSD = 0.92 %) were obtained with a coil length of 140 cm. The poor precision value of the 100 cm coil (2.23 %) is an indication that the sample zone may have entered the peristaltic pump resulting in sample zone distortion.

4.7.1.2.3 Holding coil geometry

Mainly three geometries, normally used in flow and sequential injection, were evaluated during the optimisation of the coil geometry, namely straight, coiled and knitted reactors. For the straight coil, the 140 cm tube was kept as straight as possible. In the second case the tube was tightly wound around a perspex cylinder with a 10 mm outside diameter while for the knitted coil the tube was tightly knitted in such a way that the tube changed direction constantly.

Not one of the holding coil geometries out-performed the others in any way, but since compactness of the analytical system does play a role in the industry, a coiled tube was decided upon.

4.7.1.3 Reaction coil 1

The main reason for the inclusion of the first reaction coil (Fig. 4.1) in a SI setup is that it is supposed to influence the penetration of the different injected zones in a positive or a negative way, depending on the requirements of the reaction. For the determination of nitrite, three zones had to penetrate each other, *viz.* sample, buffer and colour reagents, with dispersion values between D = 2 and D = 10. The reaction coil (RC 1) should be designed in such a way that it holds the entire reagent zone and the non-cross-contaminated sample zone [21]. The degree of penetration between the sample and reaction zones depend on the tube diameter, coil length and the geometry of the coil and all three of these parameters have to be optimised

4.7.1.3.1 Tube diameter

Tube inside diameters between 0.38 and 1.02 mm were evaluated (Table 4.6, Fig 4.7). According to Marshall [21] a larger reaction coil tube diameter should lead to a lower penetration and a lower response. The sensitivity of the manifold, initially improved with an increase in the tube diameter and then decreased as was expected. Since the presision increased (% RSD decreased) at first, it is possible to conclude that other secondary factors also played a role in increasing the sensitivity of the manifold.

Table 4.6 Influence of tube diameter on peak height and % RSD.

Tube diameter(mm)	**0.38**	**0.51**	**0.64**	**0.76**	**1.02**
Peak height	3.15	3.24	3.53	3.51	3.49
% RSD	3.53	2.84	1.61	1.10	1.66

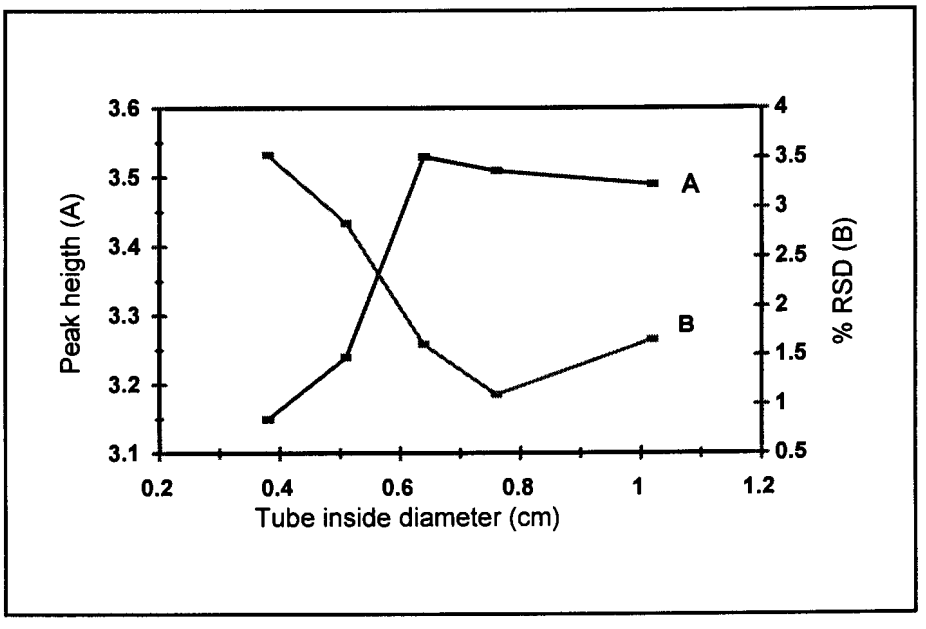

Fig. 4.7 Influence of RC 1 tube diameter on peak height (A) and % RSD (B).

4.7.1.3.2 Coil length

Coil lengths shorter and also longer than the required length (120 cm) were evaluated. Coil lengths were varied between 50 and 150 cm to observe the influence on the zone penetration. The results obtained are shown in Table 4.7 and graphically depicted in Fig. 4.8. The coil length had little influence (2.4 % difference between the highest and lowest values) on the penetration of the zones.

A far more important factor was the coil lengths influence on the % RSD, which decreased and then increased again as the coil was lengthened. In the case of the 50 cm coil the high % RSD value obtained was caused by sample entering the pump through the holding coil causing zone distortion. The best precision (1.01 %) was obtained with a coil length of 120 cm, which could hold the entire reacting zone. With coil lengths longer than 120 cm, an increase in the % RSD values were obtained with a negative effect on the peak height.

Table 4.7 Influence of coil length on peak height and % RSD.

Length (cm)	**50**	**70**	**90**	**110**	**120**	**130**	**150**
Peak height	4.17	4.14	4.14	4.12	4.13	4.11	4.07
% RSD	2.80	1.50	1.49	1.25	1.01	1.57	1.37

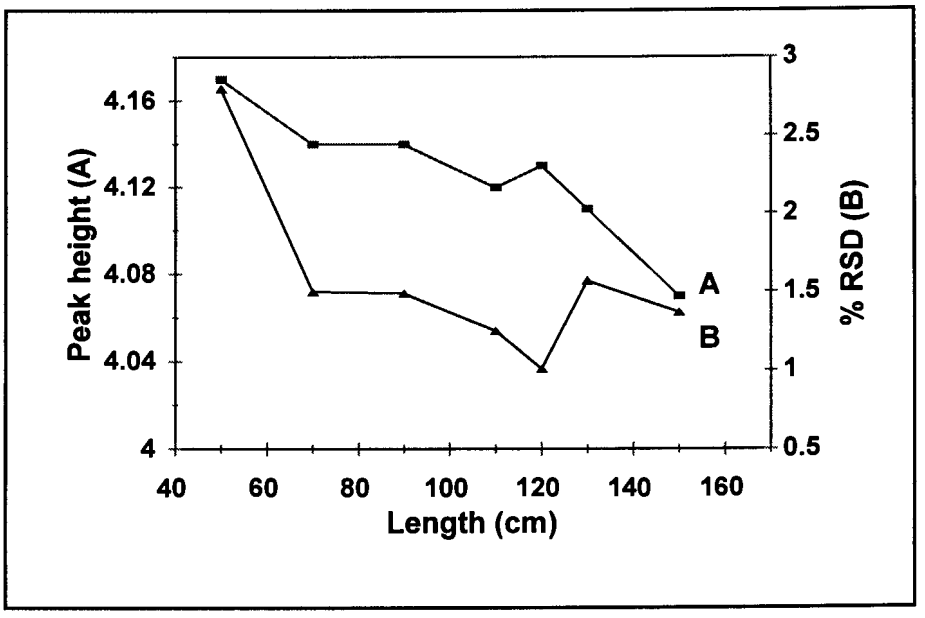

Fig. 4.8 Influence of RC 1 tube length on peak height (A) and % RSD (B).

4.7.1.3.3 Coil geometry

Coil geometry influences the penetration of the different zones as a result of the change in axial dispersion. Three geometries were tested, namely straight, coiled and knitted. Table 4.8 shows the results obtained.

Table 4.8 Influence of coil geometry on peak height and % RSD

Geometry	Straight	Coiled	Knitted
Peak height	3.35	3.53	4.01
% RSD	0.97	0.58	1.66

With coiled and knitted reactors, axial dispersion is decreased resulting in narrower peaks and an increase in sensitivity. Although straight coils should have given the best sensitivity, it was found that enough zone penetration could take place within the coiled and knitted reactors with the added advantage of the peaks being narrower. Narrow peaks also led to better sensitivity for the coiled and knitted reactors with the best sensitivity achieved with the knitted reactor.

The best precision (0.58 %) was obtained with the coiled reactor, while the knitted reactor's precision decreased by more than 180 %. The coiled reactor was chosen as the optimum configuration and was subsequently used in the rest of the optimisations.

4.7.1.4 Reaction coil 2

The second reaction coil connects the valve with the detector and the reacted zones normally flow non-stop through this reactor on its way to the detector. The effective length of this reactor is measured from the selector valve outlet to the point of detection in the flow cell. The length of the coil, the tube diameter and the geometry of the coil was optimised.

4.7.1.4.1 Tube diameter

Tube diameter had an important effect on both the sensitivity and precision. According to Fig. 4.9 and Table 4.9 the sensitivity decreased with an increase in the tube diameter, as a result of an increase in dispersion. The precision increased (% RSD decreased) for diameters up to

0.76 mm and decreased again thereafter. Both the 0.64 and 0.76 mm inside diameters coils produced good results, but the 0.76 mm diameter was chosen, for it is also used in the holding and first reaction coils, simplifying the manifold slightly.

Table 4.9 Influence of coil diameter on peak height and % RSD of RC 2.

Inside diameter (mm)	0.38	0.51	0.64	0.76	1.01
Peak height	5.96	5.19	5.01	4.88	4.53
% RSD	2.57	2.03	1.60	1.58	1.86

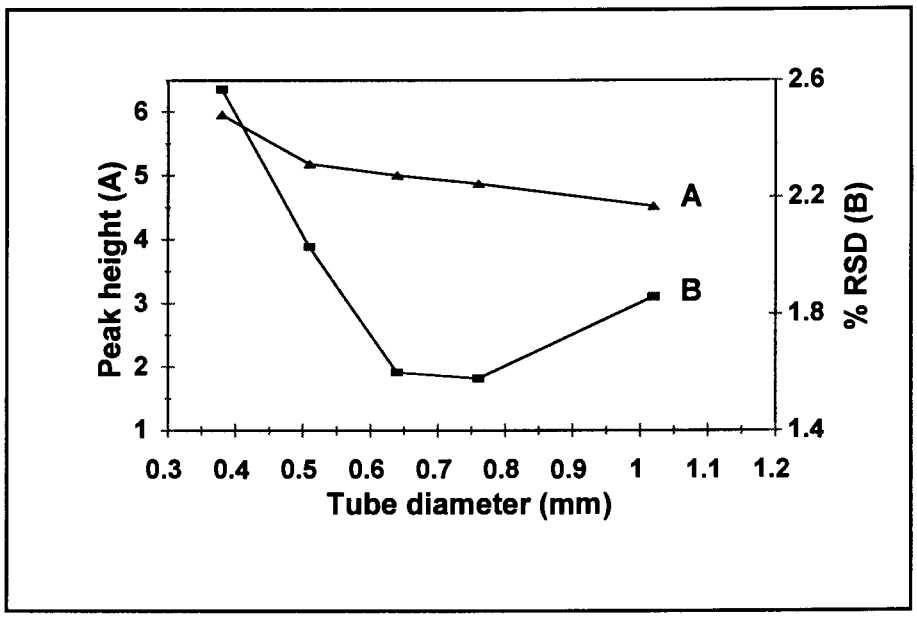

Fig. 4.9 Influence of RC 2 tube diameter on peak height, and % RSD.

4.7.1.4.2 Coil length

Longer coil lengths cause more dispersed product zones. In this proposed method the reaction between the colour reagent and nitrite is almost immediate and by the time the product zone enters the second reaction coil, the reaction is complete. At this point, the dispersion has to be prevented in order to increase the sensitivity of the method. An effective way of doing this is to shorten RC 2 to an acceptable length. RC 2's length was varied between 29 and 37 cm. The expected trend mentioned earlier is observed in Table 4.10 and Fig. 4.10

Table 4.10 Influence of RC 2's length on peak height and % RSD.

Length (cm)	29	31	33	35	37
Peak height	5.36	5.15	4.98	4.74	4.56
% RSD	1.98	1.89	1.49	0.52	1.58

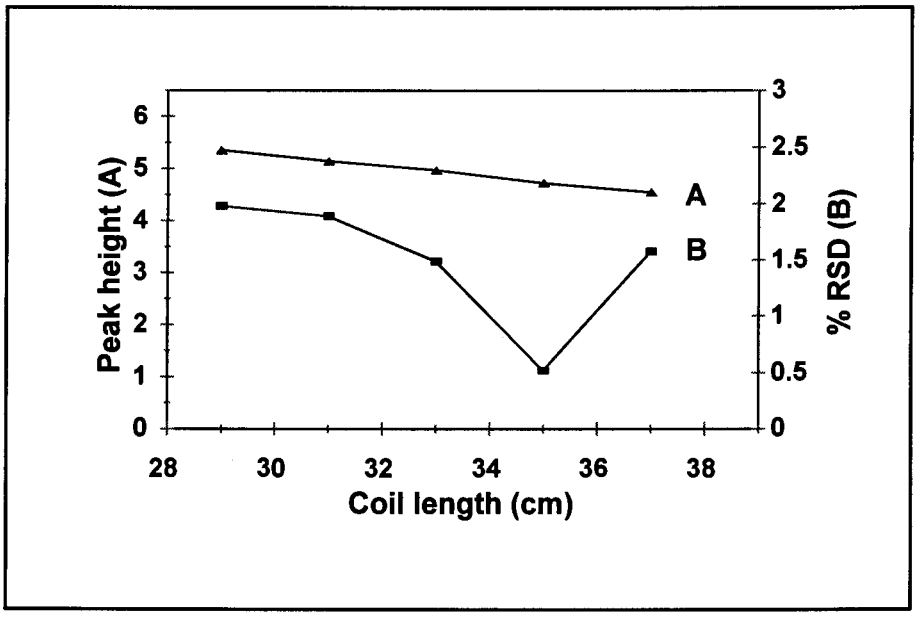

Fig. 4.10 Influence of RC 2's length on peak height (A) and % RSD (B).

4.7.1.4.3 Coil geometry

With the second reaction coil, the coil geometry plays an important role in limiting the dispersion of the zones that took place within RC 1. A study of the three possible geometries (straight, coiled, knitted) revealed that the geometry had only limited influence within this specific setup. A coiled second reaction coil was therefore used for the rest of the optimisation to limit any dispersion that could occur in this reactor.

4.7.1.5 Up-take tubes

Up-take tubes must be as large as possible in order to minimize back-pressure. When too small diameter up-take tubes are used, a low pressure system develops between the pump and the valve. When the valve moves to the next port, before this low pressure system is corrected, a small amount of the next solution in the sequence will be aspirated due to the low pressure, leading to volumes that may differ from the theoretical values. Large diameter tubing prevent this low pressure system from developing. For the setup in Fig. 4.1 up-take tubes with diameters of 1.01 mm were used without developing any problems.

4.7.1.6 Order of injection

The order of injection of a manifold is determined by its application. For the determination of nitrite, buffering of the colour reagent and sample was necessary in order to keep the pH levels within the limits. The sample was introduced first and the reagent third, with the buffer sandwiched between these two zones. An alternative order for this type of reaction, suggested

by Marshall [21], is to include the buffer in the wash solution, sandwiching the reagent and sample between two buffer zones. Both these orders worked equally well, but the former order simplified the procedure by reducing the number of steps (Table 4.1) necessary.

4.7.2 Chemical parameters

The Shinn reaction is very sensitive to variations in the pH as well as sulphanilamide and N-(1- naphthyl)ethylenediamine (N1NED) concentrations. The volumes of the different zones aspirated influence the pH indirectly by changing physical parameters, for example the amount of dispersion that is taking place. The concentration and volume of each solution aspirated should, therefore, be carefully optimised in order to determine the ideal conditions for the Shinn reaction to take place.

4.7.2.1 Carrier stream

Two solutions were evaluated for use as the carrier stream, namely, deionised water and an ammonium chloride solution. With deionised water, as well as solutions containing low ammonium chloride concentrations, the precision obtained was poor with RSD values ranging between 1 and 3 %. As the ammonium chloride concentration in the carrier stream was increased, the sensitivity improved slightly and the precision improved remarkably to RSD values below 1 %. An optimum concentration of 10 $g.\ell^{-1}$ ammonium chloride was chosen for the proposed SIA system. To this solution, 1 $g.\ell^{-1}$ EDTA was added to prevent other ions from interfering with the signal obtained for nitrite. Larger amounts of EDTA suppressed the signal obtained for nitrite and is thus not recommended (Table 4.11, Fig. 4.11).

Table 4.11 Influence of the ammonium chloride concentration on the peak height and % RSD.

NH_4Cl	0	2	5	8	10	20	30
Peak height	4.05	4.22	4.28	4.36	4.46	3.65	3.52
% RSD	2.24	0.83	0.42	0.73	0.67	0.46	1.46

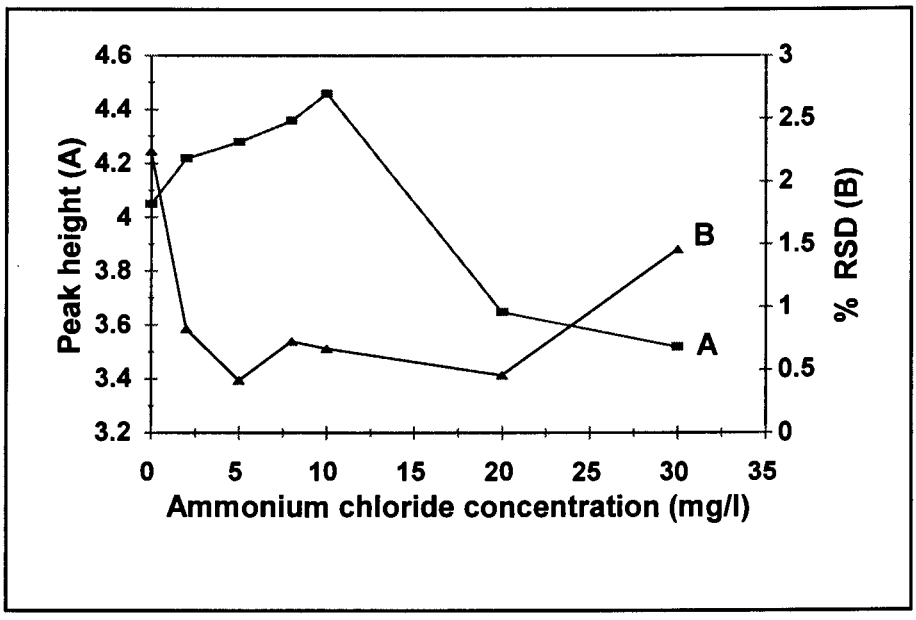

Fig. 4.11 Influence of ammonium chloride concentration on peak height (A) and % RSD (B).

4.7.2.2 Chromogenic reagent

Different concentrations of sulphanilamide and N1NED were evaluated in order to obtain the best reaction conditions for the SIA system. N1NED concentrations between 0.5 and 2 $g.\ell^{-1}$ (Table 4.12, Fig. 4.12) and sulphanilamide concentrations between 10 and 40 $g.\ell^{-1}$ [5, 11, 13, 17, 23, 24] were evaluated (Table 4.12, Fig. 4.13). The best sensitivity was obtained with 2 $g.\ell^{-1}$ N1NED and 40 $g.\ell^{-1}$ sulphanilamide.

Table 4.12 Influence of N1NED concentration on peak height and % RSD

N1NED (mg.ℓ^{-1})	0.5	1.0	1.5	2.0	2.5	3.0
Peak height	2.10	2.23	2.36	2.41	2.43	2.44
% RSD	1.47	1.25	1.13	1.05	1.13	1.07
Sulphanilamide (mg.ℓ^{-1})	**10**	**20**	**30**	**40**	**50**	**60**
Peak height	1.56	1.78	1.91	2.14	2.19	2.17
% RSD	1.31	1.24	1.13	0.96	1.23	1.19

Different dilutions of the optimum solution were evaluated to determine its influence on the calibration curve. The chromogenic reagent was diluted with water to the following ratios; 1:2 (pH = 2.2), 1:1 (pH = 2) and undiluted. The more diluted solutions worked well with the samples containing low nitrite concentrations. With the more concentrated solutions (> 4 mg.ℓ^{-1}) the calibrations tend to flatten and an undiluted chromogenic reagent was preferred for those solutions. This should be kept in mind when consumption of expensive reagents play a role in process analysers.

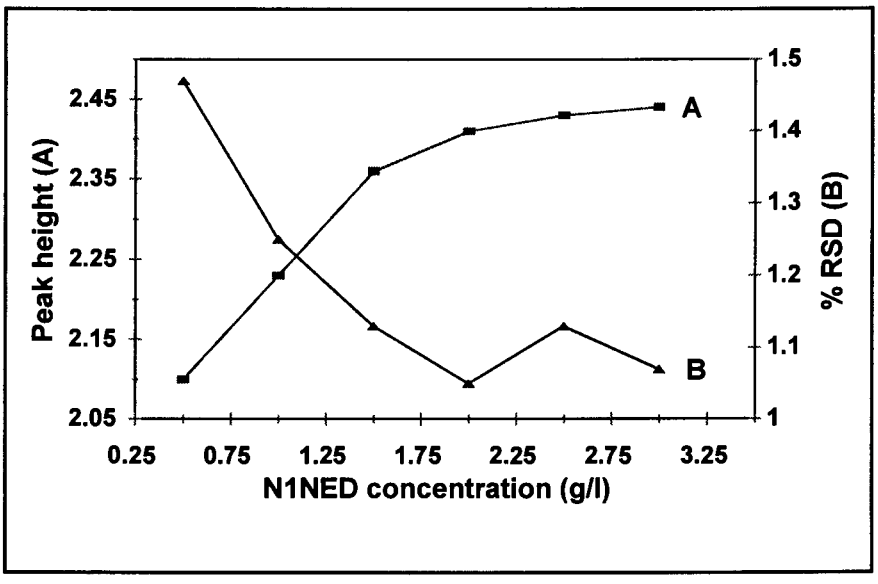

Fig. 4.12 Influence of the N1NED concentration on peak height(A) and % RSD (B).

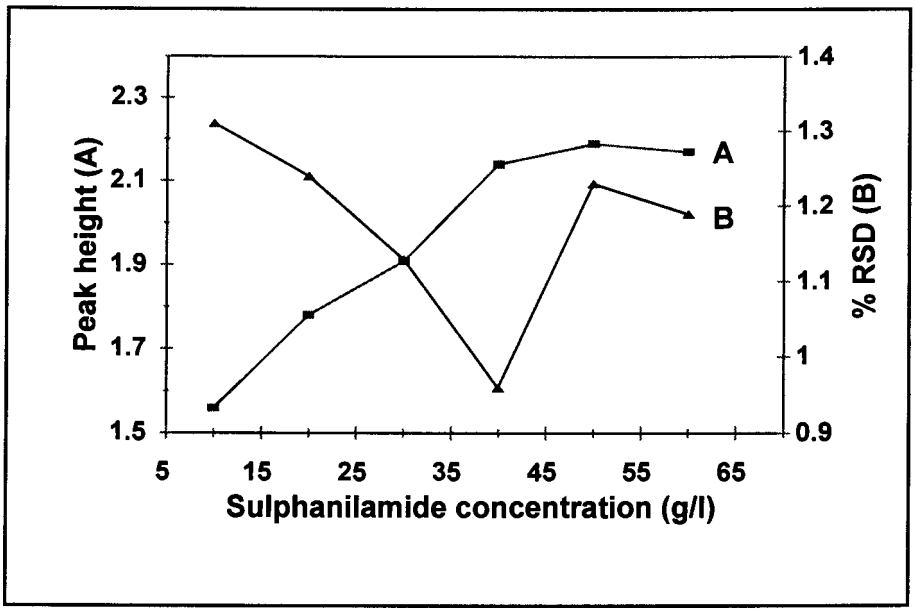

Fig. 4.13 Influence of sulphanilamide concentration variation on peak height (A) and % RSD (B)

4.7.2.3 Buffer solution

The pH of the buffer solution plays a very important role in the modified version of the Shinn [10] reaction. The pH values between pH 5.4 and pH 10.2 were evaluated. The sensitivity as well as the precision deteriorated at low as well as high pH values. The best results were obtained with a buffer solution at pH 6.6 giving a RSD value of 0.84 % (Table 4.13).

Table 4.13 Influence of buffer pH on peak height and % RSD.

pH	5.4	6.6	7.8	9.0	10.2
Peak height	1.98	2.31	2.10	1.86	1.74
% RSD	1.02	0.84	1.13	1.43	1.32

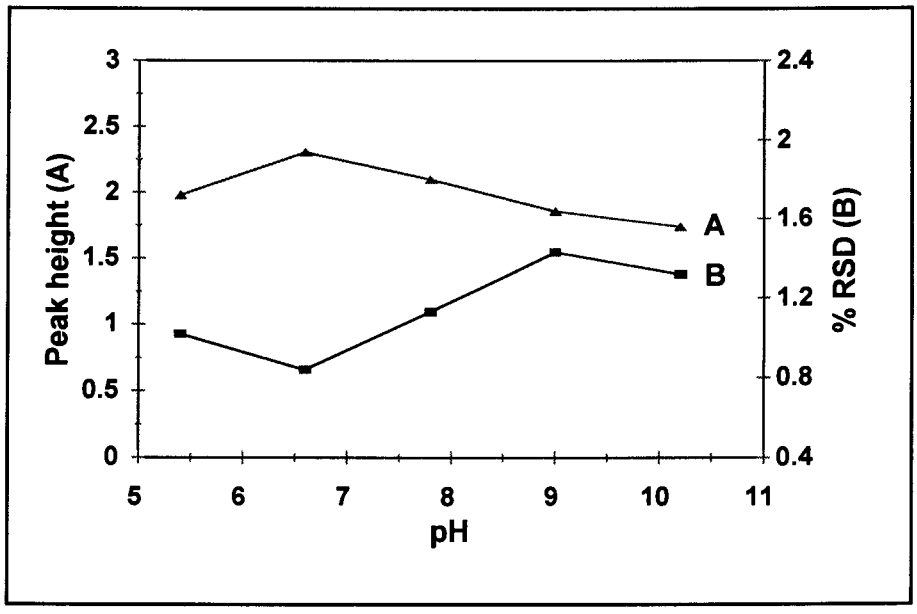

Fig. 4.14 Influence of the pH on peak height (A) and % RSD (B).

4.8 Evaluation of method

4.8.1 Linearity

The linearity of the SIA system was evaluated under the optimum operating conditions. The relationship for the relative peak height versus nitrite concentration was:

$$y = 1.353x - 0.032 \; ; \; r = 0.996$$

where y = relative peak height and x = nitrite concentration in $mg.\ell^{-1}$. The calibration graph is linear for nitrite concentrations between 0 and 5 $mg.\ell^{-1}$ and levels off at higher concentrations

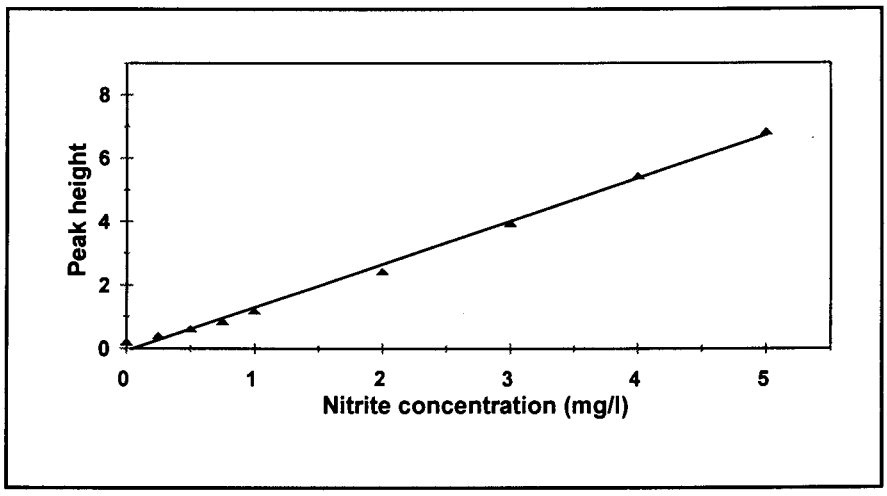

Fig. 4.15 Graph obtained for nitrite concentrations between 0 and 5 mg.ℓ^{-1}.

4.8.2 Accuracy

Real samples were analysed with the proposed SIA system to determine its accuracy. The accuracy of the SIA analyser was determined by comparing results obtained with the proposed SIA system, with that obtained with a standard procedure [25]. The results given in Table 4.14 revealed good correlation between the two methods. Values obtained for the water samples compare well with those obtained with the standard procedure, while the value obtained for the fertilizer sample is slightly higher than that of the standard procedure.

Table 4.14 Comparison of results obtained with the proposed SIA method and a standard method.

Sample	SIA method (mg.ℓ^{-1} nitrite)	Standard method (mg.ℓ^{-1} nitrite)
Boiler-feed water	0.20	0.21
Dam water	0.22	0.25
Waste water	0.24	0.25
Effluent	0.32	0.32
Liquid fertilizer	1.11	1.04

4.8.3 Precision

The precision of the optimised method was determined by 10 repetitive analyses of a number of standard nitrite solutions and samples as indicated in Table 4.15. In all cases the RSD was below 2.6 % with a best value of 0.9 %.

4.8.4 Detection limit

The detection limit of the proposed method was determined via the following formula:

$$Detection\ limit = \frac{(3\sigma+K)(K-c)}{m} \qquad (3)$$

where σ is the relative standard deviation (4.06) of the baseline, K is the average signal value of the baseline (0.220) and c (-0.03) and m (1.353) are the intercept and slope of the calibration curve respectively. The detection limit was calculated as 0.18 mg.ℓ^{-1}.

Table 4.15 Precision of the proposed SIA system.

Sample/Standard Concentration (mg/ℓ)	% RSD
0.25	2.63
0.50	1.66
0.75	0.90
1.00	1.01
2.00	1.20
3.00	1.20
4.00	2.47
5.00	2.48
Boiler feed water	2.13
Tap water	1.79
Waste water	1.83
Dam water	2.00
Liquid fertilizer	1.52

4.8.5 Interferences

As the proposed systems will be mainly employed as a process analyser in the fertilizer industry, it is very important that the ions present in fertilizers do not interfere with the signals obtained for nitrite. The following ions did not interfere at the concentrations mentioned: Cu(II) 75 $mg.\ell^{-1}$, Mg(II) 100 $mg.\ell^{-1}$, Ca 1000 $mg.\ell^{-1}$, Zn 1500 $mg.\ell^{-1}$, SO_4^{2-} 1000 $mg.\ell^{-1}$. The other ions in fertilizers are mainly micronutrients with low concentrations (below 1 $mg.\ell^{-1}$), which will not affect nitrite determination significantly.

4.8.6 Sample frequency

For a method to be industrially viable it must have a reasonable sample frequency. The total time needed for the completion of one cycle, of the proposed method, is 72.5 seconds, giving the proposed SIA system a sample frequency of 49 samples per hour.

4.9 Conclusion

Sequential injection makes direct online analysis of nitrite in water, as well as liquid fertilizer streams, possible. The proposed method is a simple, inexpensive and reliable method for nitrite analysis. The proposed method also has the added advantages of being sensitive and fast, making it ideal for routine analysis situations in the industry. The method does not suffer severe influences by ions normally present in liquid fertilizers making it a possible alternative to existing methods.

The influence of different physical and chemical parameters were evaluated in order to obtain a sensitive nitrite analyser. The sensitivity of the method improved with an increase in the flow rate while other parameters such as the holding coil diameter and geometry didn't improve the sensitivity a lot. The holding coils volume is an important factor in limiting the distortion of aspirated zones.

One of the most important parameters that were evaluated is the parameters of RC 1. For RC 1, shorter coil lengths and smaller inside diameters improved the sensitivity. RC 2 on the other hand limits the dispersion that normally takes place between the selection valve and the detector.

The Shinn reaction proved to be largely dependant on the concentration of the reagents as well as the pH of the buffer used. Optimum results were obtained with concentrations of 40 $g.\ell^{-1}$ of sulphanilamide and 2,0 $g.\ell^{-1}$ N1NED. A buffer solution at pH 6.6 kept the pH levels of the reactions within the limits.

4.10 References

1. M. Yacoob, M. A. Siddiqui, M. Masoom, **J. Ind. Chem. Soc.**, **69** (1992) 32.
2. T. M. Addiscott, A. P. Whitmore and D. S. Powlson, **Farming, Fertilizers and the Nitrate Problem**, C.A.B. International, 1991.
3. R. J. Haynes, **Mineral Nitrogen in the Plant-soil System**, Academic Press, Inc. , 1986.
4. T. Pérez-Ruiz, C. Martinez-Lozano and V. Tomás, **Anal. Chim. Act.**, **265** (1992) 103.
5. A. G. Fogg, A. Y. Chamsi and M. A. Abdalla, **Analyst, 108** (1983) 464.
6. J. Slanina, F. Bakker, A. G. Bruijn-Hes and J. J. Möls, **Fresenius'Z. Anal. Chem.**, **289** (1978) 38.
7. E. H. Hansen, A. K. Ghose and J. Ruzicka, **Analyst, 102** (1977) 705.
8. S. Sunita and V. K. Gupta, **Int. J. Environ. Anal. Chem.**, **19** (1984) 11.
9. B. A. Bashir and S. Flamerz, **Talanta, 28** (1981) 697.
10. M. B. Shinn, **Ind. Eng. Chem. Anal. Ed.**, **13** (1941) 33.
11. M. F. Giné, H. F. Bergamin, E. A. G. Zagatto and B. F. Reis, **Anal. Chim. Acta.**, **114** (1980) 191.
12. E. A. G Zagatto, A. O. Jacintho, J. Mortatti and H. F. Bergamin, **Anal. Chim. Act.**, **120** (1980) 399.
13. L. Anderson, **Anal. Chim. Acta, 110** (1980) 123.
14. A. C. Bratton, E. K. Marshall, D. Babbitt and A. R. Hendrickson, **J. Biol. Chem.**, **128** (1939) 537.
15. H. Wattenberg, **Cons. Int. Explor. Mer. Rapp. Et Proc. -Verb., 103** (1937) 1.
16. D. F. Boltz and J. A. Howell, **Colorimetric determination of non-metals**, John Wiley & Sons, 1978, 237 - 238.

17. J. F. Van Staden and M. A. Makhafola, **Fresenius J. Anal. Chem.**, **354** (1996) 251..

18. G. D. Marshall and J. F. van Staden, **Analytical Instrumentation**, **261** (1992) 11.

19. M. Varcarcél and M. D. Luque de Castro, **Flow Injection Analysis: Principles and Applications**., Horwood, Chichester, 1987.

20. J. Ruzicka and G. D. Marshall, **Anal. Chim. Acta.**, **237** (1990) 329.

21. G. D. Marshall, **Sequential Injection Analysis**, PhD Thesis, University of Pretoria, 1994.

22. J. Ruzicka and T. Gübeli, **Anal. Chem.**, **63** (1991) 1680.

23. J. R. Clinch and P. J. Worsfold, **Anal. Chim. Acta.**, **200** (1987) 523.

24. M. T. Oms, A. Cerdá and V. Cerdá, **Anal. Chim. Acta.**, **321** (1995) 330.

25. **Standard methods for Examination of Water and Waste Water**, 14th Edition, American Public Health Association, Washington, DC, 1976.

CHAPTER 5

Determination of Nitrate in Water, Water Effluents, and Fertilizers by Reduction with Copperized-Cadmium and Sequential Injection Analysis

5.1 Introduction

Adequate food and clean water are regarded as basic human rights. People in industrialised societies, however, have grown used to more than just the basics. Food has become plentiful and cheap, while our taps yield unlimited supplies of clean water suitable for drinking and cooking. Both have become expectations where 45 years ago they were no more than hopes for the future in countries stricken by war and famine. These expectations are beginning to conflict [1].

The root of this conflict lies in the particular properties of a very common place, naturally-occurring chemical entity called nitrate [2]. Nitrate is essential to life, but a nuisance and possibly a hazard in the wrong place at the wrong time. The same is true of water. Nitrate easily dissolves in water and is found in most natural water: in rain, in rivers, in dams and importantly in underground water. Tap water in South Africa may come from any of these sources.

In the past 30 years the nitrate content in these natural waters increased noticeably. This increase has coincided with increasing use of nitrogen fertilizer by farmers. Another very important

reason for the interest in nitrate is that the European Community has recently imposed a limit of 11.3 mg.ℓ^{-1} nitrate-nitrogen.

This increase in nitrate is due to only one reason namely population growth. World population increased from 3.0 billion in 1960 to 5.3 billion in 1990. The world added more people during the 1960-1990 period than it did during the first 60 years of this century or the whole of the last century. Currently, the world is adding about 97 million people - equivalent to the 1995 population of Central America - every year. More than 90 % of these additional people are added to developing countries where an estimated 1 billion people already live under conditions of poverty, hunger and malnutrition [3].

This population increase creates unprecedented pressures on the natural resource base to produce additional food, fibre and raw materials. In the past, these requirements were met mainly through technological innovations, institutional and infra structural developments that promoted growth in agricultural productivity. These technologies involved mainly the use of high yield plant varieties that required large amounts of fertilizers.

The use of fertilizer ($N + P_2O_5 + K_2O$) increased over fivefold, from 27.4 million tons in 1959/60 to 145.6 million tons in 1988/89 Fig. 5.1 [3]. While significant growth was experienced by both developed and developing countries, it was mainly the developing countries that realized higher growth; their fertilizer use increased 20-fold, from 2.7 million tons in 1960 to 61.5 million tons in 1988/89 [3].

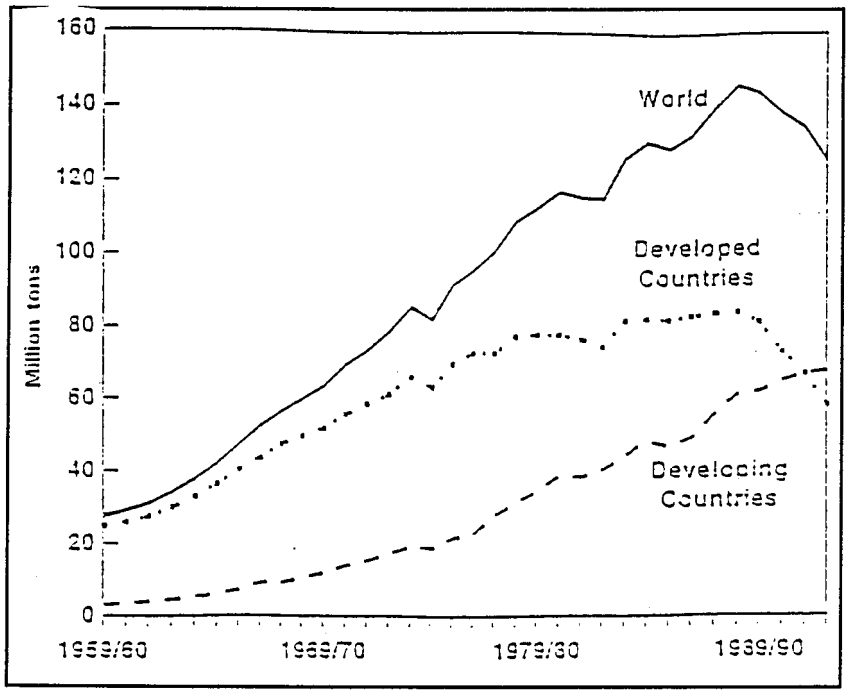

Fig 5.1 World fertilizer use, 1959/1960 to 1992/1993

To measure nitrate in fertilizers and to monitor its buildup in natural water, as a result of the increased use of fertilizers, a sensitive analytical method had to be developed. This method had to be sensitive and also versatile enough to measure both low nitrate levels in natural water, and high levels of nitrate in liquid fertilizers. Other prerequisites of the method was that it should be economical, not sensitive to changes in environment (e.g. temperature), and automated.

5.2 Uses of nitrate

Nitrate is essential for plants to grow, therefore, it is not strange to find nitrates biggest application in the agricultural industry or to be more specific, the fertilizer industry. It helps the farmer grow better crops with higher yields per unit area, resulting in higher income for the farmer. Some of the nitrates commonly used in the fertilizer industry are ammonium nitrate,

calcium nitrate, sodium nitrate and potassium nitrate.

Nitrate is also part of all the constituents of the cell: the chlorophyll that is essential for photosynthesis, the nucleic acids, DNA and RNA in which the pattern of the plant's growth and development are encoded, the proteins which include the enzymes which catalyse all chemical reactions and processes, and the walls that hold the cell together [2].

Another important application of nitrate is in the medical field. Sodium nitrate and ammonium nitrate are used to treat phosphatic kidney stones. Doses of up to 9 $g.day^{-1}$ have been used for this purpose without any adverse effect [2]. Last, but not least, is the use of nitrates, in various forms, in the explosives industry. Ammonium nitrate, for instance, is a material that needs to be treated with respect, mixed with aluminium powder it becomes 'Ammonal' one of the more powerful explosives used in the Second World War. Only mixed with a stabilizer is ammonium nitrate safe for use as a fertilizer.

5.3 Properties

Nitrate is not toxic to humans. It becomes a problem only when it is reduced, in various ways, to nitrite. This reduced form of nitrate is hazardous and an excess could lead to such illnesses as "blue baby" syndrome and stomach cancer. These ailments are described in detail in Chapter 4 (Sec. 4.1).

Nitrate easily dissolves in water. One example of nitrate's solubility is calcium nitrate. One kilogram of this salt can dissolve in a litre of water. This property is both positive and negative when it comes to fertilizers. On the positive side, nitrate salts dissolve in a small amount of water making nitrate quickly available to plants through the roots. On the negative side, nitrate ions leach from the soil easily, making less nitrogen available to the plants. The soil has no mechanism for retaining the nitrate ion under very wet conditions.

One way of coping with this drawback is the use of depot fertilizers [4]. Depot fertilizers are particularly slow-acting nitrogen fertilizers. They are synthesized by incorporating nitrogen into compounds that are particularly difficult to decompose. The nitrogen is then located in long chain or ring compounds. These fertilizers can then be used to supply nitrogen through leaching over longer periods.

5.4 Choice of analytical method

Nitrate was previously determined by methods based on the nitration of chromotropic acid [5], phenoldisulphonic acid [6], 2,6-xylenol [7] and 3,4-xylenol [8] or the oxidation by nitrate of brucine[9], diphenylamine [10] and strychnine [11]. These methods, however, produce unsatisfactory results as the nitrate is reduced by the organic material under acidic conditions [12].

Reduction of nitrate to nitrite, and the determination thereof, is an alternative to these direct methods. Numerous reducing agents are used for the reduction of nitrate namely copper [13], hydrazine [14], aluminium-nickel [15] and zinc [16], but, with these methods it is difficult to

ensure complete reduction of nitrate and preventing reduction of nitrite. The use of cadmium and copperized-cadmium reduction achieves a reliable quantitative reduction of nitrate to nitrite in an alkaline medium. This reduction method has been successfully employed by a number of authors [17, 18, 19] and was chosen as the most convenient method for the determination of nitrate.

The colorimetric reaction used with the reducing agent is a modified version [20, 21, 22] of the Shinn [23] reaction based on the well-known Griess reaction. It is the same method utilized in the direct determination of nitrite in Chapter 4 (Sec. 4.7.1.1). This is the reaction of nitrite with a primary aromatic amine to form a diazonium salt. The diazonium salt couples with a second aromatic compound to form a azo dye which is spectrophotometrically detected.

5.5 Determination of nitrate with sequential injection analysis

5.5.1 Experimental

5.5.1.1 Reagents and solutions

Only analytical-reagent grade reagents were used unless specified otherwise. Deionised water, supplied by a Modulab system (Continental Water Systems, San Antonio, TX, USA) was used to prepare auueous solutions. The solutions were degassed, by boiling it in a microwave oven, before introduction into the system and it was stored in an oxygen free environment when not in use.

Standard nitrate solution: A stock nitrate solution was prepared by dissolving 0.6071 g of oven dried (2 hours at 110°C) sodium nitrate in deionised water and diluting it to 1 litre. Approximately five drops of chloroform were added to the stock solution, to prevent the growth of bacteria, and it was stored in a cool place when not in use. Working standard nitrate solutions were made up by appropriate dilutions of the stock solution.

Carrier solution: The carrier solution was prepared by dissolving 10 g of ammonium chloride in 1.0 litre of deionised water with no adjustment of the pH (4.65).

Buffer solution: The buffer solution was prepared by dissolving 30 g of ammonium chloride and 2 g of EDTA-disodium salt [24] in 500 mℓ deionised water. The pH of this solution was adjusted to pH 6.6 [25] using a 25% (v/v) ammonia solution.

Chromogenic reagent: The chromogenic reagent was prepared by dissolving 40 g sulphanyl amide and 2 g of N-(1-naphthyl)ethylenediamine dihydrochloride (N1NED), obtained from Merck, in 200 mℓ of 80% (v/v) phosphoric acid, and diluting it to 1.0 litre with deionised water. The pH of this solution was 1.07 and it was stored in a cool place when not in use.

Copperization solution: The copperization solution was prepared by dissolving 10 g of copper(II)sulphate and 1.0 g of disodium EDTA in 1.0 litre of deionised water.

Liquid fertilizer: The liquid fertilizer sample was prepared by diluting 1mℓ of sample with 300mℓ of de-ionised water. The solution was filtered to get rid of any solid substances that formed during the dilution.

Reductor column: Pump tubing (Technicon), 11 cm in length with an inside diameter of 2.03 mm, was used to construct the reductor container. The tube was plugged with glass wool and fitted with a nipple connector at the one end. The column was filled with cadmium granules, (particle diameter between 0.3 and 1.5 mm) by means of a shaker and nozzle that fitted into the open end of the column, to a point 0.5 cm from the column top. The open end was plugged with glass wool and a nipple connector fitted. The reductor was then copperized with 6 mℓ of copperization solution using a low flow rate (1.21 mℓ.min^{-1}). Before the reductor was used, it was activated by passing a 100 mg.ℓ$^{-1}$ nitrate solution through it for 5 minutes. After activation the column was stored in the carrier solution when not in use, it can also be stored in deionised water when not incorporated into the manifold.

5.5.1.2 Equipment

The sequential injection manifold used, is shown in Fig. 5.2. The system consisted of a Gilson Minipuls peristaltic pump (Gilson Medical Electronics, (France) S. A., Villiers-le-Bel, France), with a pumping tube (inside diameter 1.42 mm), operating at a speed of 18.5 rpm. The pump was connected to a holding coil (HC) consisting of Tygon tubing, with length 100 cm and an inside diameter 0.76 mm (0.454 ml), wound around a perspex tube with an o.d. of 10 mm.

The holding coil was connected to the reductor, 11.0 cm x 2.03 mm i.d., packed with copperized cadmium (0.3 - 1.5 mm granules). The reductor was connected to the first reaction coil (RC 1) consisting of PTFE (Teflon) tubing with length 120 cm and inside diameter 0.76 mm (0.544 mℓ), wound around a perspex tube with o.d. 10 mm. RC 1 was connected to a 10-port electrically actuated selection valve (Model ESCD10P, Valco instruments, Houston, TX, USA).

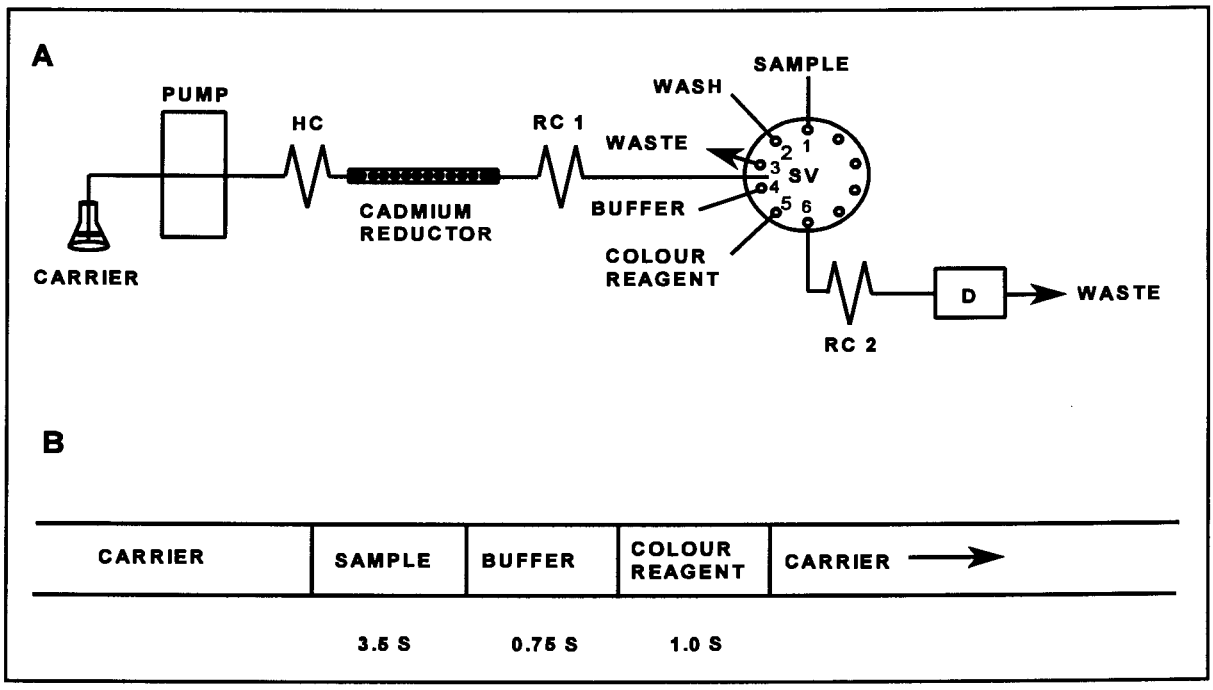

Fig. 5.2 **A** Proposed sequential injection manifold for the determination of nitrate. Carrier is pumped through the holding coil (HC), reductor, reaction coil 1 (RC 1), sequential valve (V) and the second reaction coil (RC 2). The absorbance of the azo dye is measured at the spectrophotometer (D).

B Sequence of sample, buffer and colour reagent present in RC 2.

A second reaction coil (RC 2) connected the valve to the spectrophotometer via 0.76 mm i.d. PTFE (Teflon) tubing, 120 cm in length and 0.76 mm i.d. (0.544 mℓ), wound around a perspex cylinder with o.d. 12.5 mm. A Unica 8625 UV-visible spectrophotometer equipped with a 10 mm Hellma type flow-through cell (volume 80 $\mu\ell$) was used and the absorbance was measured at 525 nm.

Data acquisition and device control were achieved using a PC 30-B interface board (Eagle Electric, Cape Town, South Africa), an assembled distribution board (Mintek, Randburg, South Africa) and a *FlowTEK* [21] software package for computer aided flow-injection.

5.5.1.3 Procedure

The device sequence for the determination of nitrate with the proposed sequential injection method is given in Table 5.1. Samples from an online source or any type of auto sampler are introduced into RC 1 with pump reversal, via port no. 1 of the sequential valve (Fig. 5.2). The valve selects port no. 2 and wash solution (same as carrier solution) is introduced into RC 1 until the tail of the sample plug reaches the end of the cadmium column nearest to the pump (the largest section of the sample zone is then enclosed by the reductor), where nitrate is reduced to nitrite.

Valve position no. 3, waste, is then selected and with forward pumping, reduced sample is pumped towards the valve and a position where the sample plug is split in half by the valve (the other halve of the sample plug is in the tube connecting the valve with the waste container). At this point valve position no. 4 is selected and with pump reversal buffer is introduced into RC 1 followed by colour reagent through port 5. In RC 1 the sulphanilamide is diazotised and couples with N1NED forming the highly coloured azo dye.

Valve position no.6 is selected, which connects RC 1 and RC 2, and with forward pumping the azo dye (the product) is flushed to the detector where the absorbance is measured at 540 nm. The product plug is then pumped towards waste, flushing the system with carrier solution. The valve now returns to position no. 1, ready for the next cycle. Fig. 5.2 shows the cycle (sample, carrier, waste, buffer, chromogenic reagent and flush to the detector) involved ports 1 to 6 of the selection valve.

Table 5.1 Device sequence for a full cycle of the sequential injection system.

Time (s)	Pump	Valve	Description
0.00	Reverse	Sample	Draw up sample
3.50	Off		Pump stop
4.00		Wash	Valve selects wash solution
5.50	Reverse		Draw up wash solution
17.50	Off		Pump stop
28.00		Waste	Valve selects the waste position
28.50	Forward		Sample is pumped towards waste
38.50	Off		Pump stop
39.00		Buffer	Valve selects the buffer position
39.50	Reverse		Draw up buffer solution
40.00	Off		Pump stop
40.50		Colour reagent	Valve selects colour reagent
41.00	Reverse		Draw up colour reagent
41.50	Off		Pump stop
42.00		Detector	Valve selects detector position
42.50	Forward		Azo dye is pumped to detector
84.50	Off		Pump stop
85.00		Home	Valve returns to the original position

5.6 Method optimisation

5.6.1 Physical parameters

Although the sequential injection manifold was optimised in Chapter 4 (Sec. 4.8), it was necessary to repeat certain aspects of the optimisation with the reductor in place.

5.6.1.1 Pump speed

The prerequisites for a good propelling system was summarised in Chapter 4 (Sec. 4.8.1.1), for the determination of nitrite in different samples. For the determination of nitrate the same propelling system, a peristaltic pump, was used with the same advantages and disadvantages.

The experimental conditions (pH, solutions used) were of such nature that standard PTFE (Teflon) tubing (Gradco, Manchester, England) could be used. The pumping tube inside diameter was optimised by choosing a constant pump head rotation, for example 10 rpm, and pump tubes with different inside diameters. Pump tubes with inside diameters between 0.127 mm and 2.794 mm are commercially available. Table 5.2 contains the results obtained for the tube inside diameter optimisation and the results are graphicly depicted in Fig. 5.3. In Table 5.2, one peak height unit is equal to an absorbance of approximately 0.1.

Table 5.2 Influence of pump tube diameter on sensitivity (peak height) and precision (% RSD) .

Tube diameter (mm)	Peak height	% RSD
1.14	3.24	0.53
1.30	4.87	0.74
1.52	4.98	0.96
1.65	5.90	0.81
1.85	6.57	1.01
2.06	6.79	0.67
2.29	7.86	0.72
2.54	8.00	0.98

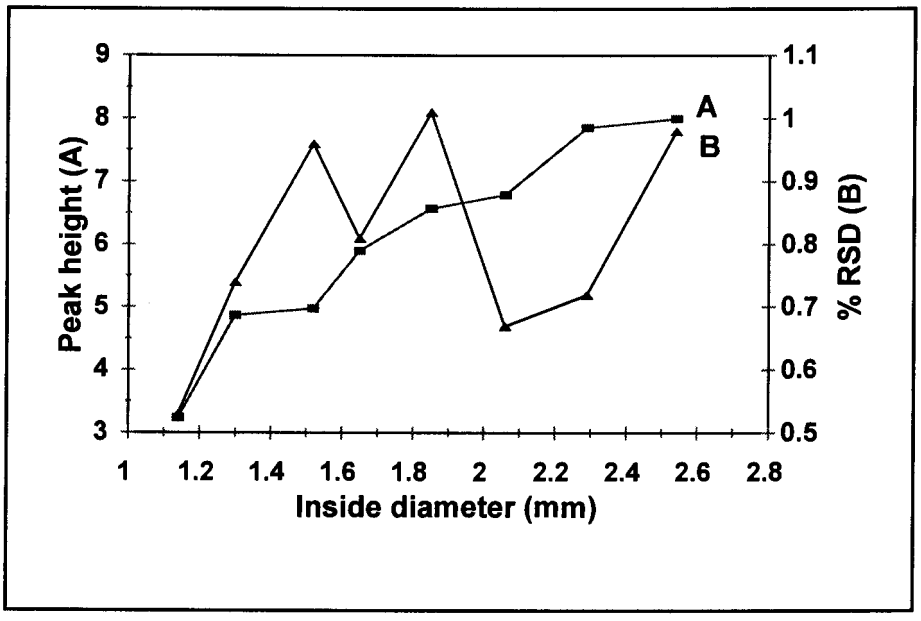

Fig. 5.3 Influence of internal diameter on peak height and %RSD.

The flow rate was further optimised keeping the optimum i.d. (1.85 mm) constant. The flow rate was varied by changing the rotational speed, variable between 12 and 20 rpm, of the peristaltic

pump head. Table 5.3 shows the results obtained for the pump speed optimisation, and it is graphically depicted in Fig. 5.4.

Fig. 5.4 shows the expected upward trend of the peak height with an increase in the flow rate. An r squared value of 0.995 was obtained for the straight line of peak height vs. pump speed. The precision increase (% RSD decrease) for the speeds up to 17 rpm, whereafter it decreases again at the higher pump speeds. In this case a definite optimum speed, in the region 17 - 18 rpm, was obtainable. The best precision was obtained with a tube inside diameter of 1.85 mm and a pump head rotation of 18 rpm (0.86 %). The pump speed was later adjusted to 18.5 rpm with a flow rate of 1.21 mℓ min^{-1} with even better results.

Table 5.3 Influence of pump speed (rpm) on peak height and % RSD.

Pump speed (rpm)	Flow rate (mℓ)	Peak height	% RSD
12	0.55	1.93	3.54
13	0.67	2.42	3.19
14	0.76	2.76	2.53
15	0.85	3.24	1.29
16	0.94	3.75	1.12
17	1.05	4.17	0.80
18	1.15	4.54	0.86
19	1.27	5.04	1.44
20	1.38	5.21	1.90

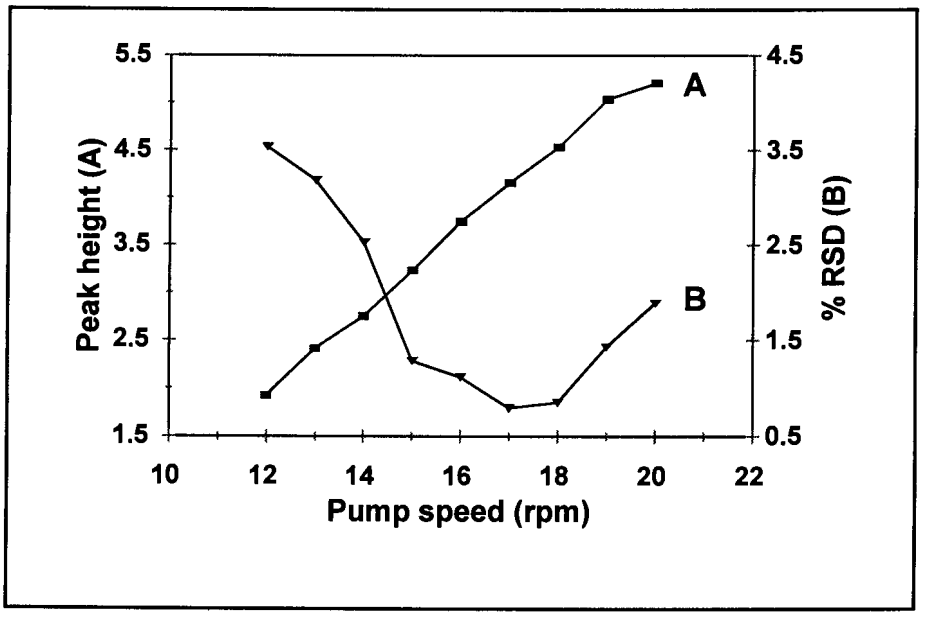

Fig. 5.4 Influence of pump speed (rpm) on sensitivity (peak height), A and precision (% RSD), B.

At the lower pump speeds, 12 - 14 rpm, dispersion increased resulting in low sensitivity and precision. As the pump speed increased to intermediate values, 14 - 18 rpm, dispersion decreased leading to better sensitivity and precision. Above 18 rpm back pressure started influencing the results and caused the low precision (high % RSD) values obtained between 19 and 20 rpm.

5.6.1.2 Holding coil

The holding coil inside diameter and configuration was kept the same as for the nitrite manifold used in Chapter 4 (Sec. 4.8.1.2). More important was the holding coil length. Dispersion was increased with the nitrate as a result of the cadmium reductor fitted between RC 1 and the holding coil. The total sample containing volume of the solution was, therefore, increased, which

necessitated the optimisation of the holding coil's length.

5.6.1.2.1 Holding coil length

The holding coil length was optimised employing the optimum tube diameter (0.76 mm) arrived at in Chapter 4 (Sec. 4.8.1.2). The total volume of the stacked zones was 0.106 mℓ, which required a holding coil length of at least 0.106 mℓ in volume (50 cm), without considering the dispersion of the zones. Lengths between 80 and 120 cm were evaluated. Table 5.4 contains the results which is graphically depicted in Fig. 5.5.

According to Fig. 5.5 an increase in holding coil length improved both the precision and sensitivity for the 100 cm holding coil only, and this length was taken as the optimum holding coil length. The 60 cm coil proved to be too short to contain the dispersed zone and a part of this zone may have entered the pump, causing low precision (high % RSD) values. Longer coil lengths improved neither precision nor sensitivity.

Table 5.4 Influence of holding coil length on peak height and % RSD.

Coil length (cm)	Volume (mℓ)	Peak height	% RSD
60	**0.272**	0.533	2.24
80	**0.363**	0.558	2.07
100	**0.454**	0.827	0.63
120	**0.544**	0.738	1.16
140	**0.635**	0.668	1.62

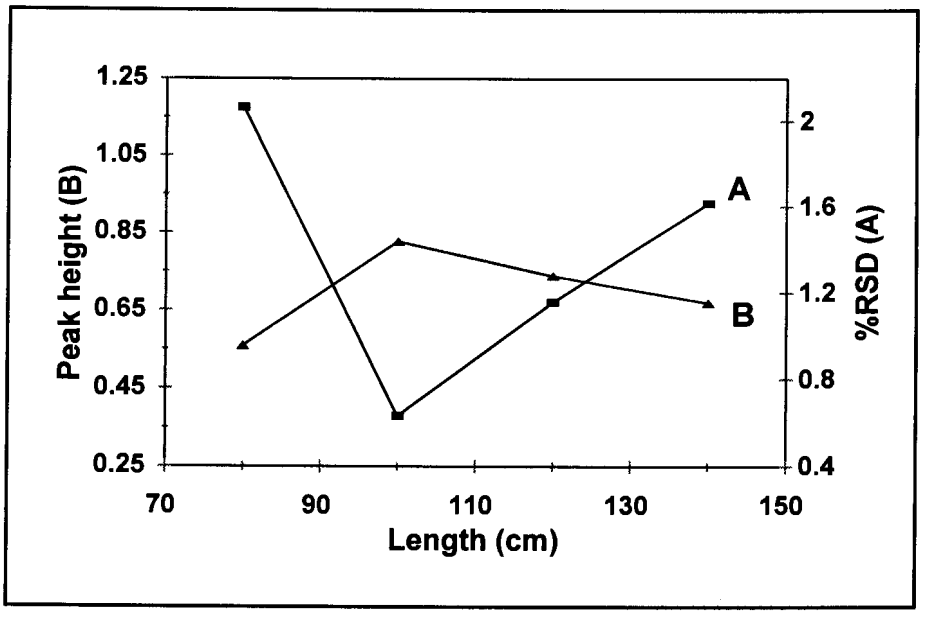

Fig. 5.5 Influence of holding coil length (cm) on precision (A) and peak height (B).

5.6.1.3 Reaction coil 1

Limited dispersion (D < 2) was needed for the sample zone to be contained within the reductor in the first part of the procedure. For the second part, the azotisation and coupling, medium dispersion (D = 2 - 10) was needed to enable the reduced nitrate (nitrite) to penetrate the chromogenic reagent zone. To satisfy both these requirements the first reaction coil had to be optimised carefully. It should also be kept in mind that optimisation with the reductor in place should be done in such a way that the nitrate sample ends up in the same position in the reductor each time. The reaction coil (RC 1) should be designed in such a way that it holds the entire reagent zone as well as the sample zone [21]. Only the tube diameter was optimised for RC 1.

5.6.1.3.1 Tube diameter

Tube inside diameters between 0.38 and 1.02 mm were evaluated. Table 5.5 shows the results, graphically depicted in Fig. 5.6, obtained for the optimisation of tube diameters.

Table 5.5 Influence of reaction coil 1 tube diameter on peak height and % RSD.

Tube diameter (mm)	0.38	0.51	0.64	0.76	1.02
Peak height	1.59	1.68	1.97	2.13	2.27
% RSD	1.97	1.29	1.10	0.84	1.66

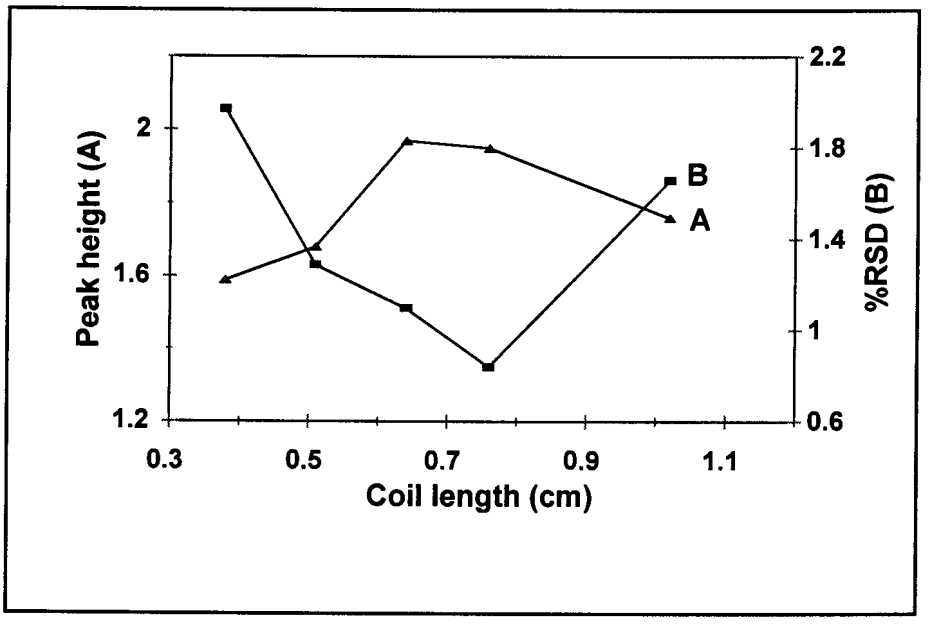

Fig. 5.6 Influence of RC1 tube diameter on sensitivity (peak height) and precision (% RSD).

According to Marshall [21] a larger diameter tube should lead to lower penetration and lower response. In Fig. 5.6 peak height increase for the first three diameters and decrease for the last

two diameters, the trend suggested by Marshall is thus only followed by the last three diameters. The best precision (0.84 %) was obtained with a tube diameter of 0.76 mm and this diameter was used for further optimisation of the proposed method.

5.6.1.4 Reaction coil 2

The second reaction coil (RC 2) played a more important role in the proposed nitrate manifold than it did in the determination of nitrite. In the case of nitrite, the sample already penetrated and completed the reaction with the chromogenic reagent zone in the first reaction coil while the second reaction coil, only served as a way of getting the reacted zone to the detector with the lowest amount of dispersion possible. With the determination of nitrate, RC 1's main purpose was the transport of the sample to the reductor. With the nitrate reaction penetration and completion of the reaction, had to take place mainly in reaction coil 2 (RC 2). For penetration of two zones in the second reaction coil, medium dispersion (D = 2 - 10) was necessary. RC 2 had to be designed in such a way that these prerequisites were met.

5.6.1.4.1 Tube diameter

RC 2 tube diameters were varied between 0.38 and 1.01 mm. According to Table 5.7 and Fig. 5.7, peak height decreased as the tube diameters were increased, but the difference between the peak heights of the largest and the smallest diameters was small in comparison with the difference between the precision of the largest and smallest diameters.

Table 5.7 Influence of the coil diameter on the peak height and % RSD of RC 2.

Inside diameter (mm)	0.38	0.51	0.64	0.76	1.01
Peak height	3.14	3.07	3.01	2.93	2.85
% RSD	1.87	1.64	1.31	1.09	1.42

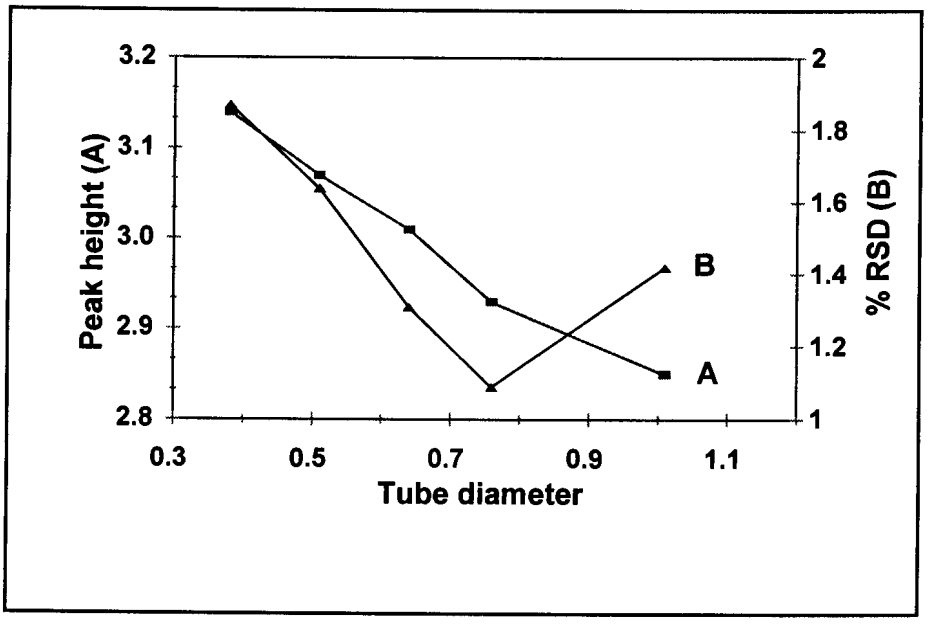

Fig. 5.7 Influence of RC 2 tube diameter on peak height and % RSD.

The best precision was obtained with a 0.76 mm tube diameter. Smaller diameters were influenced by back pressure, leading to low precision, while the 1.01 mm diameter's precision decreased as a result of less penetration [21]. A 0.76 mm inside diameter was chosen as the optimum diameter and used in the optimisation of the other parameters.

5.6.1.4.2 Coil length

The difference between the procedures followed in the determination of nitrite and that of nitrate is that penetration takes place in RC 1, in the case of nitrite. In the case of nitrate, RC 2 must be

long enough for total penetration of reacting zones to take place, since the amount of penetration that can take place in RC 1 is limited. The length of the second reaction coil was varied between 60 and 140 cm to obtain the optimum length. The expected trend mentioned in Sec. 5.6.3.1.2 is observed in Table 5.8 and Fig. 5.8.

Table 5.8 Influence of RC 2 length on peak height and precision % RSD.

Length (cm)	60	80	100	120	140
Peak height	3.21	3.13	3.09	2.97	2.83
% RSD	1.98	1.69	1.28	0.52	1.35

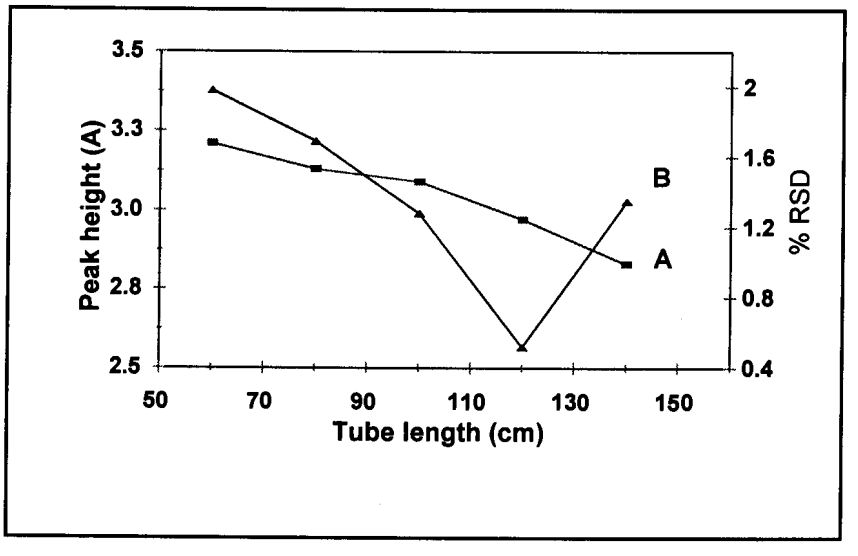

Fig. 5.8 Influence of RC 2 length on peak height and % RSD.

5.6.1.4.3 Coil geometry

The second reaction coil geometry plays an important role in determining the correct penetration needed for the reaction. From the study of the three geometries (straight, coiled, knitted), it was found that the coiled geometry had the most positive effect on the results. A coiled second reaction coil was therefore used for the rest of the optimisation.

5.6.1.5 Uptake tubes

Uptake tubes were kept large enough (1.0 mm i.d.) to prevent any possible back pressure from developing during sample and reagent aspiration. Tube lengths were kept the same as used for the determination of nitrite (30 cm) in the previous chapter.

5.6.1.6 Order of injection

The order of injection is determined by the application. For the determination of nitrate the sample was introduced first, to be reduced in the reductor. The sample was followed by enough wash solution to transport the sample into the reductor. The whole wash solution plug and a part of the sample plug were flushed towards waste via port 3. Only then was chromogenic reagent introduced into the system and pumped towards the spectrophotometer. An alternative order, is the introduction of chromogenic reagent directly behind the sample. Although time is saved, due to a shorter sequence, the results obtained with this order of injection proved to be irreproduceable.

5.6.1.7 Reductor

Several parameters, both physical and chemical, influence the reduction capabilities of reductors. It's physical parameters (diameter and length) play the most important role in determining its reduction capacity while its position and chemical parameters (e.g. degree of copperization) play a less important role. All these parameters had to be optimised in order to determine the feasibleness of such a reductor in conjunction with SIA.

5.6.1.7.1 Reductor diameter

The reductor diameter was optimised by using reductors of constant length (5 cm) while varying the inside diameters between 1.0 and 2.8 mm. The reductor was positioned between the valve and RC 1 and sample was introduced directly into the reductor through the valve (Fig. 5.9) At this stage the sample and chromogenic reagent were introduced sequentially, with no wash solution to transport the sample into the reductor.

The obvious result of increased dispersion with increased inside diameter is observed in Fig. 5.10 and Table 5.9. Only in the case of samples with high nitrate concentrations will the influence of diameter on peak height be noticeable, when smaller diameter reductors with less cadmium will be over loaded.

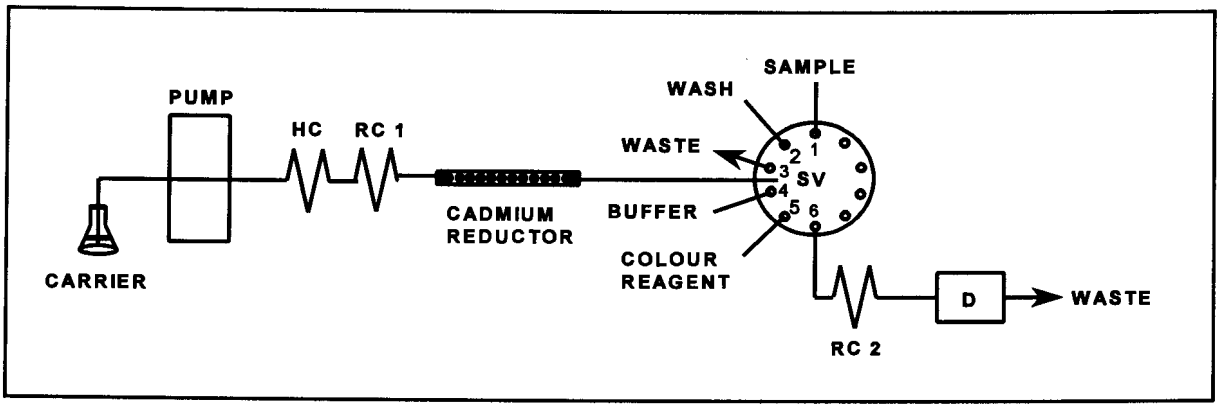

Fig. 5.9 SIA manifold used in the optimisation of the reductors physical parameters

Table 5.9 Influence of reductor inside diameter on peak height.

Diameter (mm)	1.01	1.55	2.03	2.29	2.54	2.80
Peak height	0.82	0.79	0.73	0.58	0.51	0.41

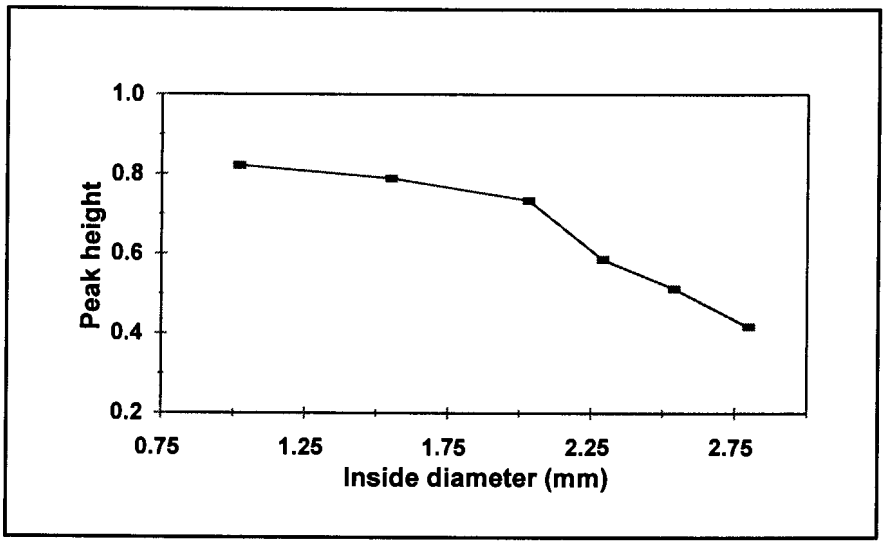

Fig. 5.10 Influence of reductor inside diameter on peak height.

If concentrations are increased beyond the reductor's capabilities the inverted graph of Fig. 5.10 is expected, with the smaller diameter reductors being overloaded and the larger diameter reductors able to cope with the load. An intermediate reductor diameter (2.03 mm), with limited

dispersion and intermediate reduction capacity, was chosen for the determination of nitrate to enable the detection of nitrate at both high and low concentrations.

5.6.1.7.2 Reductor length

The reductor length is probably the second most important parameter of the cadmium reductor. It is expected that the dispersion would be increased in some way by the variation of the reductor length and a variation in the length would also influence the reductor's reducing capacity. To determine these influences the reductor length was varied between 3 and 15 cm. Table 5.10 and Fig 5.11 shows that an increase in the reductor length leads to increased peak heights and therefore a greater reduction ability. The precision shows a similar increase up to a length of 10 cm and a decrease for a reductor length of 15 cm. The 10 cm reductor was chosen for its good precision and sensitivity.

Table 5.10 Influence of reductor length on peak height and % RSD.

Reductor length (cm)	**3**	**5**	**10**	**15**
Peak height	2.72	2.82	3.15	3.54
% RSD	3.12	1.59	1.51	1.83

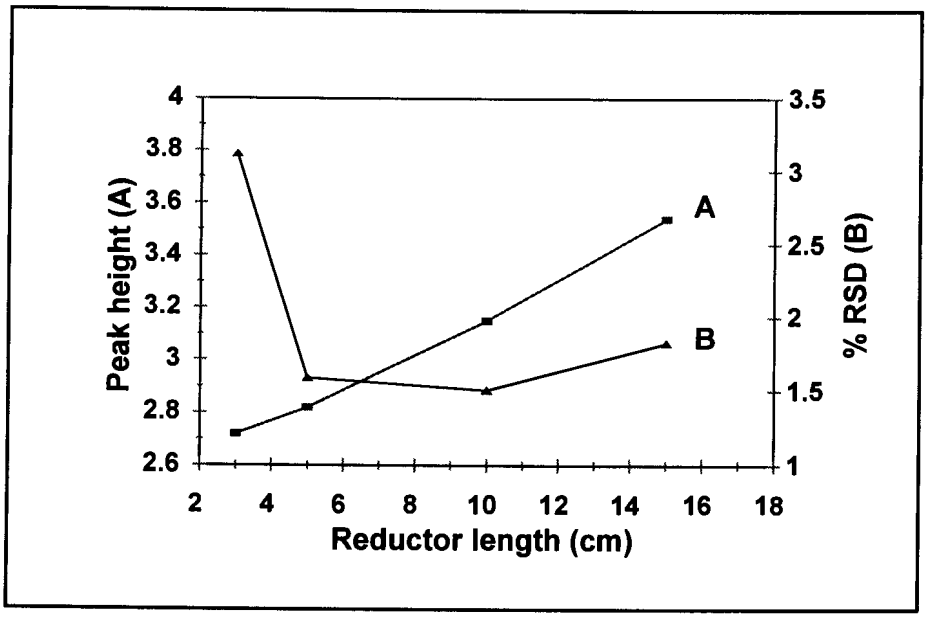

Fig. 5.11 Influence of reductor length on peak height (A) and % RSD (B)

5.6.1.7.3 Reductor position

Since reductors were not used previously in SIA systems, the question arose where it should be placed in the manifold for maximum yield. There are mainly five possible positions where the reductor may be placed, each with its own advantages and disadvantages. The five positions are: in the sample up-take stream, between the valve and RC 1, between RC 1 and the HC, in a separate line of its own and between the valve and detector in RC 2.

With the reductor in the sample uptake stream, sample is in continuous contact with the reductor. Advantages of this position are: longer reduction periods for the sample with the reduction time equal to the time it takes to complete one analysis cycle, nearly complete reduction, and it is possible for the sample and chromogenic reagents to be introduced sequentially. With all

reductors the reduction material, copperized cadmium in this case, is oxidised and needs to be replaced after a certain amount of reduction has taken place. In this particular position the reductor has to be replaced more often to keep the amount of reduction constant.

With the reductor placed between the valve and the first reaction coil (RC 1), the reductor lasts longer because contact between the sample and reductor is limited to only a few seconds per cycle. It is impossible for the sample and chromogenic reagent to be aspirated sequentially, saving time by cutting steps from the sequence (see the final position between RC 1 and HC). If the sample and chromogenic reagent are aspirated sequentially the sample has to be aspirated after the chromogenic reagent to allow the sample to remain in the reductor. Precision in this position was only average (% RSD = 2.0 %).

The third possible position is between the holding coil and RC 1. The best results were obtained with the reductor in this position by aspirating the sample and then deionised water until the sample was enclosed by the reductor. The reduced sample was then pumped towards the valve, using an additional step. More dispersion occurs but better precision was obtained (% RSD = 1.3). An added advantage is the reductor's increased lifespan as a result of the limited exposure to sample. This was the position finally chosen for the determination of nitrate with the proposed method.

The fourth possible position is to place the reductor in a separate reaction coil containing only the reductor. Sample is pumped into the reductor, and back into the main stream after reduction of nitrate has taken place. The best sensitivity was obtained in this position, but at the cost of a

decrease in the precision (% RSD = 5.3 %). The most probable reason for the decrease in precision is sample carried over from one run to the other.

The final possible position is to place the reductor in the reaction coil connecting the valve and the detector. The reduction time is increased only if the flow is stopped with the sample zone in the reductor. It is possible to aspirate the sample and chromogenic reagent sequentially, thus leading to a saving in time. An average precision (% RSD = 2.02) was obtained but the sensitivity was lower than in all the other cases. The sample is probably more dispersed in this position with lower sensitivity as the result.

5.6.2 Chemical parameters

Most of the chemical parameters were previously optimised for the determination of nitrite in the Chapter 4 (Sec. 4.9.3) and only parameters concerning the reductor were optimised. However, some of the parameters affected by the reductor had to be optimised again.

5.6.2.1 Carrier stream

Ammonium chloride [26, 27, 28] is frequently used in the carrier stream in nitrate and nitrite detection systems. Ammonium chloride concentrations between 1 and 10 $g.\ell^{-1}$ ammonium chloride [26 - 28] are mostly used. Most of the authors [26 - 28] used the same reagents in FIA and other analytical methods requiring different ammonium chloride concentrations. For the proposed system ammonium chloride concentrations between 1 and 30 $g.\ell^{-1}$ were evaluated. Table 5.11 and Fig. 5.12 shows the results obtained for these concentrations.

Table 5.11 Influence of NH_4Cl concentration on peak height and % RSD.

Concentration (mg/ℓ)	Peak height	% RSD
0	5.02	2.98
1	5.20	2.26
2	5.42	1.73
3	5.54	1.14
4	5.58	0.87
5	5.59	0.83
6	5.59	0.82
7	5.60	0.63
8	5.65	0.45
9	5.71	0.42
10	5.66	0.29
15	4.87	0.33
20	4.05	0.66
25	3.71	0.86
30	3.60	1.66

It is clear that ammonium chloride has both a positive and negative influence depending on its concentration. Ammonium chloride has an increasingly positive influence between 1 and 9 $g.\ell^{-1}$ with the peak height increasing and the RSD decreasing. Ammonium chloride concentrations higher than 15 $g.\ell^{-1}$ showed a slight increase in precision but the sensitivity decreased at high ammonium chloride concentrations.

Ammonium chloride concentrations between 9 and 15 $g.\ell^{-1}$ had little influence on precision but the sensitivity was greatly reduced. An optimum concentration of 9 $g.\ell^{-1}$ ammonium chloride was chosen as carrier stream for the determination of nitrate. This carrier stream had a pH of 4.65.

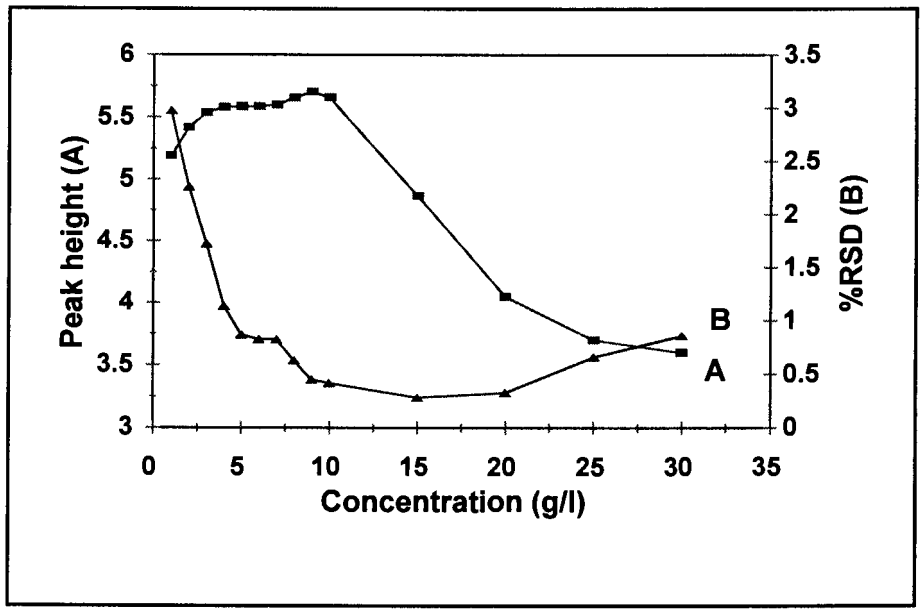

Fig. 5.12 Influence of NH_4Cl concentration on peak height (A) and % RSD (B).

5.6.2.2 Chromogenic reagent

Different concentrations of sulphanilamide and N1NED in the chromogenic reagent were optimised to obtain the best reaction conditions for the SIA system. N1NED concentrations between 0.5 and 2 $g.\ell^{-1}$ are normally used in FIA [26. 27, 28] and therefore concentrations between 10 and 40 $g\ \ell^{-1}$ of sulphanilamide [11, 13, 17, 28, 29] were evaluated for the proposed method. The best sensitivity was obtained with 2 $g.\ell^{-1}$ N1NED and 40 $g.\ell^{-1}$ sulphanilamide as the chromogenic reagent.

Hydrochloric [30], phosphoric [25, 31] and acetic acid were all used in the preparation of the chromogenic reagent in earlier work [12]. All three these acids were evaluated but the chromogenic reagents prepared with phosphoric acid (pH = 0.33, peak height = 5.50) were more

sensitive than that prepared with hydrochloric acid (pH = 1.07, peak height = 3.91) and it also had a better precision.

Different dilutions of the optimum chromogenic solution were evaluated to determine its influence on the calibration curve. The chromogenic reagent was diluted with water to the following ratios; 1:2 (pH = 1.2), 1:1 (pH = 1) and undiluted (pH = 0.33). The more diluted solutions worked well with the samples containing low nitrite concentrations but with the more concentrated solutions ($[NO_3^-] > 4$ mg.ℓ^{-1}) the calibration curve tended to flatten at high nitrate concentrations and an undiluted chromogenic reagent was preferred for those solutions. This should be kept in mind when consumption of expensive reagents play a role.

In the optimisation of the volume ratio of sulphanilamide to N1NED, Fig. 5.13 was obtained. As the volume ratio of N1NED (X) against sulphanilamide (Y) was increased, the peak height increased and levelled off at four parts N1NED to one part sulphanilamide. With an increase in the sulphanilamide volume (Y), the peak height increased for the first three values (Y = 1 to 3) and for the fourth value (Y = 4) the peak height was substantially lower than the peak height of the third value (Y = 3).

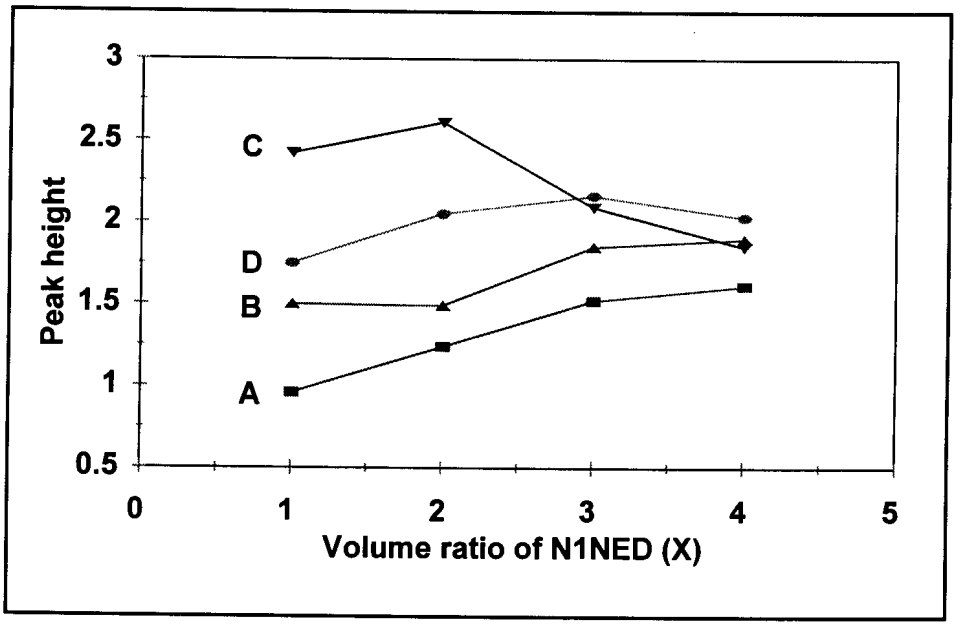

Fig. 5.13 Influence of different N1NED (X), sulphanilamide (Y) volume ratios on the sensitivity (peak height). The Y = 1 is represented by A, Y = 2 by B, Y = 3 by C and Y = 4 by D.

The best results were obtained with a ratio of three parts sulphanilamide to two parts N1NED. For the chromogenic reagent containing both its components in one solution, as used in the proposed method, the volume aspirated had to be determined for the combined solution. According to Fig. 5.14 and Table 5.12 the optimum chromogenic reagent volume is in the order of 40 μℓ or an aspirating time of 2 sec. Larger chromogenic reagent volumes gave better precision, at the cost of a loss in sensitivity, and too small chromogenic volumes resulted in low precision values and sensitivity.

Table 5.12 Influence of the chromogenic reagent volume on the peak height and % RSD.

Volume($\mu\ell$)	0	20	40	60
Peak height	0.12	7.21	7.23	6.80
% RSD	2.35	1.96	1.56	0.83

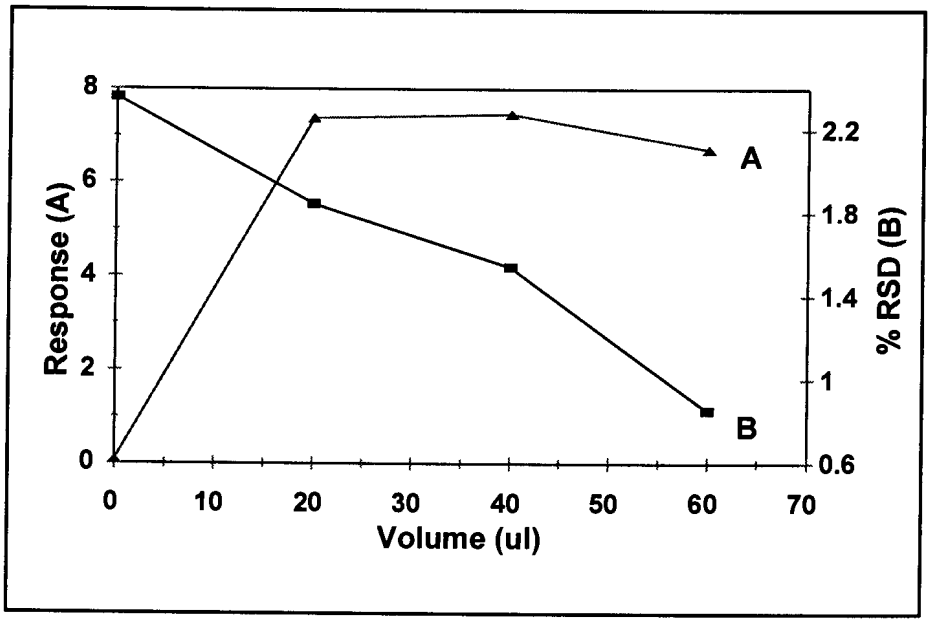

Fig. 5.14 Chromogenic reagent volume influence on peak height (A) and % RSD (B).

5.6.2.3 Sample volume

Nitrate samples used in the optimisation of the method were made up in deionised water keeping interferences from other elements to a minimum. The sample volume was optimised by varying the volume aspirated into the proposed system. This was necessary to allow just the right volume of sample into the reductor for optimum results. An intermediate sample concentration (5 mg.ℓ^{-1}) was used in the optimisation. Sample volumes between 10 and 90 $\mu\ell$ were evaluated (Table 5.13, Fig. 5.15).

Table 5.13 Sample volume influence on peak height and % RSD.

Volume (µℓ)	Peak height	% RSD
10	0.721	1.97
20	0.122	1.51
30	0.201	1.11
40	0.286	0.83
50	0.370	0.65
60	0.458	0.36
70	0.550	0.19
80	0.641	0.23
90	0.721	0.32

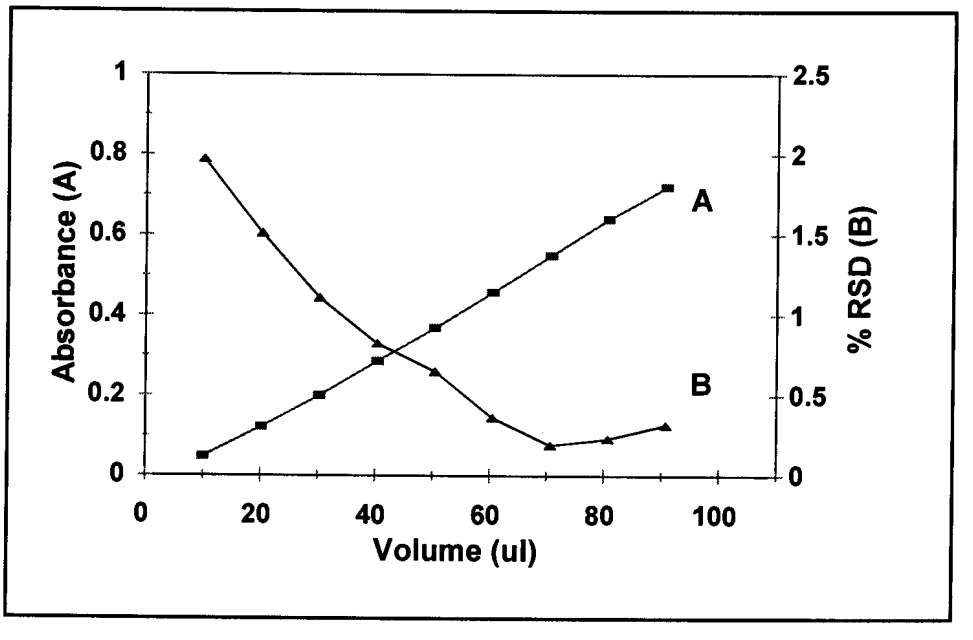

Fig. 5.15 Sample volume influence on peak height (A) and % RSD (B).

According to Fig. 5.15 the optimum sample volume is 70 µℓ of sample with a % RSD value of only 0.19 %. An r squared value of 0.999 was obtained for the straight line graph, showing the accuracy with which sample could be aspirated with a peristaltic pump. In this case the precision is a good indication of the optimum sample volume with a definite minimum value of 0.19 % at

the turning point of the precision graph.

5.6.2.4 Reduction material

A copperized-cadmium reductor [17, 18, 19] is normally used for the reduction of nitrate to nitrite. Several parameters surrounding this reductor has to be optimised in order to obtain maximum reduction, namely: degree of copperization of the reductor, sample position within the reductor and reduction time.

Mainly four different methods for the copperization of cadmium exists:

(1) direct batchwise copperization of untreated cadmium with a 10 $g.\ell^{-1}$ copper sulphate solution for 1-2 minutes [30],

(2) treatment of cadmium with 0.2 $mol.\ell^{-1}$ hydrochloric acid, washing with deionised water and then batchwise copperization with a 10 $g.\ell^{-1}$ copper sulphate solution for 2 minutes [32],

(3) direct copperization of the packed, untreated cadmium in the manifold with 3 ml of a 10 $g.\ell^{-1}$ copper sulphate solution [26],

(4) treatment of ready packed cadmium with a 0.1 $mol.\ell^{-1}$ hydrochloric acid solution, followed by copperization with 10 $g.\ell^{-1}$ copper sulphate for 2 minutes at a flow rate of about 0.6 $m\ell.min^{-1}$ [33].

The grey cadmium turns black with copperization. By visual inspection of the copperized cadmium, it is possible to see if the cadmium was uniformly copperized or not. Method no. 2, pretreatment of cadmium with hydrochloric acid, provided a more uniformly copperized

cadmium than method no. 1, but on the negative side it also produced a lot of small diameter copperized cadmium particles. The larger particles had to be separated from the small diameter particles to obtain more uniformly sized particles.

It is possible to get more reproducible copperization with the use of the SIA system to directly copperizing the cadmium in the system. Methods 3 and 4 were done in this way. Method 4 uses the same method of copperization as method 2, and the same problem of small particles forming during treatment of the cadmium with HCl occurred. These small particles were unable to pass through the glass wool stoppers of the reductor, resulted in blockages and a pressure build-up in the system. Method 3 was used in the proposed method with good results and very little problems.

To determine the influence of the amount of copperization, both the sensitivity and precision of the proposed method, reductors were copperized with different volumes of a 0.1 mol.ℓ^{-1} $CuSO_4$ solution. Table 5.14 and Fig. 5.16 shows the results obtained for this optimisation. According to Fig. 5.16 the sensitivity is not greatly influenced by the amount of copperization up to 6 mℓ.

Table 5.14 Influence of the amount of copperization on peak height and % RSD.

Volume (mℓ)	1.39	2.78	4.17	5.86	6.95	8.34
Peak height	3.59	3.54	3.51	3.38	3.16	2.58
% RSD	3.10	2.50	1.59	1.18	0.73	1.17

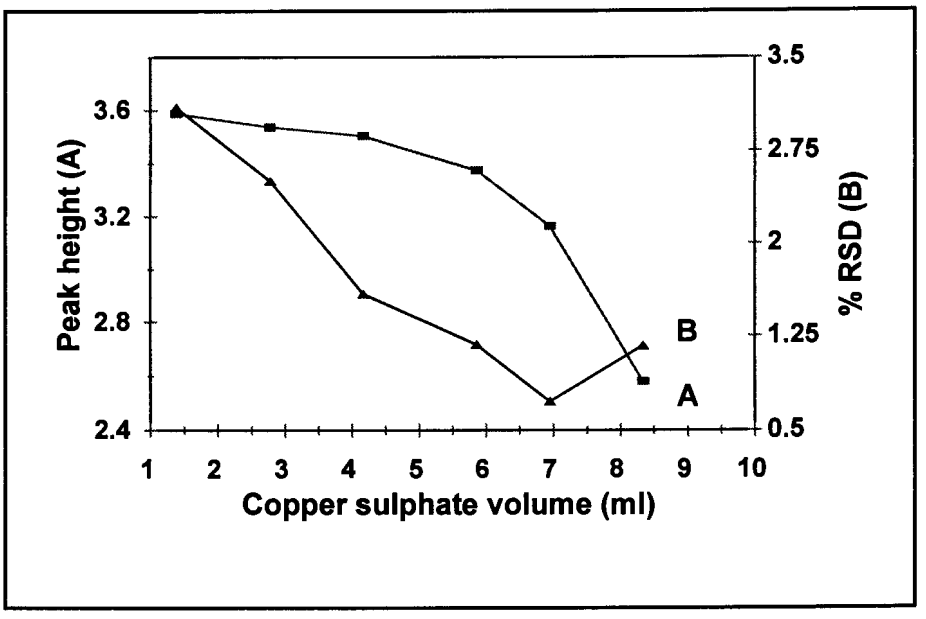

Fig. 5.16 Influence of copperization on peak height (A) and % RSD (B).

There is however a noticeable difference in the precision from a RSD value of 3.10 %, for a volume of 1 mℓ, to 1.18 %, for a volume of 6 mℓ. Above 6 mℓ the sensitivity decreased substantially from a peak height value of 3.38 units for 6 mℓ to a value of 2.58 units for 8 mℓ. The precision increased to its best value of 0.73 % with a volume of 6.95 mℓ and it decreased for larger volumes. For the copperization of the cadmium 6 mℓ of a 0.1 mol.ℓ^{-1} copper sulphate solution were pumped through the reductor at 1.21 mℓ.min^{-1}.

The time needed for reduction to occur varies from reductor to reductor. To determine the time needed for a complete reduction, sample was left in the reductor for different periods. Table 5.15 and Fig. 5.17 show that in this particular case reduction occurred almost immediately. Longer reduction times caused samples to disperse causing a loss in sensitivity. Precision deteriorated as reduction times increased except for very short reduction periods in which case the precision was very low. The best results were obtained with reduction times in the region of 10 to 15

seconds. For the proposed method a reduction time of 10 seconds were chosen.

Table 5.15 Influence of reduction time on peak height and % RSD.

Time (sec)	0	20	40	60	80	100	120
Peak height	0.45	0.41	0.40	0.39	0.39	0.38	0.39
% RSD	2.66	0.58	0.70	0.80	0.89	0.93	1.43

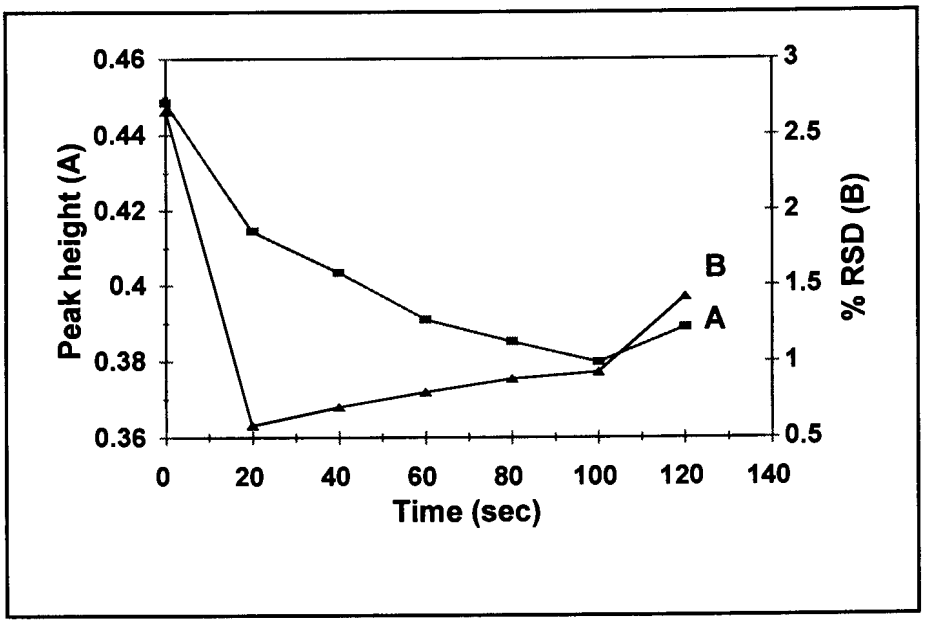

Fig. 5.17 Optimisation of reduction time, and influence of reduction time on peak height (A) and % RSD (B).

5.7 Evaluation of method

5.7.1 Linearity

For a method to be industrially viable it should have a flexible concentration range to enable it to be used in different situations. A method with a wide linear range is, therefore, more useful. The linearity of the SIA system was determined under the optimum operating conditions. The relationship for the relative peak height versus nitrate concentration was:

$$y = 0.550x - 0.433 \; ; \; r = 0.997$$

where y = relative peak height and x = nitrate concentration in $mg.\ell^{-1}$. The calibration graph is linear for nitrate concentrations between 0 and 15 $mg.\ell^{-1}$ and deviate from the expected value for concentrations above 15 $mg.\ell^{-1}$ (Fig. 5.17). The absorbance obtained in the absence of any nitrate is the result of the small refractive index differences between the carrier stream and the combination of the chromogenic reagent and the buffer solutions. Concentrations below 0.5 $mg.\ell^{-1}$ would be difficult to detect as a result of these differences.

5.7.2 Accuracy

Real samples were analysed with the proposed SIA system to determine the accuracy. The accuracy of the SIA analyser was determined by comparing results obtained with the SIA system

to that obtained with a standard procedure [34]. The results given in Table 5.16 revealed good correlation between the two methods.

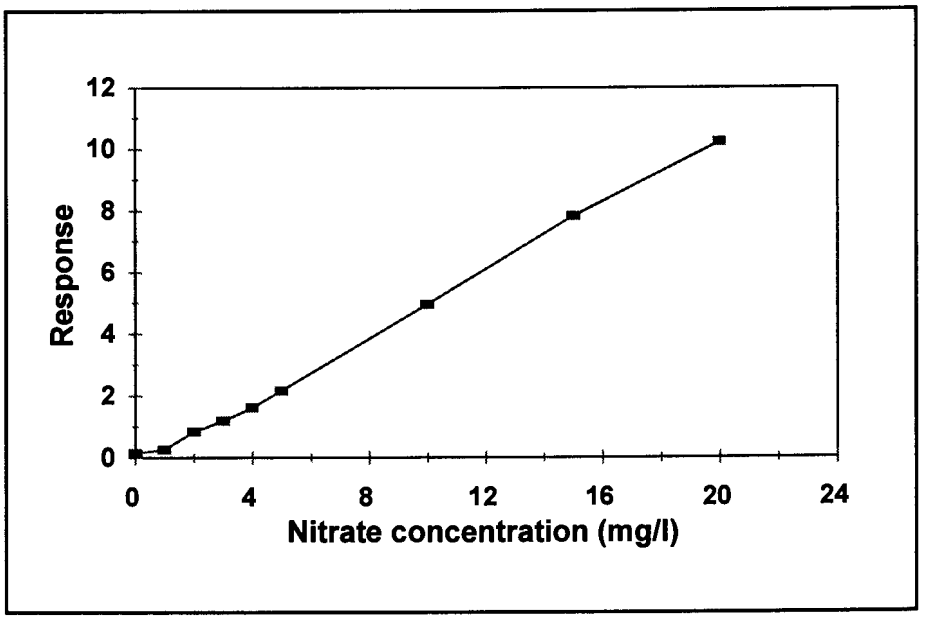

Fig. 5.17 Graph obtained with the proposed method for nitrate concentrations between 0 and 20 mg.ℓ^{-1}.

Table 5.16 Comparison of results obtained with the proposed nitrate SIA method and a standard method.

Sample	SIA method (mg.ℓ^{-1} nitrate)	Standard method (mg .ℓ^{-1} nitrate)
4	1.70	1.67
13	1.72	1.70
18	1.67	1.65
32	1.58	1.57
38	1.46	1.46
Liquid fertilizer	122*	126*

* g.ℓ^{-1} with dilution taken into account

5.7.3 Precision

The precision of the optimised method was determined by 10 repetitions of a number of standard nitrate solutions and samples as indicated in Table 5.17. In all cases the RSD was below 2.4 % with a best case scenario of 1.07 % for a nitrate concentration of 1 mg.ℓ^{-1}.

Table 5.17 Precision of the proposed SIA method at various concentrations.

Sample/Standard Concentration (mg.ℓ^{-1})	% RSD
0.00	0.44
1.00	1.07
2.00	1.18
3.00	1.18
4.00	1.70
5.00	2.06
10.00	2.39
15.00	2.37
Liquid fertilizer	2.51

5.7.4 Detection limit

The detection limit of the proposed method was determined via the following formula:

$$Detection\ limit = \frac{3\ x\ (S_k)\ x\ K}{100} \qquad (1)$$

where S_k is the relative standard deviation of the baseline (Sk = 0.44) and K is the average signal value of the baseline (K = 1.50). The detection limit was calculated as 0.018 mg.ℓ^{-1}.

5.7.5 Interferences

Because the proposed system will be mainly employed as a nitrate process analyser, it is important that the ions present in fertilizers and effluent water do not interfere with the signal obtained for nitrate. The influence of these ions were evaluated by adding the same amount of nitrate to samples containing different amounts of other ions (Table 5.18).

The ions tested had limited to no influence on the proposed method. It should, however, be noted that the interferences were studied with EDTA absent from the samples tested. If the interferences from other ions do become a problem, the addition of EDTA to the solutions may solve the problem.

5.7.6 Sample frequency

For a method to be industrially viable it must have a reasonable sample frequency. The total time needed for the completion of one cycle of the proposed method, is 85 seconds, giving the proposed SIA system a sample frequency of 42.5 samples per hour. The frequency is a little lower than the 49 samples per hour obtained with the nitrite analyser of Chapter 4 as a result of the extra ten seconds needed for the reduction of nitrate.

Table 5.18 Possible interfering ions and their influence on the signal obtained with the proposed method

Ion	Ion concentration ($mg.\ell^{-1}$)	Peak height	% Influence
PO_4^{3-}	0	8.09	0.00
	100	8.05	0.50
	1000	7.81	3.48
Cu^{2+}	0	7.19	0.00
	10	7.84	9.00
	50	7.90	9.80
	100	7.90	9.86
Mg^{2+}	0	7.87	0.00
	20	8.10	2.92
	100	7.24	8.00
Ca^{2+}	0	8.07	0.00
	50	8.2	1.80
	500	8.14	0.90
	1000	7.78	3.60
K^{1+}	0	8.07	0.00
	100	8.44	4.50
	1000	8.87	10.0
Zn^{2+}	0	7.82	0.00
	20	8.02	2.60
	100	8.11	3.70
	1000	8.59	10.0
SO_4^{2-}	0	7.81	0.00
	20	7.79	1.00
	100	7.99	2.20
	1000	8.37	7.10

5.8 Conclusion

Sequential injection makes direct on line analyses of nitrate in water and liquid fertilizer streams possible. The proposed method is a simple, inexpensive and reliable method for the determination of nitrite. The proposed method also has added advantages such as sensitivity and speed, making it ideal for routine analysis situations in the process industry. The method is not influenced by ions normally present in liquid fertilizers, but if a interference does occur the addition of a masking agent such as EDTA may solve the problem.

The position of the detector is totally dependant on the setup and reagents used. For the determination of nitrate the reductor was placed between the holding coil and RC 1 with excellent results. Once the reductor position was determined the physical size of the reductor had to be determined which was dependant on the concentration range of the sample. In the case of nitrate it was determined that bigger was not always better with an intermediate sized reductor giving the best results.

5.9 References

1. **House of Lords Select Committee**, (1989) 7.
2. T. M. Addiscott, A. P. Whitmore and D. S. Powlson, **Farming, Fertilizers and the Nitrate problem**, C. A. B. International, (1991).
3. S. D. Wullschleger and D. M. Oosterhuis, **J. Plant Nutr., 13** (1990)1141.
4. A. Finck, **Fertilizers and fertilization**, Verlag Chemie, (1982).
5. P. W. West and G. L. Lyles, **Anal. Chim. Acta, 23** (1960) 227.
6. F. B. Hora and P. J. Webber, **Analyst, 85** (1960) 567.
7. D. W. W. Andrews, **Ibid., 89** (1964) 730.
8. H. Barnes, **Ibid., 75** (1950) 388.
9. F. L. Fisher, E. R. Ibrt and H. F. Beckman, **Analyt. Chem., 30** (1958) 1972.
10. A. V. Trofimov, **Z. Phys. Chem., 9** (1935) 756.
11. O. Deniges, **Analyst., 51** (1912) 158.
12. R. J. Elliot and A. G. Porter, **Analyst, 96** (1971) 522.
13. R. H. Diven, W. J. Pistor, R. E. Reed, R. T. Trautman and R. E. Watts, **Amer. J. Vet. Res., 23** (1962)497.
14. J. B. Mullin and J. P. Riley, **Anal. Chim. Acta, 12** (1955) 464.
15. J. A. Brabson and W. G. Burch, **J. Ass. Off. Agric. Chem., 47** (1964) 1037.
16. K. Matsunaga and M. Nishimura, **Anal. Chim. Acta, 45** (1969) 350.
17. M. J. Follett and P. W. Ratcliff, **J. Sci. Fd. Agric., 14** (1963) 138.
18. K. Mohler, **Z. Lebensm. u. -Forch., 125** (1964) 337.
19. L. Kamm, G. G. McKeown and D. M. Smith, **J. Ass. Off. Agric. Chem., 48** (1965) 892.
20. **Standard methods for the Examination of Water and Waste Water**, 14th Edition, American Public Health association, Washington, DC, 1976.

21. A. Chaube, A. K Baveja and V. K. Gupta, **Anal. Chim. Acta, 143** (1982) 273.

22. S. Sunita and V. K. Gupta, **Int. J. Environ. Anal. Chem., 19** (1984) 11.

23. M. B. Shinn, **Ind. Eng. Chem. Anal. Ed., 13** (1941) 33.

24. D. F. Boltz and J. A. Howell, **Colorimetric determination of non-metals**, John Wiley & Sons, 1978, 237 - 238.

25. J. F. van Staden and M. A. Makhafola, **Fresenius J. Anal. Chem., 354** (1996) 70.

26. A. Hulanicki, W. Matuszewski and M. Trojanowicz, **Anal. Chim. Acta, 194** (1987) 119.

27. K. Nagashima, M. Masatoshi and S. Shigetaka, **Anal. Chem., 57** (1985) 2065.

28. J. R. Clinch and P. J. Worsfold, **Anal. Chim. Acta., 200** (1987) 523.

29. M. T. Oms, A. Cerdá and V. Cerdá, **Anal. Chim. Acta., 321** (1995) 321.

30. L. Anderson, **Anal. Chim. Acta, 110** (1979)123.

31. M. F. Giné, F. Bergamin, E. A. G. Zagatto and B. F. Reis, **Anal. Chim. Acta, 114** (1980) 191.

32. A. Henriksen and A. R. Selmer-Olsen, **Analyst, 95** (1970) 514.

33. A. G. Fogg, A. Y. Chamsi and M. A. Abdalla, **Analyst, 108** (1983) 464.

34. **Standard methods for Examination of Water and Waste Water**, 14th Edition, American Public Health Association, Washington, DC, 1976.

CHAPTER 6

Determination of Boron by Sequential Injection Analysis

6.1 Introduction

Boron is one of the trace elements in nature, occurring only in minute concentrations in natural systems. Yet, it is one of the most important trace elements or micronutrients of growing plants. By micronutrient is meant that it is only used in small quantities by plants, but believed to be essential to their nutrition. In biochemical and biomedical research, trace elements are considered to be those elements that are ordinarily present in plant or animal tissue in concentrations comprising less than 0.01 % of the organism. Sources of boron in the terrestrial environment is mainly soil minerals and parent material, fertilizers, irrigation waters, sewage sludges and effluents, and coal combustion.

Sodium tetraborate ($Na_2B_4O_7 \bullet 5H_2O$) and Borax are the most commonly used boron fertilizers. Other sodium borates such as sodium pentaborate ($Na_2B_{10}O_{16} \bullet 10H_2O$) and Solubor, a mix of sodium tetraborate and sodium pentaborate ($Na_2B_4O_7 \bullet 5H_2O + Na_2B_{10}O_{16} \bullet 10H_2O$), are also used but to a lesser extend. Boric acid ($B(OH)_3$) is only used sparingly. Boron deficiencies are normally corrected for by application of these types of fertilizer to the soil. The amount of fertilizer applied to the soil, depends on several factors including plant species, soil type, pH, and other factors.

Toxicologically, boron is not a great concern when compared to other trace elements. Boron concentrations in natural waters are normally in the region of less than 100 $\mu g/\ell$. This is well below the mandatory level of 5.0 $mg.\ell^{-1}$, as well as the desirable upper limit of 1 $mg.\ell^{-1}$ in drinking water. Only at levels above 30 $mg.\ell^{-1}$ does boron start to interfere with the digestive system. Boron content in food stuffs is not of great concern, and it only proved to be toxic at intakes of 4 g and higher per day.

Boron levels in food and drinking water is, therefore, not as important as the level of boron in agricultural soil is to the farmer. Boron deficiency in agricultural soil can lead to huge losses for the farmer, which is easily prevented by correct fertilization. Correct fertilization is only possible with the correct boron concentration in the applied fertilizer.

6.2 Uses of boron

Fertilizers are one of the biggest industrial applications of boron. Another common application is in the glass industry and more recently, insulation products, fire retardants, and glass fibre-reinforced plastics are important consuming sectors of boron, with borax pentahydrate and ulexiteprobertite as the main sources of boron. Boron is also extensively used in the manufacture of textile-grade glass fibres for use in aircraft, motor vehicles, and sport equipment.

Borates are used in the manufacture of borosilicate glass for the glassware, pottery, and enamel industries. It is also used in cleaning and bleaching compounds especially in the production of sodium perborate detergents. Boron compounds, are also used in the manufacture of biological growth control agents for use in water treatment, algicides, herbicides, and insecticides.

Other uses of boron include metallurgical work, nuclear industries, and electroplating. Medically, boric acid is used as a mild antiseptic especially as an eyewash. In earlier times it was also used in the preservation of food. Technologically boron is important because of its application to synthetic organic chemistry. Organo borane compounds are used as chemical intermediates in the manufacture of medicines, as well as in new classes of pesticides [1]

6.3 Properties

Boron belongs to Group III-A of the periodic table, and it is the only non-metal among the plant micronutrients. Boron has an atomic weight of 10.811 $g.mol^{-1}$ and a melting point of 2300 °C [1]. Two stable isotopes occur naturally, ^{10}B (18.98 %) and ^{11}B (18.02 %). At room temperature boron is inert, except to strong oxidising agents such as nitric acid. Borates (eg. Sodium tetraborate, $Na_2B_4O_7 \bullet 5H_2O$) are formed when boron is fused with oxidising alkaline mixtures, such as NaOH and $NaNO_3$.

Boric oxide (B_2O_3) is the only important oxide which is acidic, soluble in water, and forms boric acid ($B(OH)_3$), a very weak acid (pKa = 9.15). Boron occurs naturally primarily as the borates of Ca and Na, of which Borax ($Na_2B_4O_7 \bullet 10H_2O$) is the most common compound, along with boric or boracic acid ($B(OH)_3$). The most important source of boron is the mineral Kernite ($Na_2B_4O_7 \bullet 4H_2O$), an evaporite deposit. Boron almost always occurs in chemical combination with O_2, as a borate, usually coordinated with three O atoms and occasionally with four.

6.4 Natural occurrence

The average concentration of total boron in the earth's crust is about 10 mg.ℓ^{-1}, and boron is the 37 th most abundant among the elements [2]. Concentrations in igneous rock is in the same range, but increase several fold in sedimentary rocks. Commonly observed boron concentrations (mg.ℓ^{-1}) in various environmental matrices are shown in Table 6.1.

Table 6.1 Boron concentrations in various environmental matrices.

Material	Mean (mg.ℓ^{-1})
Basalt (a)	5
Granite (a)	15
Limestone(a)	20
Sandstone (a)	35
Shale (a)	100
Phosphorites (c)	<50
Petroleum (d)	2*
Lignite (c)	70
Animal manures (d)	24
Dolomite lime (d)	4
Lichens (c)	4.1
Fungi (c)	16
Ferns (c)	77
Fresh water (c)	15*
Sea water (c)	4.4

*μg.ℓ^{-1}
(a) Krauskopf (1972) [2]
(b) Trudinger (1979) [3]
(c) Bowen (1979) [4]
(d) Adriano (1986) [1]

Some sedimentary rocks of marine origin can contain up to 500 $mg.\ell^{-1}$ or more boron [5]. Other sources are glacial clay and stratified plain deposits in Byelorussia and Amur, where boron levels between 35 and 70 $mg.\ell^{-1}$ are found. As a general rule, marine clays contain more boron than clays accumulating in lakes or flood plains.

In general, the boron contents of soils are higher than the boron contents of rocks [1]. The reason for this is that weathering of boron containing rocks gives borate in solution, chiefly as the non-ionized boric acid ($B(OH)_3$). Boric acid is a weak acid, pK = 9.14, noted for its volatility even at low temperatures [4]. In natural environments, boron solutions contain primarily boric acid and $B(OH)_4^-$, and the polymeric forms such as tetraborate ($B_4O_7^{2-}$), are likely to occur only in concentrated solutions [1].

6.5 Essentiality of boron in plants

Boron's precise biochemical role in plants is not clear, and it has not been shown to participate in any enzyme activity. That boron is an essential plant nutrient, can be determined by studying the effect of boron deficiency on plants. Plants suffering from a boron deficiency show a decrease in root elongation, followed by degeneration of meristematic tissues as a result of the limited cell division.

Once boron is utilized in the actively growing parts of the plant, it can not be translocated to other parts of the plants. A constant boron supply is, therefore, essential throughout the plant's

growth cycle. Research has also shown that boron is required for formation of new tissue, but apparently not for the maintenance of older tissue. Deficiency is, therefore, more readily noticed in younger plants than older plants.

Boron facilitates the transport of sugars through the cell membranes, involved in auxin metabolism and in the synthesis of nucleic acids and protein. Boron also plays a role in carbohydrate metabolism, and in the synthesis of cell wall components such as polyphenolic compounds [6].

It is also believed that boron plays a part in photosynthetic and transport processes in plants [7,8]. Other purposes of boron include root growth [9], regulation of seed dormancy [10], pectin synthesis, water balance relationships, and resynthesis of ATP [11].

6.6 Choice of analytical method

Several methods exist for the determination of boron in various sample types, for example isotachophoresis [12], ICP AES [13], titrimetric [14], and automated methods such as autoanalysers [15], flow-injection analysis [16], and stopped-flow injection analysis [17]. All these methods, except for the automated methods, are fairly time consuming and are, therefore, not ideally suited for industrial use. The automated methods have the advantage of possible automatic in-line sampling and analysis, making it a time and labour saving method of analysis. With the added advantages of sequential injection analysis, it is possible to design a boron analyser that is both convenient and economical.

6.7 Choice of chromogenic reagent

Sequential injection analysis coupled with a spectrophotometer is a relatively simple analytical technique. For the spectrophotometric determination of boron, several specific and sensitive colorimetric reagents have been developed [18-21]. These reagents include hydroxyanthraquinone reagents such as quinalizarin(1,2,5,8-tetrahydroxyanthraquinone) [18] and carminic acid [19], as well as other anthraquinones and their derivatives such as rufigallic acid [20] and curcumin [21].

All the above mentioned methods make use of concentrated sulphuric acid mediums, requiring expensive "Acidflex" tubing in the sequential injection manifold to withstand such acidic conditions. They also require exact acid concentrations, temperatures and heating times for optimum performance. A chromotropic acid method that was suitable for automation was developed in 1957 by James and King [22], but difficulties were experienced as both the reagent and the borate-chromotropate components were sensitive to light.

Petrovsky [23] suggested the use of Azomethine-H as a chromogenic reagent. Azomethine-H is the condensation product of salicylaldehide and H-acid (8-amino-1-naphtol-3,6-disulphonic acid). This reagent is used in aqueous solution, and is ideally suited for use in sequential injection analysis systems that utilise normal tubing.

6.8 Reaction principles

Azomethine-H is a yellowish reagent, that dissociates in aqueous solutions according to

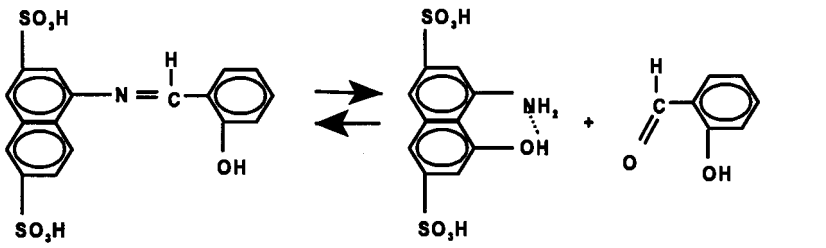

AZOMETHINE-H **H-ACID** **SALICYLALDEHIDE**

With the dissociation of Azomethine - H, the solution obtains a less intense yellow colour as a result of the formation of one of the dissociation products, H-acid. Azomethine-H has a more intense yellow colour than H-acid. When boric acid is added to the solution, the existing equilibrium is displaced towards the left, increasing the intensity of the yellow colour (Azomethine-H), proportional to the boron concentration. This displacement is totally dependant on the pH of the aqueous solution, and could be very slow at the incorrect pH.

6.9 Determination of boron by sequential injection analysis

6.9.1 Experimental

6.9.1.1 Reagents and solutions

Only analytical-reagent grade reagents were used unless specified otherwise. Deionised water, supplied by a Modulab system (Continental Water Systems, San Antonio, TX, USA), was used to prepare aqueous solutions.. The solutions were degassed, by boiling it in a microwave oven, before introduction into the system and it was stored in an oxygen free environment when not in use.

Standard boron solution: The standard boron solution was made up by dissolving 1.143 g of boric acid in 1 ℓ of de-ionised water. This solution was stored in a polythene container, and used to prepare working boron standards by suitable dilutions with 0.1 mol.ℓ^{-1} hydrochloric acid [15].

Buffer solution: The buffer solution was prepared by dissolving 132 g of ammonium phosphate and 25 g of disodium EDTA in 500 mℓ of de-ionised water. The pH of this solution was adjusted to 7.0 with an alkali addition [16].

Carrier solution: The carrier solution was prepared by adding 11.4 mℓ of 32 % (v/v) hydrochloric acid to de-ionised water and diluting it to 1 ℓ.

Chromogenic reagent: The Azomethine-H (Azo-H) solution was prepared by dissolving 0.163 g Azomethine-H, 0.500 g disodium EDTA and 0.500 g ascorbic acid in 2.0 mℓ of warm de-ionised water (50°C). This solution was stirred, diluted to 25 mℓ with cold de-ionised water and stored in a polythene container.

Liquid fertilizer: The liquid fertilizer was prepared by diluting 1mℓ of liquid fertilizer with 20 mℓ of de-ionised water. The solution was filtered to get rid of any solid substances that formed during the dilution.

6.9.1.2 Equipment

The sequential injection manifold used, is shown in Fig. 6.1. The system consisted of a Gilson Minipuls peristaltic pump (Gilson, Villiers-le-Bel, France), operating at a speed of 17 rpm with a pumping tube inside diameter of 1.85 mm. The pump was connected to a holding coil (HC), consisting of 0.76 mm inside diameter Tygon tubing wound around a Perspex tube with an outside diameter of 10 mm.

The holding coil was connected to the first reaction coil (RC 1). Tygon tubing with an inside diameter of 0.76 mm wound around a 10 mm perspex tube was used as RC 1. RC 1 was connected to a 10 port electrically actuated selection valve (Model ECSD10P, Valco Instruments, Houston, TX, USA), using Tygon tubing with 0.76 mm inside diameter. The second reaction coil (RC 2) connected the selection valve and spectrophotometer, and consisted of 0.76 mm inside diameter Teflon tubing wound around a 12.5 mm Perspex tube.

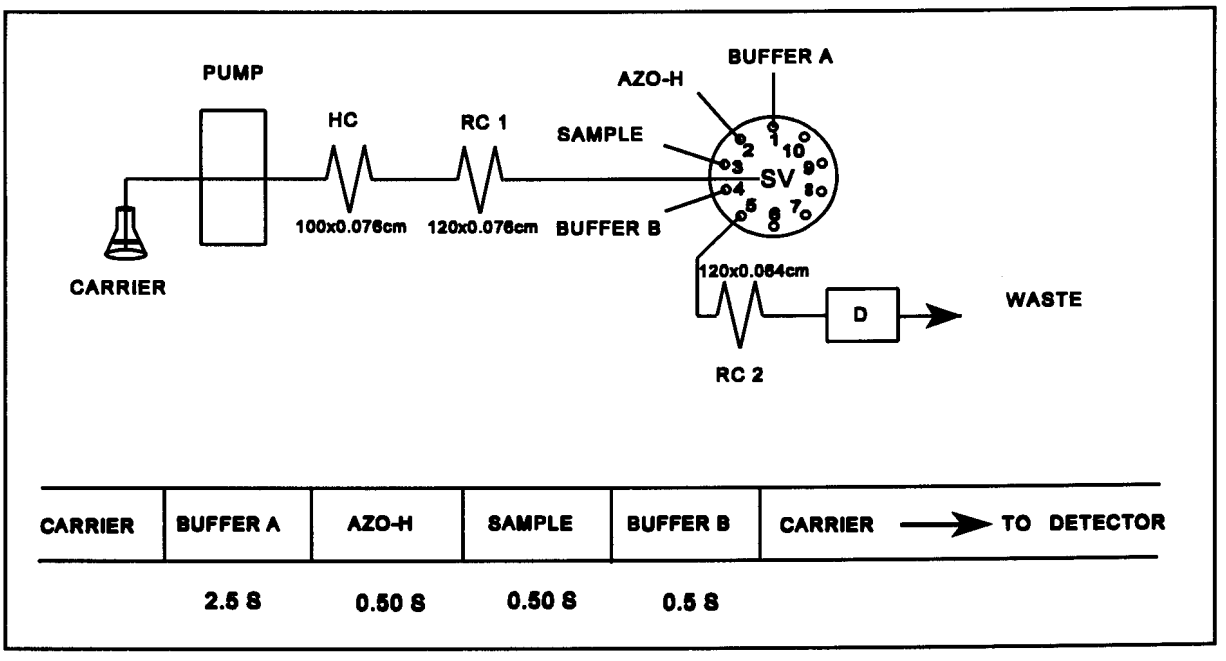

Fig. 6.1 Sequential injection manifold for the determination of boron. Buffer A, Azo-H, sample, and buffer B solution plugs are aspirated through the sequential valve (SV) into the first reaction coil (RC 1). Carrier solution, propelled by the peristaltic pump through the holding coil (HC), flushes the reacted zone towards the detector (D) and waste, via the second reaction coil (RC 2).

A Unicam 8625 UV-Visible spectrophotometer, equipped with a Hellma type flow through cell (volume 80 $\mu\ell$) was used as detector. The absorbance was measured at 420 nm. Data acquisition and device control were achieved by using a PC30-B interface board (Eagle Electric, Cape Town, South Africa) as well as an assembled distribution board (MINTEK, Randburg, South Africa). The FlowTEK software package (MINTEK, Randburg, South Africa), for computer-aided flow-analysis, was used throughout for device control and data acquisition.

6.9.1.3 Procedure

The device sequence for the determination of boron by sequential injection is presented in Table 6.2. The sequential injection system depicted in Fig 6.1 involved ports 1 to 5 of the selection valve.

Table 6.2 Device sequence for a full cycle of the sequential injection system for boron determination.

Time (s)	Pump	Valve	Description
0.00	Reverse	Buffer A	Draw up buffer A solution
2.50	Off		Pump stop
3.00		Azo-H	Valve selects Azo-H solution
3.50	Reverse		Draw up Azo-H solution
7.10	Off		Pump stop
7.60		Sample	Valve selects sample solution
8.10	Reverse		Draw up sample solution
10.60	Off		Pump stop
11.10		Buffer B	Valve selects buffer B solution
11.60	Reverse		Draw up buffer B solution
13.60	Off		Pump stop
14.10		Detector	Valve selects detector position
44.10	Forward		Pump stacked zones to detector
120.00	Off		Pump stop
120.50		Home	Return valve to starting position

6.10 Method optimisation

6.10.1 Physical parameters

Physical parameters were evaluated by comparing the sensitivity (degree of zone penetration) and precision (reproducibility of zone penetration) obtained for the different parameter changes. The following physical parameters were optimised: flow rate, holding coil (tube inside diameter), reaction coil 1(tube inside diameter, and tube length), reaction coil 2 (tube inside diameter, tube length) and temperature. All physical parameters were optimised by using the actual reagents used in the determination of boron.

6.10.1.1 Flow rate

The flow rate plays an influential role in the dispersion of the reacting zones, and therefore the sensitivity and precision (% RSD) of the analytical method. Flow rates were varied between 2.08 mℓ.min^{-1} and 4.34 mℓ.min^{-1}, by changing the speed at which the pump head rotates while the inside diameter of the pump tube is kept constant (Table 6.3, Fig. 6.2).

An increase in the flow rate increased the sensitivity of the method up to a flow rate of 3.81 mℓ.min^{-1}. With higher flow rates no useful increase in intensity was observed. The precision improved with an increase in the flow rate, up to a value of 0.76 % for a flow rate of 3.81 mℓ.min^{-1} and deteriorated for higher flow rates as a result of back pressure that developed in the system. Therefore, a flow rate of 3.81 mℓ.min^{-1} was chosen as the optimum flow rate.

Table 6.3 Effect of an increased flow rate on peak height (sensitivity) and % RSD (precision).

Flow rate (mℓ.min^{-1})	Peak height	% RSD
2.08	2.32	2.17
2.32	2.94	1.94
2.59	3.85	1.90
2.85	4.48	1.87
3.06	4.82	1.91
3.31	5.33	1.54
3.56	5.86	0.83
3.81	6.13	0.76
4.07	6.21	1.27
4.34	6.30	2.27

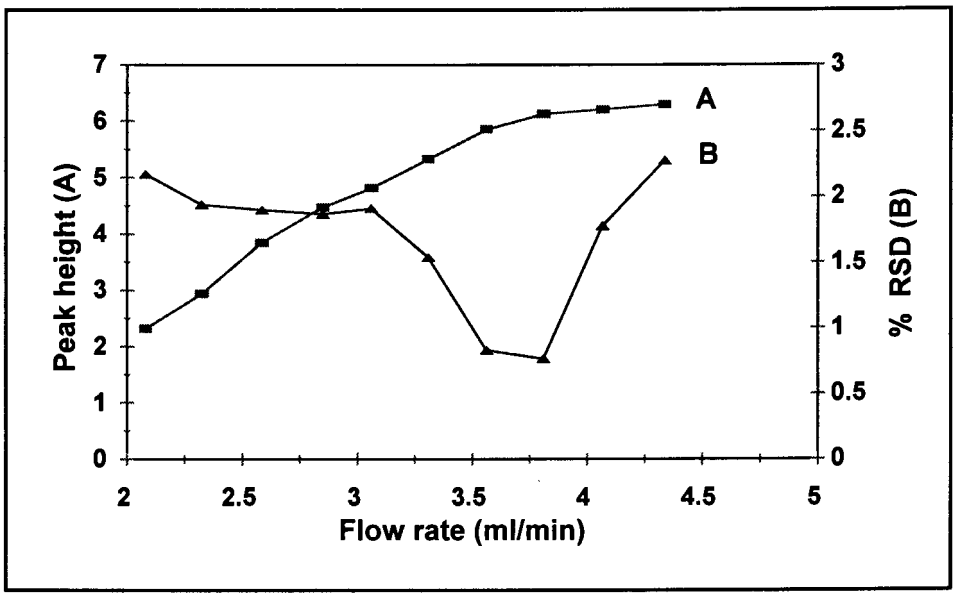

Fig. 6.2 Effect of an increased flow rate on peak height (sensitivity) and % RSD (precision).

6.10.1.2 Holding coil/RC 1

In sequential injection analysis it is possible to use the first reaction coil (RC 1, Fig 6.1) as both a reaction coil and a holding coil, by simply elongating the first reaction coil. In such a case, RC 1 has to be large enough to contain the whole aspirated zone, as well as prevent any part of the dispersed zone from penetrating the peristaltic pump. This type of setup was used in the optimisation of this method.

For the optimisation of the reaction coil's inside diameter, the minimum required length for each diameter was determined before optimising the inside diameter, to ensure that none of the analytical zones enter the peristaltic pump. A coil length of 120 cm was sufficient for the diameters used in the optimisationof the coil diameter. Diameters between 0.64 and 1.60 mm were used in the optimisation with the following results:

Table 6.3 Influence of RC 1 inside diameter on peak height (sensitivity) and % RSD (precision).

Inside diameter (mm)	**0.64**	**0.76**	**0.89**	**1.02**	**1.14**	**1.60**
Peak height	4.23	4.30	4.32	4.30	4.27	4.28
% RSD	1.85	1.56	1.35	1.20	1.25	1.26

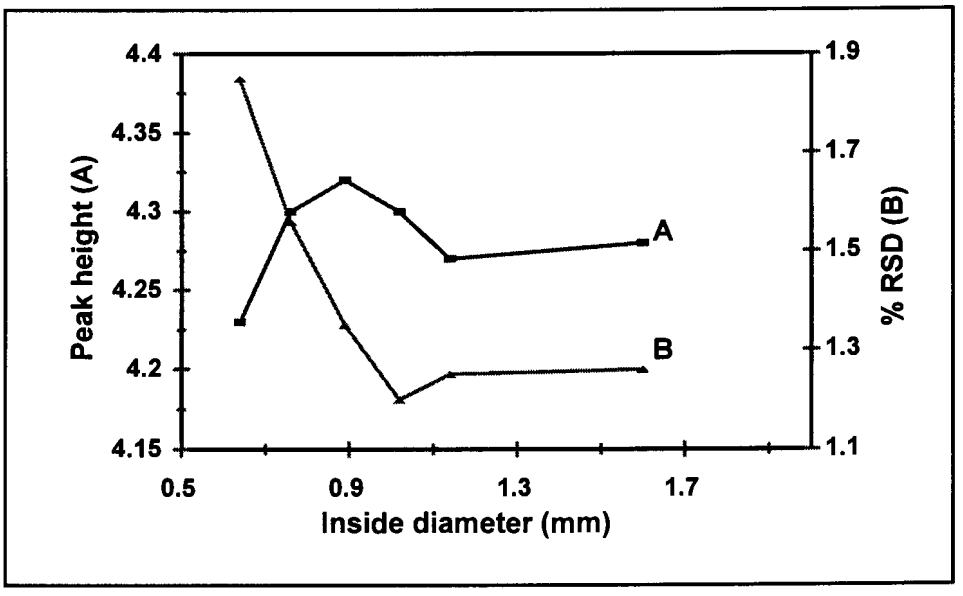

Fig. 6.3 Influence of reaction coil 1's inside diameter on peak height (A) and precision (B)

The 0.76 mm tube diameter was chosen for its superior presicion. With tube inside diameters larger than 0.89 mm the dispersion increased noticeably, indicated as a decrease in the peak height in Fig 6.3. The tube with the smaller inside diameter (0.64 mm) resulted in a significant decrease in the precision.

6.10.1.3 Reaction coil 2

The second reaction coil connects the selection valve to the detector. The reacted zones normally flow non-stop through this reactor to the detector (Fig. 6.1). This reactor's length is measured from the selection valve outlet, to the point of detection in the flow cell. The tube inside diameter, tube length, as well as the geometry of the coil were optimised.

6.10.1.3.1 Tube diameter

The shift of the Azo-H : H-acid equilibrium towards the more intensely coloured Azo-H compound requires a certain amount of time. The procedure of the proposed boron method was setup in such a way that the shift towards Azo-H was complete when the reacted zone entered RC 2. Therefore , limited dispersion (D < 2) was needed in RC 2. Tube inside diameters were varied between 0.38 mm and 0.89 mm, with the results shown in Table 6.4 and Fig. 6 4.

Table 6.4 Influence of the tube diameter on peak height (sensitivity) and precision (% RSD) of RC 2.

Inside diameter (mm)	**0.38**	**0.51**	**0.64**	**0.76**	**0.89**
Peak height	4.27	5.60	6.08	5.49	4.89
%RSD	3.58	1.25	0.37	0.82	0.48

According to Fig 6.4 and Table 6.4, the sensitivity of the method increased with an increase in the tube diameter up to 0.64 mm (6.08 units), and decreased again for diameters larger than 0.64 mm. The precision increased (% RSD decrease) for diameters up to 0.64 mm (0.37 %) and levelled off at larger diameters. The 0.64 mm diameter was chosen as the optimum tube diameter for its combination of high sensitivity and precision.

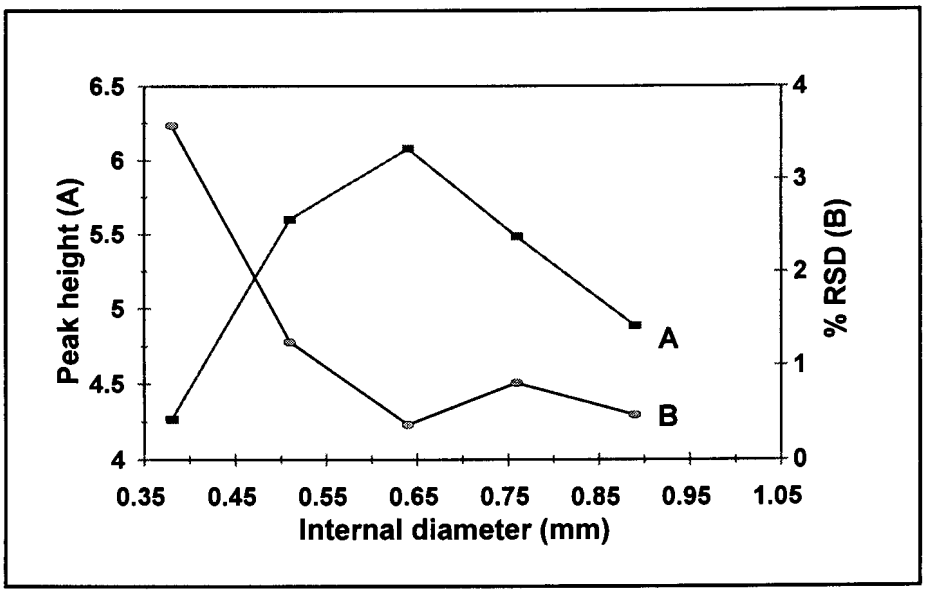

Fig. 6.4 Influence of RC 2 tube diameter on peak height (A) and % RSD (B).

6.10.1.3.2 Coil length

Under non-ideal conditions the colorimetric reaction used in this method can take up to 800 seconds (see reaction kinetics, Sec. 6.10.1.8), to complete. Therefore, longer reaction times favour this reaction. An increase in the coil length of RC 2 leads to an increase in the residence time of reacting zones in the manifold, allowing the reaction more time to complete. In the first minute the reaction is taking place particularly fast, and a small variation in time within the first minute, leads to a significant difference in the sensitivity of the method.

One way of increasing the reaction time by using the proposed method, is to change the length of RC 2. To determine the optimum length for the proposed method, RC 2's length was varied between 100 and 140 cm. The results is shown in Table 6.5 and Fig. 6.5. According to Fig. 6.5, the suggested method's sensitivity increased (Fig 6.5) by using tube lengths up to 110 cm and decreased for lengths longer than 110 cm. Longer coil lengths only increased the dispersion of the reacting zones, resulting in lower sensitivities.

The precision showed the same tendency as the sensitivity, and increased with tube length. It is possible to explain this if one keeps the reaction kinetics mentioned earlier in mind. With a short reaction time, especially below one minute, a small variation in the reaction time leads to a significant variation in the sensitivity. If the reaction time is, for example, longer than 600 seconds (Fig. 6.6) the influence of a small variation in time on the peak height is insignificant. The best combination of results (peak height = 0.28 units, %RSD = 0.88) were obtained by using a tube length of 120 cm.

Table 6.5 Influence of coil length on peak height (sensitivity) and % RSD (precision).

Length (cm)	**100**	**110**	**120**	**130**	**140**
Peak height	0.23	0.29	0.28	0.27	0.26
% RSD	1.77	1.38	0.88	1.20	2.07

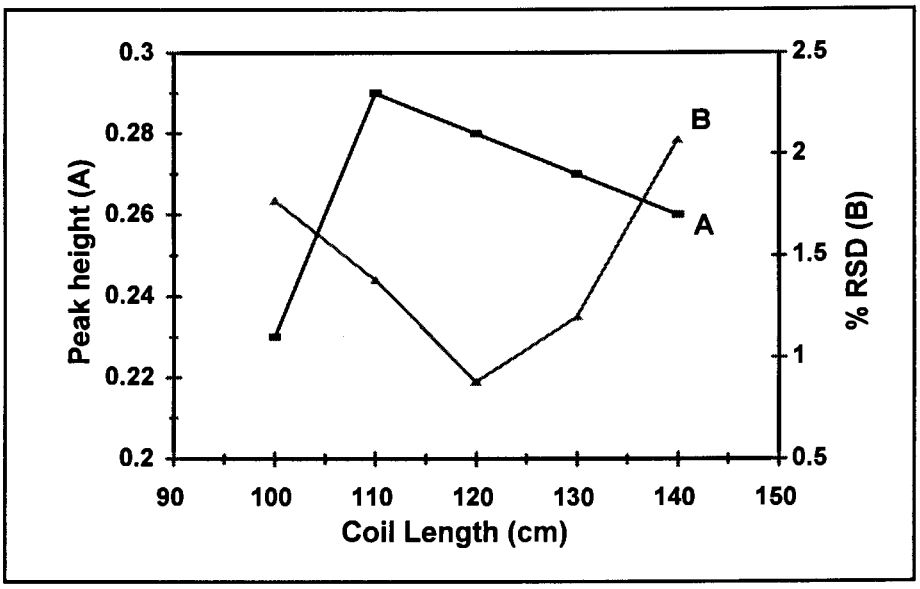

Fig. 6.5 Influence of RC 2's length on peak height (A) and %RSD (B).

6.10.1.3.3 Coil geometry

The second reaction coil's geometry plays an important role in the limitation of the dispersion that takes place in the first reaction coil (RC 1). From the previous study (Chapter 5) of the three possible geometries (straight, coiled, knitted), it was clear that the coiled geometry gave the best results. A coiled second reaction coil was therefore used for the rest of the optimisations.

6.10.1.4 Uptake tubes

The uptake tube diameter and length was optimised in Chapter 4 (Sec. 4.8.1.5), for the determination of nitrite (1.01 mm i.d. x 30 cm). Since the influence of the uptake tube diameter is independent of the reaction, it was not necessary to re-optimise the uptake tubes for this method.

6.10.1.5 Order of injection

With the optimisation of the nitrite and nitrate methods, the order of injection did not have a great influence on neither the precision nor the sensitivity. With the determination of boron, it did however play an important role, influencing both the precision and sensitivity. The three possible injection sequences, with the respective results obtained are shown in Table 6.6. If the sample was aspirated before the Azo-H solution, the peak height increased for the first 10 runs and then stabilized (method 1). In the reverse order, that is Azo-H aspirated first and then the sample (method 2), the peak height stabilized within 3 runs. This is possibly an indication of sample carry-over that took place with the former sequence, since the distance the sample travels within RC 1 is shorter and a slightly larger volume (the volume of Azo-H is additional) of reagents are used to flush out the sample with the second method. With Azo-H aspirated first, less sample is carried over to the next cycle, and the peak height stabilizes within three runs. With the sample sandwiched between two Azo-H plugs (method 3), with a total volume equal to the Azo-H volumes used in methods 1 and 2, both the precision and sensitivity decreased. The effect of order of injection on precision (% RSD) and sensitivity (peak height) is evident from Table 6.6, with best results (Peak height = 3.24, %RSD = 0.85) obtained by using the second order of injection.

Table 6.6 Effect of order of injection on peak height (sensitivity) and %RSD (precision).

Order of Injection	Peak height	%RSD
1) Buffer A - Sample - Azo-H - Buffer B	2.75	1.65
2) Buffer A - Azo-H - Sample - Buffer B	3.24	0.85
3) Buffer A - Azo-H - Sample - Azo-H - Buffer B	2.96	4.54

6.10.1.6 Temperature

According to both Chen *et al* [24] and Basson *et al* [15], the temperature has no effect on sensitivity and precision at temperatures below 35 °C. Basson [15] observed that at temperatures above 40 °C the percentage transmission increased, absorbance decreased, and therefore, sensitivity decreased. When the temperature of the suggested method was raised, it had a similar effect than that experienced by Basson. Room temperature is, therefore, suggested for the proposed method.

6.10.1.7 Reaction kinetics

One of the most convenient advantages of sequential injection analysis is the fact that the sample and reagent zones can be stopped within the detector. Fig. 6.6 was obtained by stopping the flow when the reacting zone was within the detector. The peak height increased as more of the product was formed. After 800 seconds, only a small amount of product was formed over a large period of time. Most of the product formed within the first two minutes, and therefore the total cycle should be at least two minutes in length to allow sufficient product to be formed.

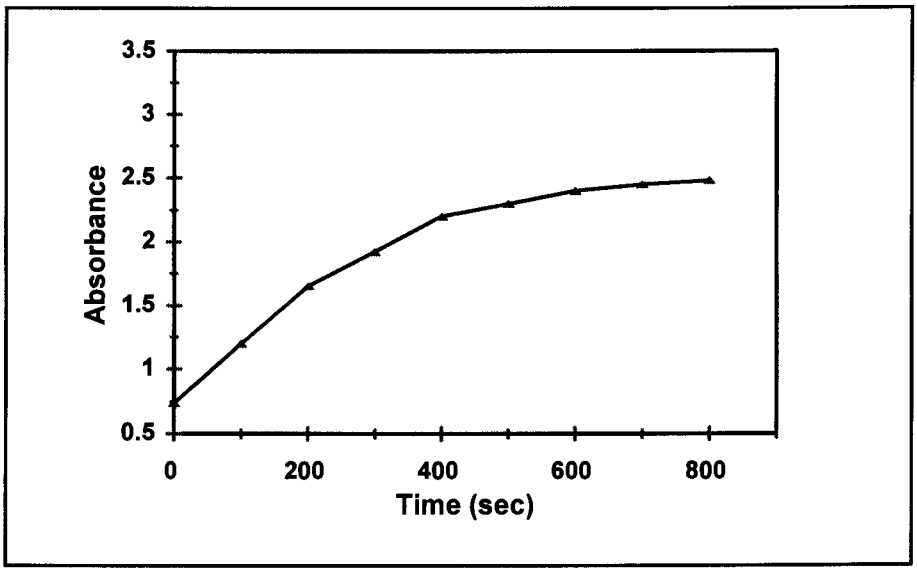

Fig. 6.6 Influence of time on absorbance at a pH of 6.0.

According to Fig. 6.6 the reaction takes about 800 sec (13 min) to obtain its maximum absorbance at a pH of 6.0. At pH 7.3, the optimal pH, only one sixth of the time (2 min) was needed for the reaction to go to completion, while more or less the same sensitivity was obtained. The influence of the pH on reaction kinetics is discussed in section 6.10.2.3.

6.10.2 Chemical parameters

The reaction between boric acid and Azo-H is heavily dependant on the chemical parameters that influence the kinetics, precision, and sensitivity of the method. Although the carrier solution, buffer, Azomethine-H and sample concentrations influence the above mentioned parameters, the pH at which the reaction takes place is possibly the most important chemical parameter of this method. In order to determine the optimum conditions of the reaction, the solutions affecting the pH should be optimised. The solutions that had to be optimised were the carrier stream, chromogenic reagent, Azomethine-H, ascorbic acid and the buffer solution.

6.10.2.1 Carrier stream

The carrier stream is used to flush the reacted zone towards the detector, and is not used to influence the reaction in any specific way. Several workers [16, 17, 24, 25] used a 0.1 mol.ℓ^{-1} hydrochloric acid carrier solution in conjunction with the Azomethine-H chromogenic reagent. De-ionised water may be used as an alternative solution, but the carry-over increased slightly when compared to the carry-over of the 0.1 mol.ℓ^{-1} hydrochloric acid solution.

6.10.2.2 Chromogenic reagent

Two chromogenic reagent preparation methods were evaluated in the optimisation of the chromogenic reagent. The first method is that of Chen *et al* [24], where Azo-H is dissolved in de-ionised water at 50°C and diluted to 100 mℓ. The second method is that of Krug *et al* [16] where 2 g of ascorbic acid is diluted in 40 mℓ de-ionised water, at 50°C, into which Azo-H is then dissolved. The best sensitivity was obtained by using Krug's method, and therefore this method was used to prepare the chromogenic reagent

6.10.2.2.1 Azomethine-H

Azomethine-H concentrations between 0.010 and 0.045 mol.ℓ^{-1} were evaluated, with the results shown in Table 6.7 and Fig. 6.7.

Table 6.7 Influence of Azo-H concentration on peak height (sensitivity) and % RSD (precision).

Concentration (x10^{-2} mol.ℓ^{-1})	1.010	1.123	1.235	1.347	1.459
Peak height	0.76	0.97	1.08	1.35	1.42
%RSD	2.32	1.96	1.04	1.21	1.14

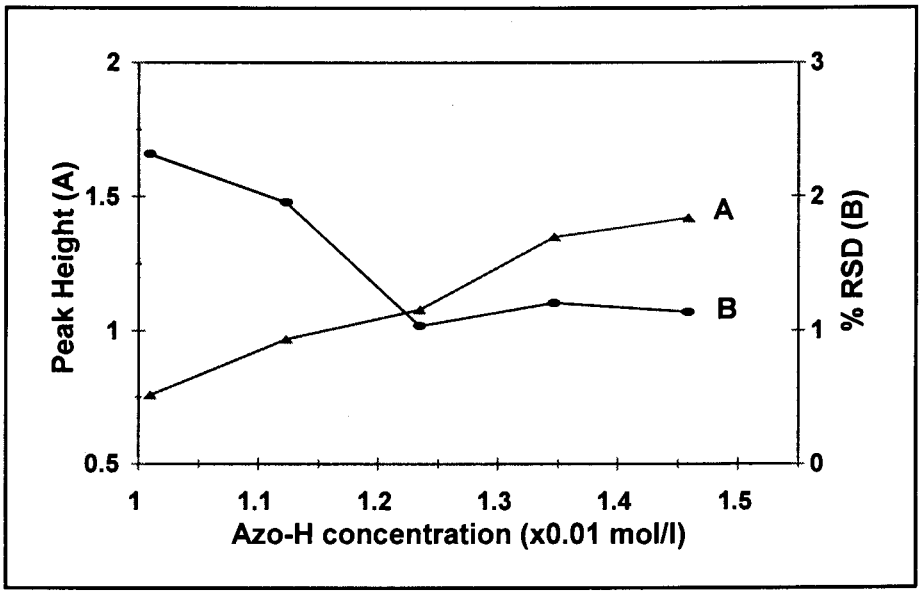

Fig. 6.7 Influence of Azo-H concentration on peak height (sensitivity) and % RSD (precision)

The linear relationship between the sensitivity (peak height) and the Azo-H concentration, obtained by other authors [16, 17], was also obtained with the proposed SIA method. An Azo-H concentration of 1.459 x 10^{-2} mol.ℓ^{-1} had the best sensitivity with good precision (1.14 %). For concentrations higher than this, the Azo-H did not dissolve completely and difficulty was experienced in obtaining a clear solution.

The chromogenic reagent volume was optimised next. The volumes were varied between 0 and 407 $\mu\ell$ with the results shown in Table 6.8 and Fig. 6.8.

Table 6.8 Influence of Azo-H volume on peak height and precision (% RSD).

Volume ($\mu\ell$)	Peak height	% RSD
0	6.03	1.29
41	5.79	1.03
81	5.72	1.03
122	5.83	1.00
163	5.94	1.02
203	6.13	1.40
244	5.86	2.32
285	5.66	1.92
325	5.60	1.99
366	5.30	3.21
407	5.20	2.65

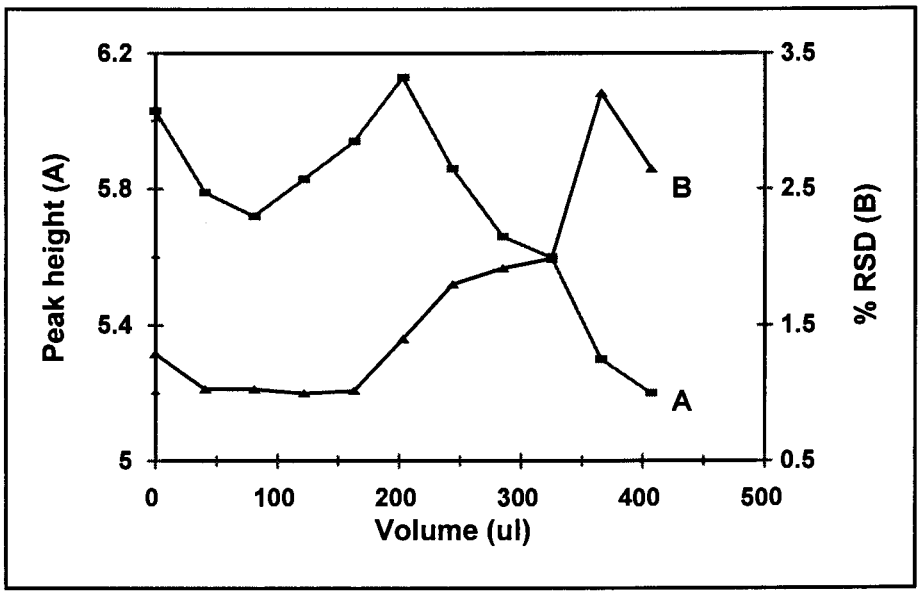

Figure 6.8 Influence of Azo-H volume on peak height (A), and precision (B).

The sensitivity increased slightly from a peak height of 6.03 to a value of 6.13 units for a volume of 203 $\mu\ell$ and decreased (% RSD increased) for larger volumes, The reason for this is not clear. The precision stayed more of less constant for volumes up to 163 $\mu\ell$, and decreased for larger volumes. A volume of 203 $\mu\ell$ of Azo-H was chosen as optimum for the proposed method.

6.10.2.2.2 Ascorbic acid

The ascorbic acid, which is added to the chromogenic reagent, alters the pH of the solution and should therefore influence the kinetics of the reaction. Variation of the ascorbic acid concentration between 2.84 x 10^{-2} and 1.70 x 10^{-1} mol.ℓ^{-1} revealed no definite relationship between the sensitivity, precision and concentration. The concentration proposed by Krug *et al* [16], 1.14 x 10^{-1} mol.l^{-1}, was therefore used in the preparation of the chromogenic reagent.

6.10.2.3 Buffer solution

The Azo-H solution is normally buffered with ammonium acetate [15], $(NH_4)_2HPO_4$ [16] and $(NH_4)H_2PO_4$ [26] or combinations [25] of these compounds. The buffer proposed by Krug *et al* [16], 132 g $(NH_4)_2HPO_4$ and 25 g disodium EDTA in 500 mℓ de-ionised water, did not have any side effects when used with the SIA system.

The first buffer solution parameter that had to be optimised was the pH of the buffer. Krug *et al* [16] suggested a pH of 7.3, while others [25, 26] suggested pH values between 5.1 and 7.6. At pH values below 6.0 the results were poor and inconsistent, while pH values between 6.0 and 7.3 gave much better results (Table 6.9, Fig 6.9).

Table 6.9 Influence of buffer pH on peak height (sensitivity) and % RSD (precision).

pH	Peak height	% RSD
6.00	1.91	3.31
6.27	3.07	0.81
6.57	4.27	0.76
6.77	5.01	1.10
6.94	5.69	0.63
7.10	6.09	0.58
7.30	6.50	0.87

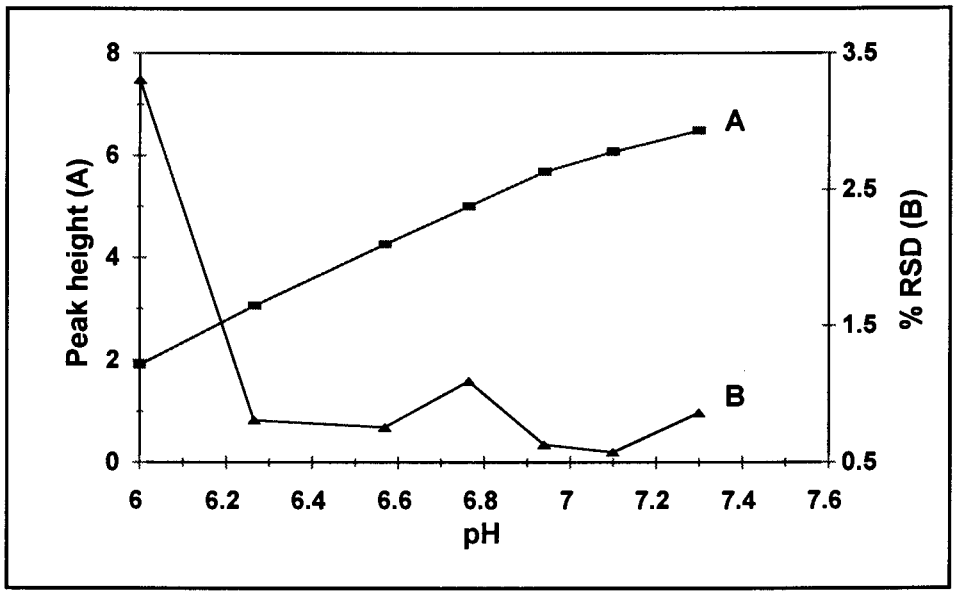

Fig. 6.9 Influence of pH on peak height (sensitivity) (A) and % RSD (precision) (B).

The pH curve in Fig 6.9 indicates that an increase in the pH was beneficial to the reaction. At pH levels above 7.1, sensitivity increased less with the same increase in pH. At pH levels above 7.3 worse values of the %RSD were anticipated. The precision was influenced in the same way as the sensitivity, with very low accuracy at pH levels below 6.2. The best precision (0.58 %) was obtained at pH 7.1 and this pH value was used for the buffer solution in further optimisations

of the proposed SIA system.

The kinetics of the colour forming reaction is dependent on the pH of the buffer. At a pH of 5.0, the reaction is complete within 2 hours, whereas at pH 7.3 maximum absorbance is obtained within 2 minutes [16]. The buffer solution was introduced into the system in front of the Azo-H plug (buffer A), as well as behind the sample plug (buffer B, Fig. 6.1). A change in volume of any one of these buffer zones, influenced the sensitivity and precision of the method, which consequently required that the two buffer volumes be optimized separately. The results of this optimization is shown in Table 6.10 and Fig 6.10.

Table 6.10 Influence of different buffer volumes on peak height (sensitivity) and % RSD (precision).

Volume (mℓ)		**0.000**	**0.025**	**0.050**	**0.075**	**0.100**	**0.125**
Buffer A	**Peak height**	0.62	1.10	1.96	3.11	3.86	4.47
	%RSD	5.72	3.95	1.46	1.10	0.58	0.76
Buffer B	**Peak height**	2.27	2.84	3.16	3.53	3.79	4.03
	%RSD	4.48	2.88	1.67	1.38	0.88	1.20

The influence of both the buffer volumes on the reaction is clearly shown in Fig 6.10. Little or no buffer resulted into very low precision values (high % RSD) and sensitivity. As the buffer volumes were increased, these two parameters improved accordingly for both the buffer zones, although the buffer volume had the greatest effect on the parameters of buffer A. The best results were obtained with a volume of 0.125 mℓ for buffer A, and 0.100 mℓ for buffer B. Buffer A should have a greater volume, since this buffer is aspirated first and consequently undergoes more dispersion, requiring a larger volume to deliver the same amount of buffering.

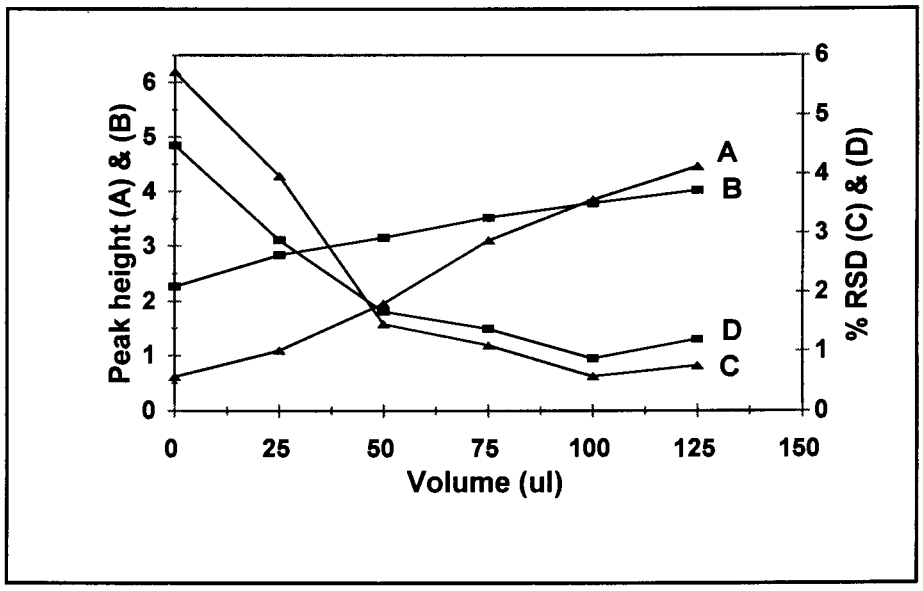

Fig. 6.10 Influence of the buffer volume on the peak height and %RSD of the proposed method. For buffer A the peak height is represented by graph A and the %RSD by graph C. For buffer B the peak height is represented by graph B and the %RSD by graph D.

6.10.2.4 Disodium EDTA

EDTA is used as a masking agent in the determination of boron [15]. Other possible masking agents include potassium cyanide, thioglycollic acid, oxalate, and citrate. EDTA is the most effective complexing agent for removing large amounts of interfering metals. The EDTA concentration should be high enough to mask possible interfering elements, but low enough not to effect the reaction itself. A 20 $g.\ell^{-1}$ disodium EDTA solution proved to be most effective, with little influence on the reaction. EDTA should be able to mask the metal ions present in both the micro and macro-nutrients in liquid fertilizers

6.10.2.5 Sample

The sample volume had to be optimised in order to determine the optimum sample to chromogenic reagent ratio. The sample volume was optimised at an optimum flow rate of 3.0 $m\ell.min^{-1}$, by changing the time at which the sample is drawn up. The results obtained is shown in Table 6.11 and Fig. 6.11. According to the results, the sensitivity did not improve much at volumes larger than 125 μl although a small increase in the precision was observed.

Table 6.11 Optimisation of sample volume and its influence on peak height and % RSD.

Volume ($\mu\ell$)	0	25	50	75	100	125	150
Peak height	2.27	2.84	3.16	3.53	3.79	4.03	4.05
% RSD	4.48	2.88	1.67	1.38	1.20	0.88	0.60

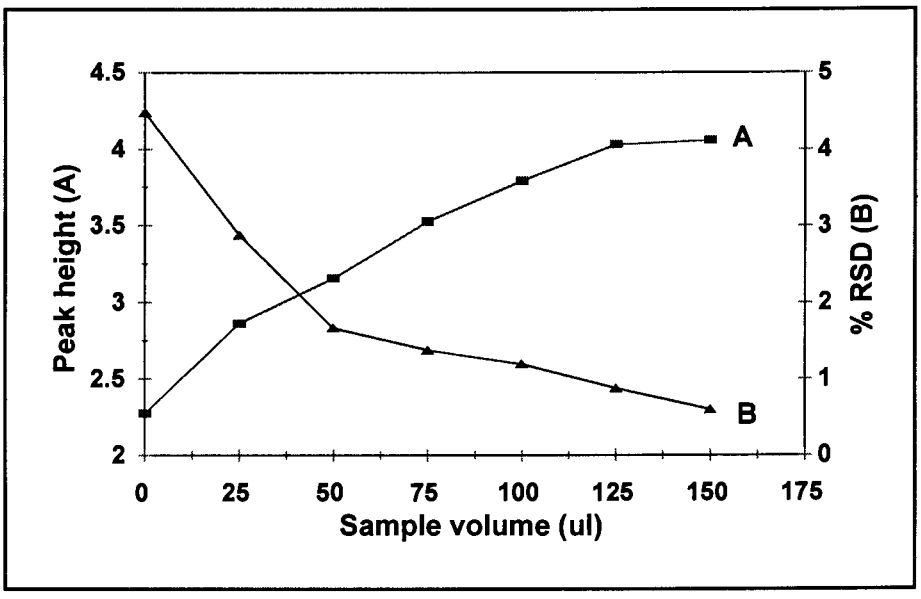

Fig. 6.11 Influence of sample volume on peak height(A) and % RSD (B).

6.11 Evaluation of method

One of the most important factors of an analytical instrument, for the user, is its capabilities and limitations. In order to determine this, the system developed in this chapter, had to be evaluated. In its optimised form the system consisted of a peristaltic pump, pumping at a rate of 3.81 mℓ.min^{-1}. The holding coil/RC 1 combination consisted of 0.76 mm inside diameter tubing with a total length of 220 cm. RC 2 consisted of 0.64 mm inside diameter tubing with a length total of 120 cm.

6.11.1 Linearity

The linearity of the SIA system was evaluated under the optimum operating conditions. The relationship between the relative peak height and boron concentration was:

$$y = 0.0504x + 1.496 \; ; \; r = 0.997$$

where y = relative peak height and x = boron concentration in mg.ℓ$^{-1}$. According to Fig. 6.12, and the above mentioned equation, the calibration graph is linear for boron concentrations between 0 and 100 mg.ℓ$^{-1}$. The absorbance obtained in the absence of boron is the result of the differences in the refractive indices of the carrier stream, chromogenic reagent and the buffer solutions, as well as the absorbance of H-acid in the solution which absorbs at the same wavelength as Azo-H.

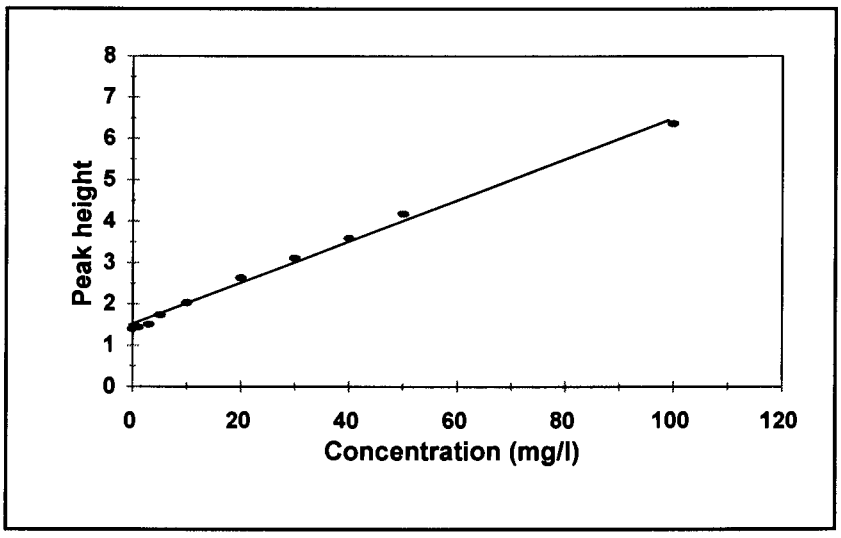

Fig. 6.12 Calibration graph for the proposed SIA method.

6.11.2 Accuracy

Samples spiked with boric acid,were analysed by the proposed SIA system to determine the accuracy. The results obtained with the SIA system, were compared to those obtained by using a standard procedure [27]. The results shown in Table 6.12, revealed a good correlation between the two methods.

Table 6.12 Comparison of results obtained with the proposed SIA method and a standard method of boron determination.

Sample	SIA method (mg.ℓ$^{-1}$ boron)	Standard method (mg.ℓ$^{-1}$ boron)
Water sample A	0.96	0.90
Water sample B	0.78	0.78
Water sample C	1.05	1.02
Water sample D	0.90	0.93
Water sample E	0.87	0.84
Spiked water sample A	2.54	2.48
Spiked water sample B	5.09	4.97
Liquid fertilizer	37.4	35.8

6.11.3 Precision

The precision of the optimised method was determined by 10 repetitive analyses of a number of standard boron solutions and samples, as indicated in Table 6.13. In all cases, the RSD was below 1.59 % with a best case of 0.56 %. The method proved to be more precise at higher boron concentrations, but the precision at lower concentrations is well below 2.0 %.

Table 6.13 Precision of the proposed SIA system.

Sample/Standard Concentration (mg/ℓ)	% RSD
1.0	1.59
3.0	1.32
5.0	1.32
10	1.17
20	0.82
30	1.16
40	0.64
50	0.82
100	0.56
Liquid fertilizer	0.81

6.11.4 Detection Limit

The detection limit of the proposed method was determined via the following formula:

$$Detection\ limit = \frac{(3\sigma + K)(K - c)}{m} \quad \textbf{(1)}$$

where σ is the relative standard deviation of the baseline (2.12), K is the average signal value of the baseline (1.50), c is the intercept (1.496) and m is the slope of the calibration graph (0.0504). With the above mentioned formula, a detection limit of 0.62 $mg.\ell^{-1}$ was obtained.

6.11.5 Interferences

Basson [15] and his co-workers tested the following ions for interferences: copper(II), iron(II), manganese(II), sink(II), calcium, magnesium, aluminium, sodium, potassium, phosphate, sulphate, and nitrate.

Table 6.14 Effect of some ions and anions on peak height of boron determination.

Sample (50 mg.ℓ^{-1} B + X mg.ℓ^{-1})	Without EDTA	With EDTA (2%)
No ions added	4.86	4.74
50 Ca^{2+}	4.05	4.75
100 Ca^{2+}	3.50	4.66
1000 Ca^{2+}	3.35	4.58
50 Mg^{2+}	3.40	4.32
100 Mg^{2+}	3.63	4.60
500 Mg^{2+}	3.60	4.59
50 Zn(II)	3.94	4.10
100 Zn(II)	3.70	4.03
50 NO_3^-	3.63	4.53
100 NO_3^-	3.70	4.58
500 NO_3^-	3.69	4.49
50 SO_4^{2-}	3.82	4.45
100 SO_4^{2-}	3.49	4.41
500 SO_4^{2-}	3.45	4.39
50 K^+	3.45	4.58
100 K^+	3.58	4.72

Sample (50 mg.ℓ^{-1} B + X mg.ℓ^{-1})	Without EDTA	With EDTA (2%)
500 K^+	3.14	4.18

Since the proposed SIA method was developed for use in the fertilizer industry where fertilizers contain a number of different elements, the effect of some common elements present in fertilizers were studied, with the results shown in Table 6.14. Some of the ions had little effect on the proposed method (e.g. Zn^{2+} and Mg^{2+}) with added EDTA while others depressed the boron signal to a certain extend (e.g. high K^+ concentrations).

6.11.6 Sample frequency

The proposed method employed a 125 second procedure giving the method a sample frequency of 28 samples per hour. It is possible to increase this frequency, by shortening the waiting period of 30 seconds by up to 10 seconds, with only a small decrease in the precision of the method.

6.12 Conclusion

This proposed sequential injection method makes direct online analyses of boron in water and liquid fertilizer possible. The method is a simple, inexpensive and reliable method of boron determination. The proposed method also has the added advantage of being a sensitive method with a wide linear range, making it ideal for routine analysis in the industry. Ions and anions that do interfere with the method can be masked with the addition of 20g.ℓ^{-1} EDTA to the buffer, with a limited effect on the sensitivity of the method.

6.13 References

1. D. C. Adriano, **Trace elements in the terrestrial environment**, 1986, Springer-Verlag, New York Inc.
2. K. B. Krauskopf, **Micronutrients in agriculture**, 1972, Soil Sci. Soc. Am. Inc., Madison, WI.
3. P. A. Trudiger and D. J. Swaine, **Biogeochemical cycling of mineral-forming elements**, 1979, Elsevier, Amsterdam.
4. J. E. Bowen, **Crop soils**, 1977, 12.
5. H. Aubert and M. Pinta, **Trace elements in soils**, 1977, Elsevier, New York.
6. D. J. D. Nicholas and E. R. Egan, **Trace elements in soil-plant-animal systems**, 1975, Academic press, New York.
7. H. G. Gauch, **Organic plant nutrition**, 1972, Dowden, Hutchinson and Ross, Strousburg, PA.
8. I. Bonilla, C. Cadahia and O. Carpena, **Plant soil, 57** (1980) 3.
9. R. A. Wildes and T. E. Neales, **J. Exp. Bot., 20** (1969) 591.
10. C. F. Crosswell and L. C. Nelson, **Soil science, 52** (1941) 351.
11. V. Sauchelli, **Trace elements in nature**, 1969, Van Nostrand Reinhold, New York,
12. A. L. Dawidowicz, J. Matusewicz and J. Wysocka-Lisek, J., **Talanta, 36** (1989) 581.
13. A. J. Jeffrey and L. E. McCallum, **Commun. Soil. Sci. Plant Anal., 19** (1988) 663.
14. J. R. Melton, **Assoc. Off. Anal. Chem., 65** (1982)234.
15. W. D. Basson, R. G. Bohmer and D. A. Stanton, **Analyst, 94** (1969) 1135.
16. F. J. Krug, J. Mortatti, L. C. R. Pessenda and E. A. G. Zagatto, **Anal. Chim. Acta, 125** (1981) 29.
17. M. A. Z. Arruda and E. A. G. Zagatto, **Anal. Chim. Acta, 199** (1987) 137.

18. A. J. Johnson and M. J. Toogood, **Analyst**, **79** (1954) 493.

19. R. C. Calkins and V. A. Stenger, **Ibid.**, **28** (1956) 399.

20. L. Rosenthaler, **Michrochemie**, **23** (1937) 194.

21. D. F. Boltz, **Colorimetric determination of non-metals**, Interscience Publishers, New York, 1958, *VIII*, 345.

22. H. James and G. H. King, **Automation in analytical chemistry**, Technicon symposia, Mediad Inc., New York, Volume I, 123.

23. V. Petrovsky, **Talanta**, **10** (1963) 175.

24. D. Chen, F. Lázaro, M. D. Luque de Castro and M. Valcárcel, **Anal. Chim. Acta**, **226** (1989) 221.

25. P. Carrero J. L. Burguera, M. Burguera and C. Rivas, **Talanta**, **40** (1993) 1967.

26. I. Sekerka and J. F. Lechner, **Anal. Chim. Acta**, **234** (1990) 199.

CHAPTER 7

Automated *in situ* Preparation of Azomethine H and the Subsequent Determination of Boron in Fertilizers with Sequential Injection Analysis

7.1 Introduction

Azomethine H is a chromogenic reagent used in the detection and quantitation of boron in various aqueous solutions. It can be obtained from chemical suppliers and works well under a variety of physical and chemical conditions. One draw back of this chromogenic reagent is that it is unstable unless stored in a desiccator. Results obtained are, therefore, inconsistent and calibration curves have to be adjusted as the reagent is used over longer periods [1]. It was found that aqueous solutions of azomethine H hydrolyses rapidly, when stored for periods longer than one day, with a loss in it's sensitivity if not refrigerated properly.

This problem may be solved with the preparation of azomethine H just prior to use. The immediate use of freshly prepared azomethine H ensures better sensitivity and accuracy for longer periods, without the need for recalibration as the reagent deteriorates. Basson and his coworkers accomplished the *in situ* preparation of azomethine H with the use of an Autoanalyser [1] and the two components of azomethine H, salicylaldehyde and H-acid (8-amino-1-naphthol-2,6-disulphonic acid). In this chapter a sequential injection procedure is described for the *in situ*

preparation of azomethine H, and its subsequent use in the determination of boron in aqueous solutions and liquid fertilizers.

7.2 Reaction principles

Azomethine H is prepared by mixing its two components salicylaldehyde and H-acid (8-amino-1-naphthol-3,6-disulphonic acid). Basson [1] described the formation of a Schiff bases from a carbonyl compound and a primary amine, in the presence of an acid catalyst. First a carbinol amine (A) is formed, then water is eliminated to form the Schiff base (B):

$$RR'CO + R''NH_2 \rightleftarrows \underset{\mathbf{A}}{R-\overset{\overset{OH}{|}}{\underset{\underset{R'}{|}}{C}}-NHR''} \rightleftarrows \underset{\mathbf{B}}{RR'C=NR''} + H_2O \qquad \textbf{(1)}$$

Hammett [2] concluded that the addition of a proton to the carbonyl group gives a carbonium ion, $RR'COH^+$, which rapidly forms the base by deprotonation. This deprotonation is the rate determining step leading to the formation of the carbinol amine (A).

For the preparation of azomethine H by the sequential injection method the same reaction principles apply. The reaction rate, however, is changed as the conditions of the deprotonation is changed.

7.3 *In situ* preparation of azomethine H and the determination of boron by sequential injection analysis

7.3.1 Experimental

7.3.1.1 Reagents and solutions

Only analytical-reagent grade reagents were used unless specified otherwise. Deionised water, supplied by a Modulab system (Continental Water Systems, San Antonio, TX, USA), was used to prepare aqueous solutions. The solutions were degassed, by boiling it in a microwave oven, before introduction into the system and it was stored in an oxygen free environment when not in use.

Standard boron solution: The standard boron solution was prepared by dissolving 1.143 g of boric acid in 2 litres of deionised water. This solution was stored in a polythene container and used to prepare working boron standards by suitable dilutions with 0.1 mol.ℓ^{-1} hydrochloric acid.

Buffer solution: The buffer solution was prepared by dissolving 132 g of ammonium phosphate and 25 g of disodium EDTA in 500 mℓ of deionised water. The pH of this solution was adjusted to 7.0 with alkali addition.

Carrier: The carrier stream was prepared by adding 11.39 mℓ of 32 % hydrochloric acid to de-ionised water and diluting it to 1 litre.

H-acid: The H-acid (8-amino-1-naphthol-3,6-disulphonic acid, Merck) solution was prepared by dissolving 2.5 g of H-acid in 250 mℓ of de-ionised water and adjusting the pH of this solution to 2.25 with a 16 % hydrochloric acid solution.

Salicylaldehyde: The salicylaldehyde solution was prepared by diluting 1.0 mℓ of salicylaldehyde (Merck) in 250 mℓ of an 80 % ethanol solution.

Liquid fertilizer: The liquid fertilizer was prepared by diluting 1mℓ of liquid fertilizer with 20 mℓ of de-ionised water. The solution was filtered to get rid of any solid substances that formed during the dilution.

7.3.1.2 Equipment

The sequential injection manifold used, is shown in Fig. 7 1. The manifold consisted of a Gilson Minipuls peristaltic pump (Gilson Medical Electronics, (France) S. A., Villiers-le-Bel, France), with a pumping tube inside diameter of 1.85 mm, operating at a speed of 17 rpm. The pump was connected to a holding coil (HC), consisting of a 0.76 mm inside diameter Tygon tubing wound around a perspex tube with an outside diameter of 10 mm.

The holding coil was connected to the first reaction coil (RC 1) via PTFE (Tygon) tubing with an inside diameter of 0.76 mm wound around a perspex tube with a 10 mm outside diameter. RC 1 was connected to a 10 port electrically actuated selection valve (Model ECSD10P, Valco Instruments, Houston, TX, USA) using PTFE tubing with a 0.76 mm inside diameter. A single bead string reactor (SBSR) was incorporated into RC 1 to ensure proper mixing with minimal

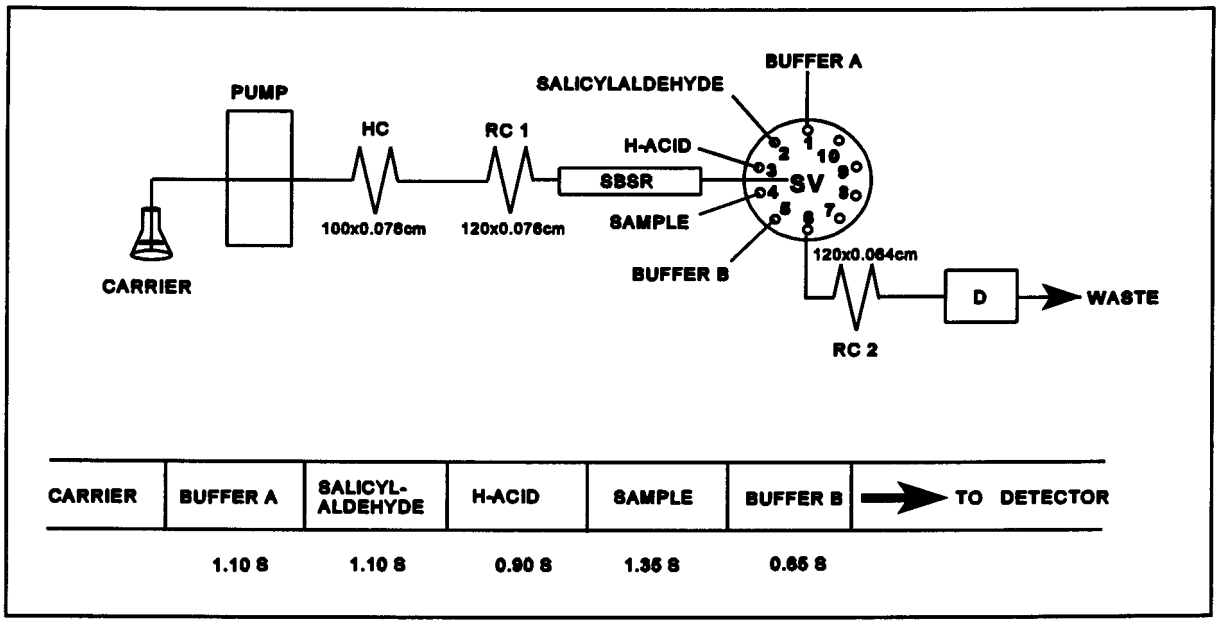

Fig. 7.1 Sequential injection manifold used in the determination of boron with *in situ* preparation of azo-methine H. Buffer A, salicylaldehyde, H-acid, sample, and another buffer B solution plug are aspirated through the sequential valve (SV) into the first reaction coil (RC 1) through the single bead string reactor (SBSR). Carrier solution, propelled by the peristaltic pump is pumped through the holding coil (HC), flushing the reacted zone towards the detector (D) and waste (W), via the second reaction coil (RC 2).

band broadening. The SBSR consisted of a PTFE tube (100 mm x 3 mm inside diameter) which was packed with boron free beads with an inside diameter slightly smaller than 3.0 mm.

The second reaction coil (RC 2) connected the sequential valve (SV) and the spectrophotometer via 0.76 mm inside diameter PTFE tubing wound around a perspex tube with a 12.5 mm outside diameter.

A Unicam 8625 UV-Visible spectrophotometer equipped with a Hellma type flow through cell (volume 80 $\mu\ell$, as supplied by the manufacturer) was used as detector and the absorbance was measured at 420 nm. Data acquisition and device control were achieved using a PC30-B

interface board (Eagle Electric, Cape Town, South Africa), as well as an assembled distribution board

(MINTEK, Randburg, South Africa). The FlowTEK [3] software package (MINTEK, Randburg, South Africa) for computer-aided flow-analysis was used throughout for device control and data acquisition.

7.3.1.3 Procedure

The device sequence for the *in situ* preparation of azomethine H, and subsequent determination of boron by sequential injection, is given in Table 7.1. As seen from the sequential injection system depicted in Fig 7.1, one cycle of the sequence (buffer A, salicylaldehyde, H-acid, sample, buffer B and flush to the detector) involves ports 1 to 6 of the selection valve. Buffer A and B are the same buffer solution, of which the volumes were optimized separately in order to obtain the optimum conditions.

7.4 Method optimisation

7.4.1 Physical parameters

The physical parameters were evaluated by comparing the sensitivity (degree of zone penetration) and precision (reproducibility of zone penetration) obtained for different parameter changes. Some of the parameters, such as the dimensions of RC 1 and RC 2, were already optimised in

Table 7.1 Device sequence for one full cycle of the sequential injection system used in the determination of boron

Time (s)	Pump	Valve	Description
0.00	Reverse	Buffer A	Draw up buffer A solution
1.10	Off		Pump stop
1.60		Salicylaldehyde	Valve selects salicylaldehyde solution
2.10	Reverse		Draw up salicylaldehyde solution
3.20	Off		Pump stop
3.70		H-acid	Valve selects H-acid solution
4.20	Reverse		Draw up H-acid solution
5.10	Off		Pump stop
5.60		Sample	Valve selects sample solution
6.10	Reverse		Draw up sample solution
7.45	Off		Pump stop
7.95		Buffer B	Valve selects buffer B solution
8.45	Reverse		Draw up buffer B solution
9.10	Off		Pump stop
9.60		Detector	Valve selects detector position
10.10	Forward		Pump stacked zones to detector
119.00	Off		Pump stop
120.00		Home	Return valve to starting position

Chapter 6 (paragraph 6.10.1.2 and paragraph 6.10.1.3) for the determination of boron.

Physical parameters, optimised for the *in situ* preparation of azomethine H and the subsequent determination of boron, were flow rate, order of injection and mixing chamber parameters. The physical parameters were optimised by using the actual reagents used in the determination of boron.

7.4.1.1 Flow rate

The flow rate plays an important role in the dispersion of the reacting zones, and consequently the sensitivity and precision of the analytical method. Flow rates were varied between 7.6 and 14.5 mℓ.min^{-1} by changing the pump speed, and keeping the pump tube inside diameter constant at 0.76 mm. The results obtained for the optimisation of the flow rate, is summarised in Table 7.2 and is graphically depicted in Fig. 7.2.

Table 7.2 Effect of an increased flow rate on peak height (sensitivity) and % RSD (precision).

Flow rate (mℓ.min^{-1})	Peak height	% RSD
7.6	2.95	3.82
8.4	3.13	3.63
9.2	3.31	3.58
9.9	3.34	3.36
10.7	3.46	2.83
11.4	3.89	2.77
12.2	4.39	2.13
13.0	4.69	1.61
13.7	4.98	1.35
14.5	5.10	2.05

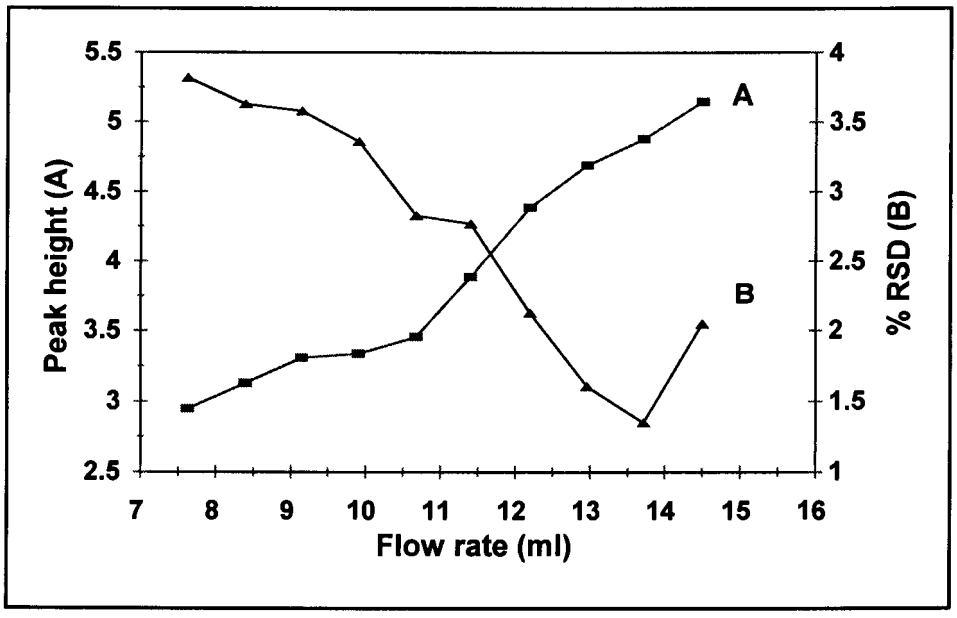

Fig. 7.2. The effect of an increased flow rate on the peak height (sensitivity) and % RSD (precision).

An increase in the flow rate improved both the sensitivity and precision, up to a flow rate of 13.7 mℓ.min^{-1}. Higher flow rates increased the sensitivity, but the precision decreased due to the development of back pressure in the system. The best precision (1.35 %) was obtained with a flow rate of 13.7 mℓ.min^{-1}. This flow rate was used for further optimisation of the method.

7.4.1.2 Order of injection

In sequential injection, the order of injection plays an important role in the determination of factors such as sensitivity, precision, and carry over. With the *in situ* preparation of azomethine H the order of injection of five separate solutions (buffer A, salicylaldehyde, H-acid, sample, buffer B) had to be determined. The four possibilities in Table 7.3 were evaluated.

Table 7.3 The effect of a change in order of injection on the peak height and % RSD.

Order of Injection	Peak height	% RSD
1) Buffer A - H-acid - Sample - Salicylaldehyde - Buffer B	4.22	2.28
2) Buffer A - Salicylaldehyde - Sample - H-acid - Buffer B	4.47	2.10
3) Buffer A - Salicylaldehyde - H-acid - Sample - Buffer B	4.56	1.90
4) Buffer A - H-acid - Salicylaldehyde - Sample - Buffer B	4.44	2.43

For the *in situ* preparation, the sample had to be aspirated after the chromogenic reagents to prevent carry over between successive runs of the method. The best precision and sensitivity were obtained with salicylaldehyde aspirated first followed by H-acid and the sample.

7.4.1.3 Mixing devices

While optimising the sequence, it was noticed that the individual zones did not mix properly. The buffer solution used in the proposed method contained 264 $g.\ell^{-1}$ ammonium hydrogenphosphate, and as a result of this high salt content, its refractive index differed a lot from that of the other solutions used. Without proper mixing of the plugs containing different salt concentrations, the absorption detected by the spectrophotometer would fluctuate leading to poor and inconsistent results.

This problem could be solved in one of three ways. Firstly by the addition of a salt (e.g. sodium chloride) to the solutions with low salt content until the difference in refractive index are negligible. Secondly by measuring the absorbance of the product zone at the wavelength that the chromotropic compound absorbs as well as at a wavelength that none of the reacting species absorbs. The last option is by using a mixing device (e.g. a mixing chamber), that will be able

to homogenise the refractive index of the reacting zones.

The addition of sodium chloride to the solutions with low salt content, had a negative effect on the sensitivity of the method, excluding it as a possibility. In order to implement the second option, additional software was required to measure the absorbance at two different wavelengths and, as a result, this possibility could not be evaluated. A mixing device, such as a mixing chamber or a single bead string reactor (SBSR), was the only option left to consider.

SBSR's (Fig. 7.3) reduce the refractive index differences by mixing the solutions of high salt content with those solutions containing less salt and more reproducible mixing is obtained for consecutive runs. Due to the mixing of the different zones, an increase in dispersion is obtained. The dispersion of the system was calculated by using the following equation:

$$D^{max} = \frac{C^o}{C} \qquad \textbf{(2)}$$

where D^{max} is the dispersion coefficient, C^o is the concentration of the sample before the dispersion process begins, and C is the concentration of the sample after dispersion has taken place [4]. Without the SBSR a dispersion coefficient of 2.8 was obtained, and with the SBSR a value of 3.91. The precision of the method improved substantially from 1.2 % to 0.8 % with only a small loss in sensitivity.

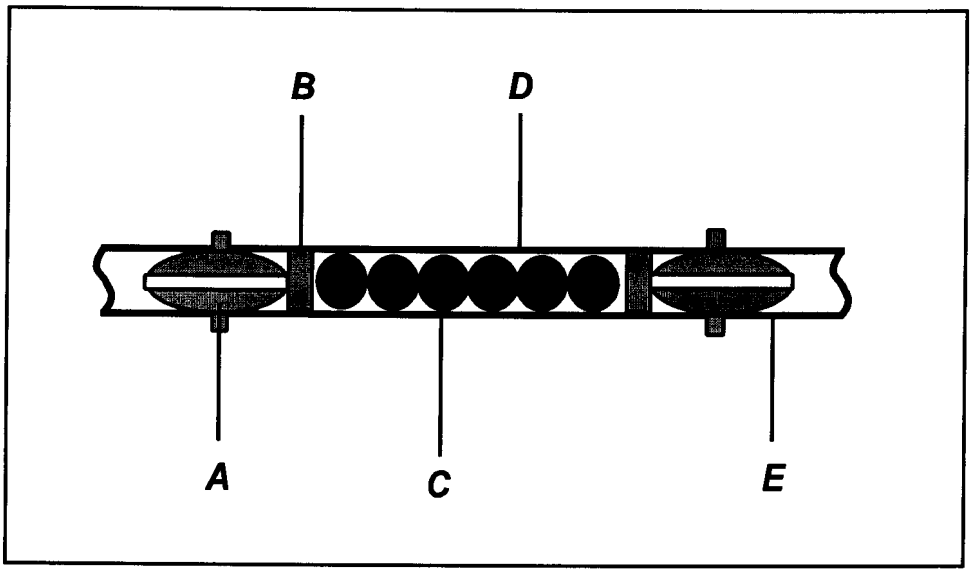

Fig. 7.3. Construction of the SBSR used in the determination of boron, with *in situ* prepared azomethine H. PTFE (Teflon) connectors (A) are used to connect the SBSR to the PTFE tubing of RC 1 (E). A polythene stopper (B) was used to keep the beads (C) in place. A PTFE tube (D) was used in the construction of the reactor.

An alternative to the SBSR is the mixing chamber [5, 6], as illustrated in Fig. 7.4. A magnetic stirrer mixes the different solutions as it enters the mixing chamber. An increase in dispersion (D = 3.5) was obtained as a result of the relatively large volume of the mixing chamber used (1.5 ml). The precision of the method improved from a value of 4.9% to a value of 0.6% with the use of the stirrer.

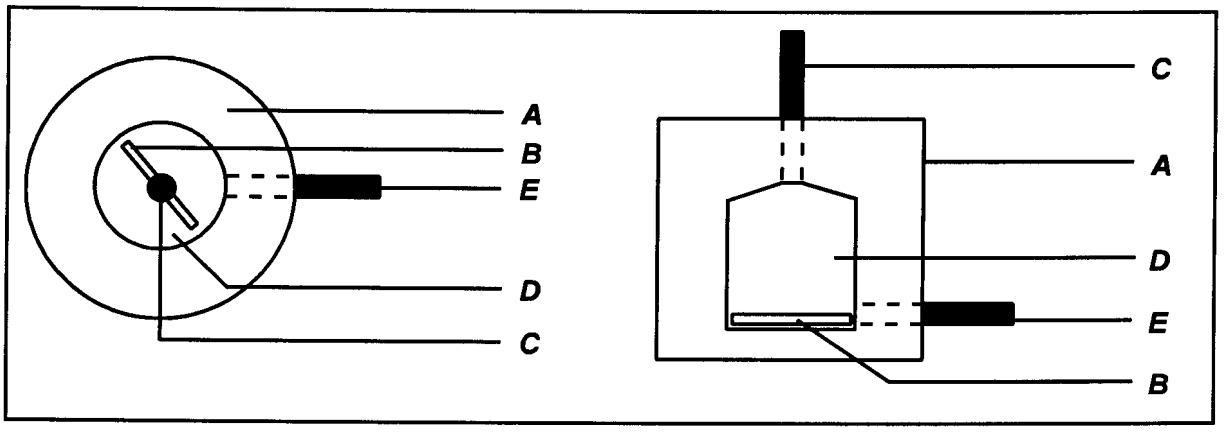

Fig. 7.4. Construction of the mixing chamber used in the determination of boron. Sample, from the selection valve, enters the mixing chamber (D) through a stainless steel tube (E) and is mixed in the chamber with the stirrer (B). Carrier solution is pumped through the stainless steel tube (C), connected with RC 1, into the chamber and flush the reacted zone towards the detector. The chamber body (A) is made out of perspex, machined to the specified dimensions.

It is possible to change the amount of dispersion experienced by the product zone in the mixing chamber, by varying the speed of the stirrer inside the mixing chamber (Table 7.4 and Fig. 7.5).

Table 7.4 Influence of mixing speed (rpm) on peak height and % RSD.

Mixing speed (rpm)	0	250	300	500	700	1000
Peak height	4.93	1.65	1.29	1.28	1.27	1.23
% RSD	2.98	2.28	1.84	1.32	1.19	0.62

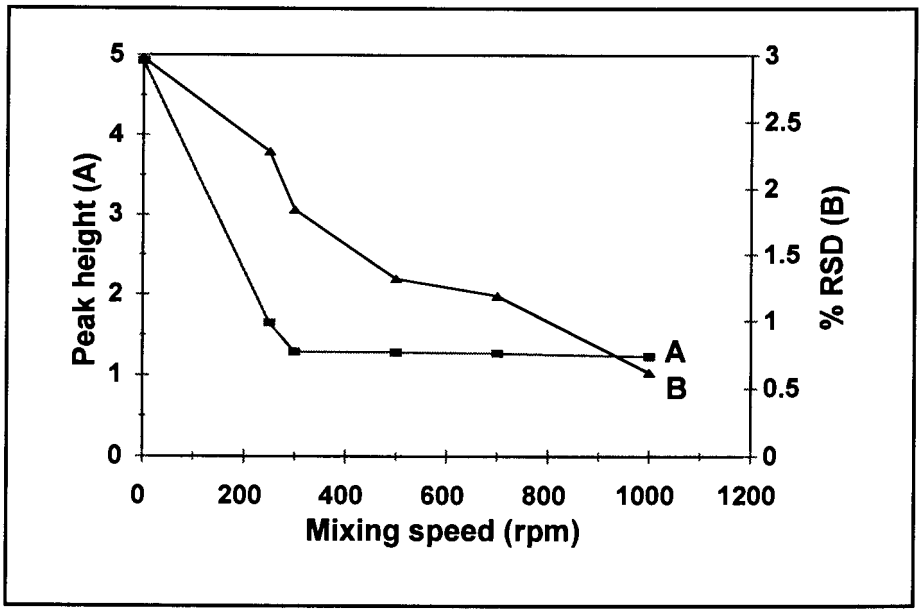

Fig. 7.5. Influence of mixing speed (rpm) on peak height and % RSD.

According to these results, the mixing speed had a negative effect on the sensitivity but a positive effect on the precision. With no stirring, the absorbance was high due to less dispersion taking place (the dispersion that did take place was due to the large dead volume of the mixing chamber).

7.4.2 Chemical parameters

7.4.2.1 Carrier stream

The same carrier solution (0.10 mol.ℓ^{-1} hydro chloric acid) was used for both the *in situ* method, and the azomethine H method proposed in Chapter 6. One aspect of the carrier solution that was evaluated, was the influence of a salt (sodium chloride) on the refractive indice of the carrier solution. As was the case in section 7.4.1.3, negative results were obtained with an increase in

the salt content of the carrier solution. Therefore the carrier solution was kept unchanged.

7.4.2.2 Salicylaldehyde

Basson *et al* [1] suggested a salicylaldehyde, ethanol (80 %) ratio of 1:250 (v/v) and this ratio was also used in the proposed method with good results. One aspect of the salicylaldehyde solution that was evaluated was the volume aspirated (varied between 0 and 280 $\mu\ell$) with the following results:

Table 7.5 Influence of salicylaldehyde volume on peak height and % RSD.

Volume ($\mu\ell$)	0	40	80	120	160	200	240	280
Peak height	0.42	2.15	2.89	3.72	5.03	5.68	6.17	6.32
% RSD	5.78	5.02	2.78	1.71	1.49	1.55	1.01	1.24

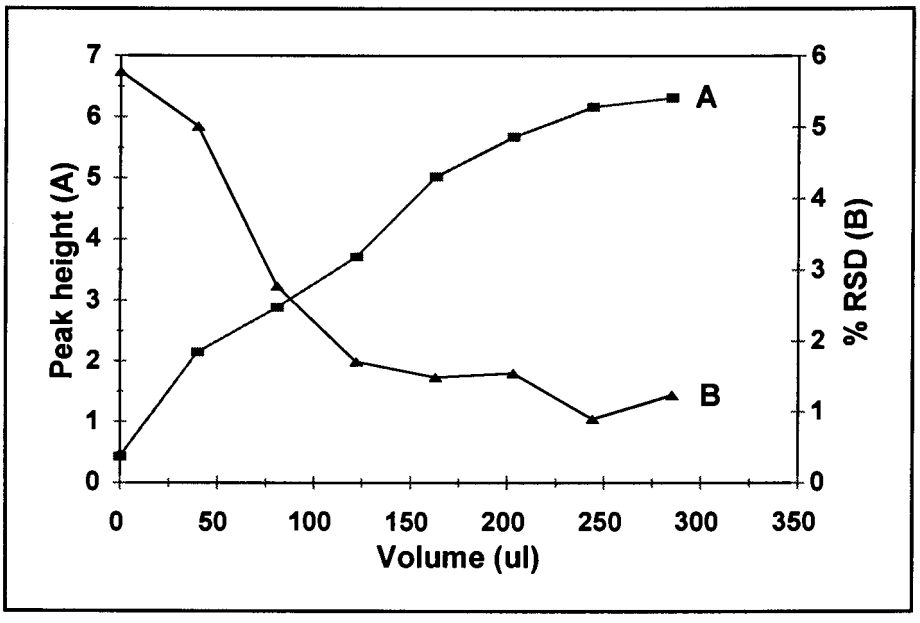

Fig. 7.6 The effect of salicylaldehyde volume on the peak height (sensitivity) and % RSD (precision).

According to Basson *et al* [1], salicylaldehyde reacts with H-acid in a one to one ratio. With the H-acid concentration kept constant, the peak height should have a linear increase up to the point where both the reagents are present at the same concentration. Theoretically, a higher salicylaldehyde concentration would not increase sensitivity since the H-acid will then be the limiting reagent. This is exactly what was found when the salicylaldehyde volume was increased, with the H-acid volume kept constant (Table 7.5, Fig. 7.6). According to Fig. 7.6, there is an increase between 0 and 240 $\mu\ell$, with the sensitivity levelling off at higher salicylaldehyde volumes. The best results were obtained with a salicylaldehyde volume of 240$\mu\ell$. The absorbance obtained at 0.00 $\mu\ell$ salicylaldehyde is a result of the small refractive index difference between the solutions aspirated.

7.4.2.3. H-acid

For the flow-injection system, Basson *et al* [1] suggested a 1 % (w/w) H-acid solution. In order to determine the optimum concentration the sequential injection system's H-acid concentration was varied between 0.2 % and 1.2 % (w/w). The results obtained were used to set up Table 7.6 and Fig. 7.7.

Table 7.6 Influence of H-acid concentration on peak height and % RSD.

Concentration (% w/w)	**0.2**	**0.4**	**0.6**	**0.8**	**1.0**	**1.2**
Peak height	1.14	1.32	1.55	1.74	1.95	2.07
% RSD	4.00	2.09	1.03	1.07	0.95	1.31

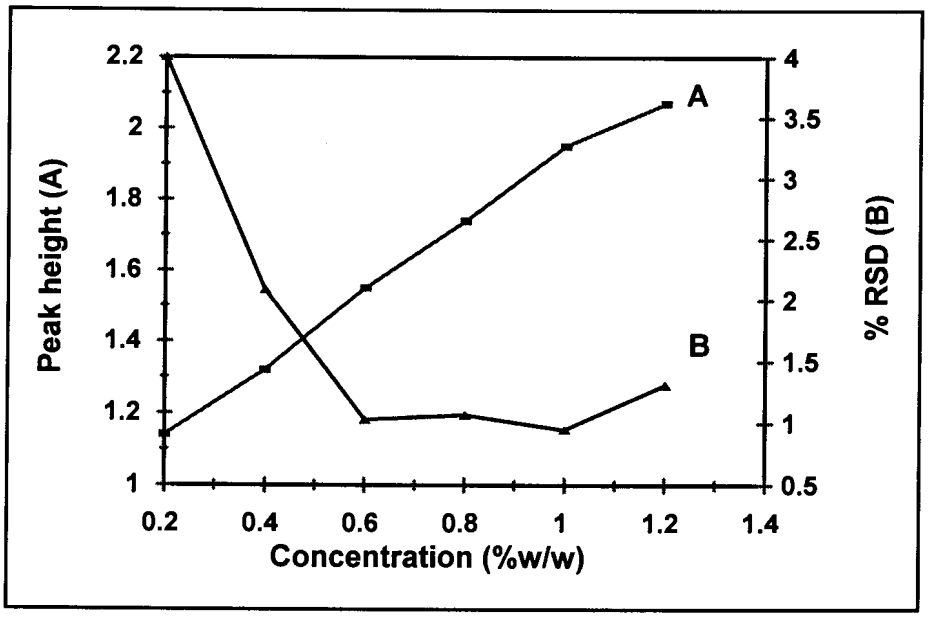

Fig. 7.7 Influence of H-acid concentration on peak height (A) and % RSD (B)

The method reached its maximum sensitivity at a H-acid concentration of 1.2 % (w/w), and its best precision (0.95 %) at a concentration of 1.0 % (w/w). The linear relationship between the salicylaldehyde concentration and peak height ended at a concentration of 1.0 %, the value at which the H-acid and salicylaldehyde concentrations are more or less equal. Higher H-acid concentration had no affect on the sensitivity, making it unnecessary to increase the concentration above this level.

With the H-acid concentration optimised the volume of H-acid aspirated had to be optimised (Table 7.8). H-acid volumes between 0 and 407 $\mu\ell$ were considered. H-acid volumes up to 203 $\mu\ell$ had positive effects on both the precision and the sensitivity, while the precision decreased (% RSD increased) for volumes larger than 203 $\mu\ell$. Under these conditions, the smaller reagent plugs gave the best reproducibility, with salicylaldehyde being able to penetrate most of the H-acid plug.

Table 7.8 The influence of H-acid volume on peak height and precision.

Volume ($\mu\ell$)	Peak height	% RSD
0	6.03	1.29
41	5.79	1.03
81	5.72	1.03
122	5.83	1.00
163	5.94	1.02
203	6.13	1.40
244	5.86	1.92
285	5.66	1.65
325	5.60	1.92
366	5.30	2.32
407	5.20	3.21

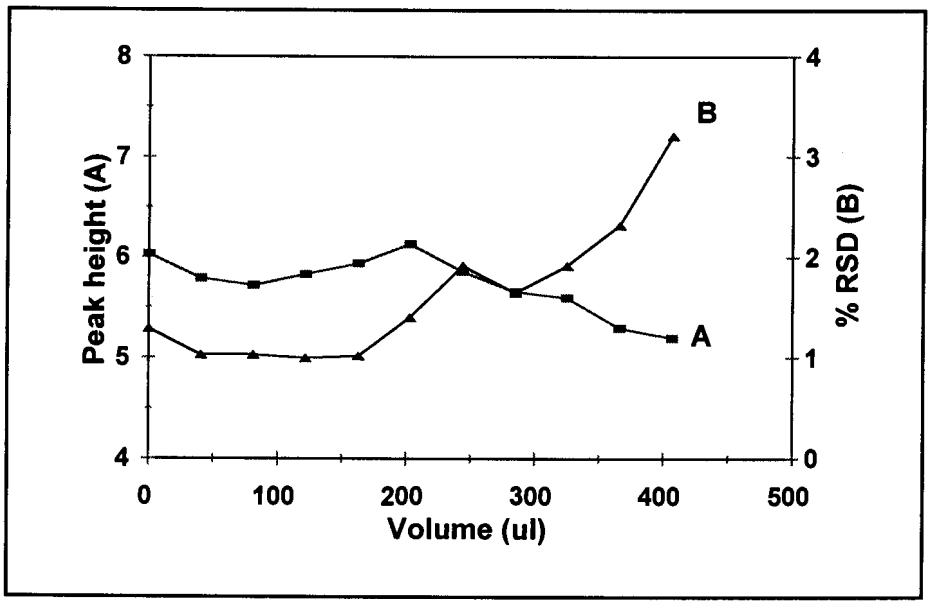

Figure 7.8 Influence of H-acid volume on peak height (A) and % RSD (B).

7.4.2.4 Sample

Tucker *et al* [7] and Růžička *et al* [8] determined that for an optimised region of mutually interdispersed sample and reagent zones, the reagent volume zone should be at least twice that of the sample zone. The optimised chromogenic reagent zones had a total volume of 453 $\mu\ell$. Therefore, according to the above mentioned report, the sample should have a theoretical optimal volume in the region of 225 $\mu\ell$. The results obtained are shown in Table 7.9 and Fig. 7.9.

Table 7.9 Influence of a change in sample volume on the peak height and % RSD.

Volume ($\mu\ell$)	0	50	100	150	200	250	300	350	400
Peak height	5.09	4.60	4.19	4.42	4.51	4.47	4.31	4.44	3.95
%RSD	1.88	1.59	1.86	2.20	1.75	0.94	0.69	2.38	2.64

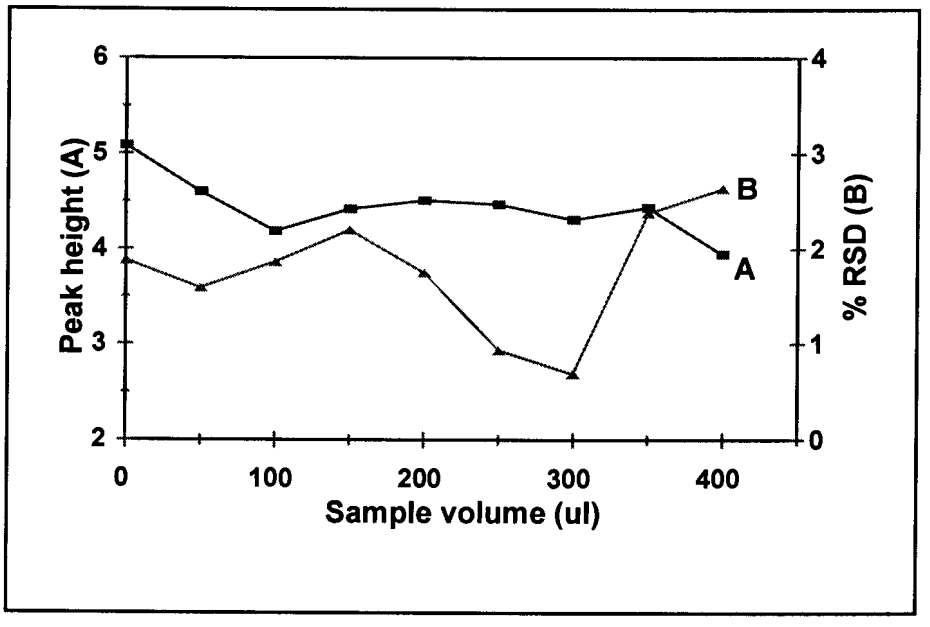

Fig. 7.9 Influence of sample volume ($\mu\ell$) on sensitivity (A) and %RSD (B).

According to Fig. 7.9, the sensitivity did not change much with an increase in the sample volume. The % RSD, on the other hand, shows that the best precision values are obtained between 250 and 300 $\mu\ell$ of sample. In this region, the sample volume is a little more than half the reagent volume, confirming the theory of Tucker [7] and Rûžička[8]. The best % RSD was obtained with a 300 $\mu\ell$ sample volume, that is two thirds the volume of the reagent zone.

7.4.2.5 Buffer solution

A buffer solution consisting of 132 g ammonium hydrogenphosphate and 25 g disodium EDTA dissolved in 500 mℓ deionised water [9] was used in the determination of boron. With the *in situ* preparation of azo-H and the subsequent determination of boron, the procedure and order of injection of the method changed. This change necessitated the re-optimisation of the buffer volumes.

The buffer solution was introduced into the system in front of the azo-H plug (Buffer A) as well as after the sample plug (Buffer B, see Fig 7.1). A change in volume of any one of these buffer plugs, influenced the sensitivity and accuracy of the method, making it necessary to optimize the two buffer volumes separately. The results of the optimization is shown in Table 7.10 and Fig 7.10.

Table 7.10 Influence of different buffer volumes on peak height and % RSD.

Volume	($\mu\ell$)	0.00	50.00	102.00	152.00	203.00	254.00	305.00	355
Buffer A	**Peak height**	2.90	2.90	3.40	3.41	3.55	3.75	4.26	4.14
	%RSD	1.04	1.07	0.70	1.10	0.65	0.41	0.85	0.95
Buffer B	**Peak height**	3.63	3.91	3.77	3.74	4.00	3.79	3.75	3.82
	%RSD	1.82	0.94	1.18	0.79	0.93	2.07	1.87	0.79

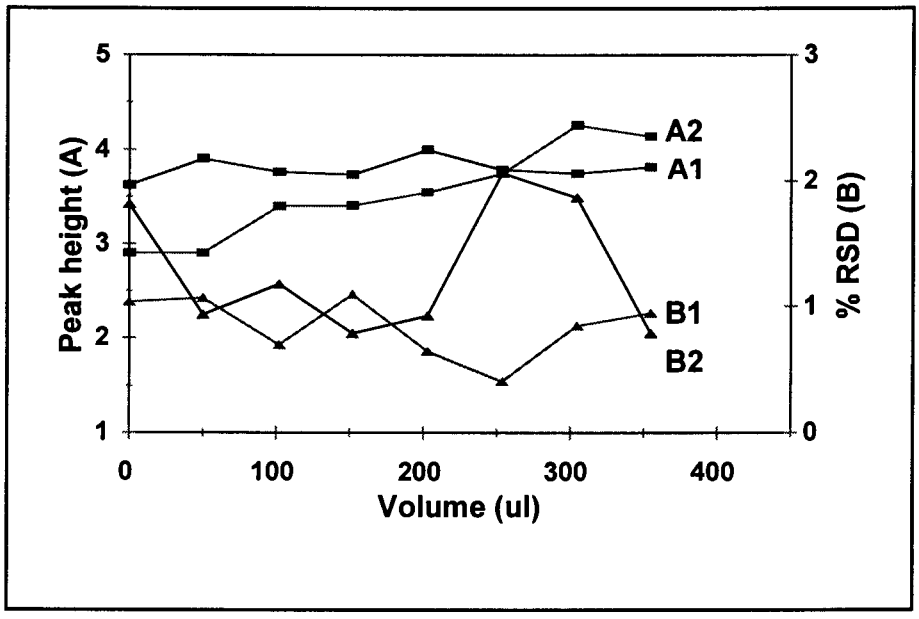

Fig. 7.10 Influence of a change in buffer volume on peak height (A1 for buffer A and A2 for buffer B) and % RSD (B1 for buffer A and B2 for buffer B)

According to Fig. 7.10 the two buffer zones reached their optimum conditions at different volumes. For buffer A it is at a volume of 254 $\mu\ell$ and for buffer B it is at 152$\mu\ell$, volumes larger than this had only a limited effect on the sensitivity.

7.4.2.6 Disodium EDTA

EDTA is used as a masking agent in the determination of boron [5]. It is the most effective complexing agent for removing large amounts of interfering metals and it was used in the determination of boron with commercial azomethine H as well. The EDTA concentration should be high enough to remove all possible interfering elements and low enough not to effect the reaction itself. A 20 $g.\ell^{-1}$ disodium EDTA solution proved to be the most effective with little influence on the reaction.

7.5 Evaluation of the method

7.5.1 Linearity

The linearity of the SIA system was evaluated under the optimum operating conditions, determined by the optimisation of the physical and chemical parameters. The relationship of the relative peak height versus the boron concentration is:

$$y = 0.0504x + 1.520 \; ; \; r = 0.995$$

where y = relative peak height and x = boron concentration in $mg.\ell^{-1}$. The calibration graph (Fig.7.11) is linear for boron concentrations between 0 and 100 $mg.\ell^{-1}$. The value of r decreased by a small amount (from 0.997 to 0.995), when compared to the value obtained for the method described in Chapter 6. However, the coefficient of x as well as the constant, changed very little.

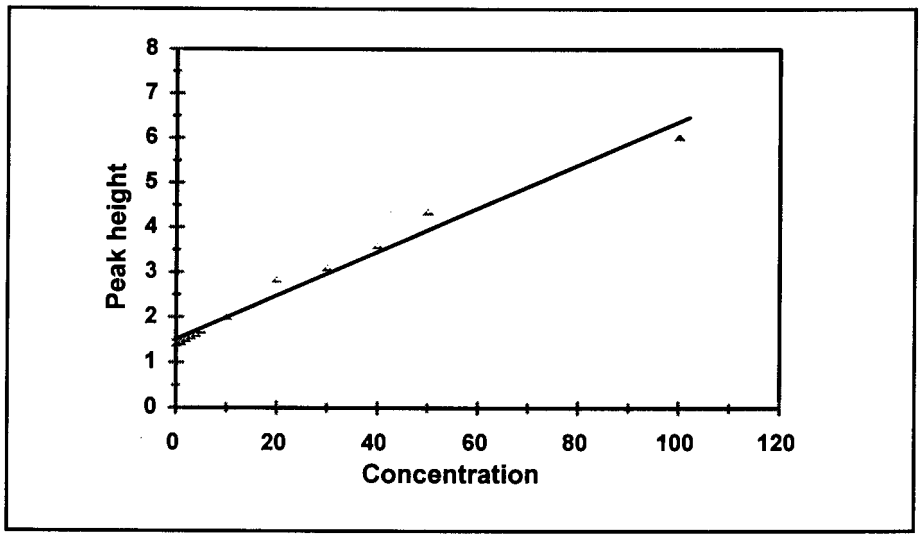

Fig. 7.11 Calibration graph of the proposed *in situ* SIA method.

7.5.2 Accuracy

Spiked water samples were determined by the proposed SIA system to determine the accuracy of the system. The accuracy was determined by comparing the results obtained with the SIA system, to that obtained by the standard procedure [**10**]. The results given in Table 7.11, revealed a good correlation between the two methods. The results obtained by the proposed method were slightly higher than those obtained by the standard method. This difference increased as the boron concentration in the samples were increased, which was an indication of the sensitivity of the method in the linear range.

Table 7.11 Comparison of the results obtained by the proposed SIA method to that of a standard method.

Sample	SIA method (mg.ℓ$^{-1}$ boron)	Standard method (mg.ℓ$^{-1}$ boron)
Water sample A	0.93	0.87
Water sample B	0.81	0.72
Water sample C	1.08	0.99
Water sample D	0.99	0.90
Water sample E	0.90	0.87
Spiked water sample A	2.63	2.50
Spiked water sample B	5.12	4.96
Liquid fertilizer	37.1	35.5

7.5.3 Precision

The precision of the optimised method was determined by 10 repetitive analyses of a number of standard boron solutions and samples, as indicated in Table 7.12. For all the cases, the RSD was below 1.40 %, with a best case scenario of 0.49 % for a boron concentration of 100 mg.ℓ$^{-1}$. The method proved to be more accurate at higher boron concentrations, although the accuracy at lower concentrations was still well below 2.0 %.

When these results are compared with those obtained in Chapter 6, it could be concluded that the accuracy of the *in situ* method is better than that of the direct method. The general trend observed in Chapter 6, that of being more precise at higher boron concentrations, was still present in the results obtained with the *in situ* method.

Table 7.12 Precision of the proposed *in situ* SIA system.

Sample/Standard Concentration (mg.ℓ^{-1})	% RSD
1.0	1.31
3.0	1.33
5.0	1.37
10	1.35
20	1.17
30	0.93
40	0.55
50	0.54
100	0.49
Liquid fertilizer	0.66

7.5.4 Detection Limit

The detection limit of the proposed method was determined via the following formula:

$$Detection\ limit = \frac{(3\sigma + K)(K - c)}{m} \qquad (3)$$

where σ is the relative standard deviation of the baseline (1.55), K is the average signal value of the baseline (1.515), c is the intercept (1.520) and m is the slope of the calibration graph (0.0504). By using the above mentioned formula a detection limit of 0.61 mg.ℓ^{-1} was obtained. When this was compared to the detection obtained by the direct method of Chapter 6 (Par. 6.11.4) only a minor increase could be observed.

7.5.5 Interferences

Since the reaction principles of the method proposed in this chapter (*in* situ preparation of Azomethine H), and that of the method proposed in Chapter 6 were the same, it was expected that the interferences from different ions would be more or less the same. This was exactly what was found when the interference of the ions evaluated in Chapter 6 (Par. 6.11.5) were determined. The same amount of interference were observed in all the cases, and this could be rectified by the addition of 2.0 % EDTA (w/w) to the buffer solution.

7.5.6 Sample frequency

The proposed method employed a 120 second procedure, giving the method a sample frequency of 30 samples per hour. This is a two samples per hour increase over the frequency obtained by the direct determination of boron with azomethine H. It is possible to increase the frequency even further by shortening the waiting period of 30 seconds, at a cost of a small amount of precision.

7.6 Conclusion

The proposed sequential injection method with *in situ* preparation of azomethine H makes direct on-line analysis of boron in water and fertilizers possible. The proposed method is a simple, inexpensive and reliable method for the detection of boron at low and intermediate

concentrations. This method has the added advantage of being sensitive over a wide linear range, making it ideal for use in routine analysis in industry. Ions and anions that interfere with the method can be masked by the addition of 2.0% (w/w) EDTA. When this method is compared to the direct method described in Chapter 6, some useful advantages come to light. Firstly, the H-acid and salicylaldehyde solutions are more stable at room temperature than the azomethine H in solution, which requires refrigeration when used over long periods. As a result of this stability, the sensitivities are constant over longer periods requiring fewer reagent exchanges over the same period of time. The method is slightly faster (two sample per hour) which is an important factor in the process industry. By using the *in situ* preparation, the linear range may be a little narrower but the detection limit is better, justifying the use of the *in situ* method.

7.7 References

1. W. D. Basson , P. P. Pille and A. L. Du Preez, **Analyst, 99** (1974) 168.
2. L. P. Hammett, **Physical Organic Chemistry**, McGraw-Hill Book Co., New York, 1940, p333.
3. G. D. Marshall and J. F. van Staden, **Analytical Instrumentation, 261** (1992) 11.
4. J. Rûžička and E. H. Hansen, **Flow injection analysis**, Wiley, New York, 2nd ed., 1988.
5. H. L. Pardue and B. Fields, **Anal. Chim. Acta, 124** (1981) 39.
6. H. L. Pardue and B. Fields, **Anal. Chim. Acta, 124** (1981) 65.
7. D. J. Tucker, B. Toivola, C. H. Pollema, J. Rûžička and G. D. Christian, **Analyst, 119** (1994) 975.
8. J. Rûžička and T. Gübeli, **Anal. Chem., 63** (1991) 1680.
9. F. J. Krug, J. Mortatti, L. C. R. Pessenda and E. A. G. Zagatto, **Anal. Chim. Acta, 125** (1981) 29.
10. **Standard methods for Examination of Water and Waste Water**, 14th Edition, American Public Health Association, Washington, DC, 1976.

ADDENDUM A

Method development

The sequential injection system used consist of various components, i.e. peristaltic pump, sequential valve, spectrophotometer and personal computer. In order for these components to communicate with each other an interface is used. The interface enables the user to control the actions of the peristaltic pump and sequential valve, and to receive data from the spectrophotometer. The FlowTEK [1] software package is used as the driver for the setup imployed in this dissertation.

A simple cycle will be used in order to demonstrate how a method is developed using the FlowTEK software with the devices mentioned above. The cycle will be the sequential introduction of a sample, chromogenic reagent and the flushing of the reacted zone towards the detector.

In order to initialise the digital outputs to the inactive state, the following steps are followed: The **Startup** option in the *method* menu is selected. The value **240** is entered in order to activate ports 5 to 8. The method is saved by selecting **File** from the method *menu* and entering **S** for save. It is necessary to exit the FlowTEK program here in order to initialise the device configuration file. At this point the device should be defined when the program is restarted.

To define the devices, the **Config devices** option in the *method* menu is selected. The device is defined in the following way:

Enter device defn number:	**8**
Enter device name:	**VS** (for the device you are about to define)
Enter number of device actions:	**2**
Enter action narration for action 1:	**STEP**
Enter digital output for action STEP	**1**
Enter hotkey for STEP:	**P** (At this point the user can enter any hotkey e.g. P for the P in STEP)
Enter action narration for action 2:	**HOME**
Enter digital output for action HOME:	**2**
Enter hotkey for HOME:	**H**

Each device used should be defined in a similar manner. For the cycle mentioned above the Gilson pump (GP), already defined by the software manufacturers (Fig 1), and the selection valve (VS), defined above, are used. In order for the computer to send the correct signals to the correct devices, the devices you intend to use should be chosen using the option **Type device** in the *method* menu.

UNIVERSITEIT VAN PRETORIA
UNIVERSITY OF PRETORIA
YUNIBESITHI YA PRETORIA

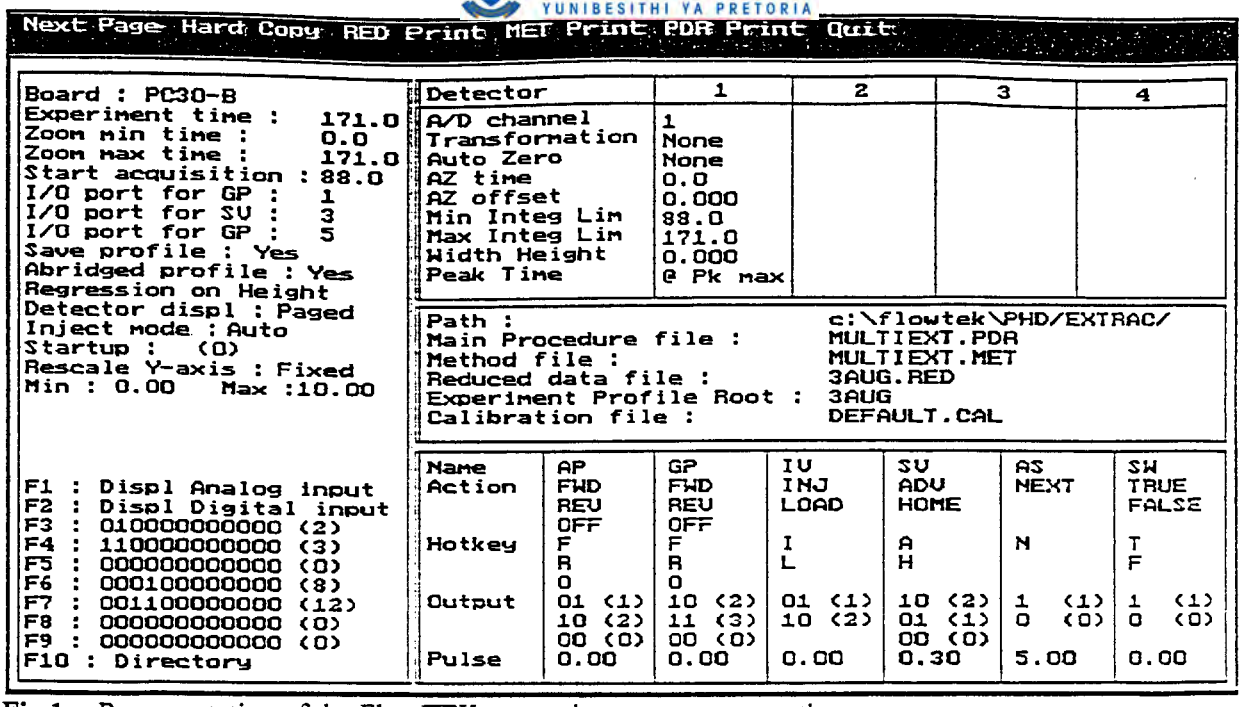

Next Page Hard Copy RED Print MET Print PDA Print Quit

Board : PC30-B
Experiment time : 171.0
Zoom min time : 0.0
Zoom max time : 171.0
Start acquisition : 88.0
I/O port for GP : 1
I/O port for SV : 3
I/O port for GP : 5
Save profile : Yes
Abridged profile : Yes
Regression on Height
Detector displ : Paged
Inject mode : Auto
Startup : (0)
Rescale Y-axis : Fixed
Min : 0.00 Max :10.00

F1 : Displ Analog input
F2 : Displ Digital input
F3 : 0100000000000 (2)
F4 : 1100000000000 (3)
F5 : 0000000000000 (0)
F6 : 0001000000000 (8)
F7 : 0011000000000 (12)
F8 : 0000000000000 (0)
F9 : 0000000000000 (0)
F10 : Directory

Detector	1	2	3	4
A/D channel	1			
Transformation	None			
Auto Zero	None			
AZ time	0.0			
AZ offset	0.000			
Min Integ Lim	88.0			
Max Integ Lim	171.0			
Width Height	0.000			
Peak Time	@ Pk max			

Path : c:\flowtek\PHD/EXTRAC/
Main Procedure file : MULTIEXT.PDA
Method file : MULTIEXT.MET
Reduced data file : 3AUG.RED
Experiment Profile Root : 3AUG
Calibration file : DEFAULT.CAL

Name	AP	GP	IV	SV	AS	SW
Action	FWD	FWD	INJ	ADV	NEXT	TRUE
	REV	REV	LOAD	HOME		FALSE
	OFF	OFF				
Hotkey	F	F	I	A	N	T
	R	R	L	H		F
	0	0				
Output	01 (1)	10 (2)	01 (1)	10 (2)	1 (1)	1 (1)
	10 (2)	11 (3)	10 (2)	01 (1)	0 (0)	0 (0)
	00 (0)	00 (0)		00 (0)		
Pulse	0.00	0.00	0.00	0.30	5.00	0.00

Fig 1 Representation of the FlowTEK notepad screen as seen on the computer.

The questions under Type device is answered in the following way:

Enter number of devices: **2**

Enter type device 1: **GP**

Enter digital point for GP: **1** (this value depends on the position the Gilson pump occupies on the interface board)

Enter type device 2: **VS**

Enter digital point for VS: **3**

As soon as this information is entered the screen divides into two sections. Each section represents a specific device (in this case GP for the Gilson pump and VS for the selection valve) with the actions of the device represented by a line in the middle of each section. By selecting each device in turn it is possible to develop a method by employing the actions, defined earlier, on the time scale (represented by the x-axis). Device events are entered by choosing the option

Insert in the *method* menu. The programming is done in the following manner:

Insert

Device number: **8** (for the selection valve as defined under Configuration of device)

Enter time of event: **0** (time in seconds)

Hotkey (P H): **H** (to enable the valve to move to its homing position, in this particular case the sample is situated at port 1 of the selection valve)

Insert

Device number: **2** (for the Gilson pump)

Enter time of event: **2**

Hotkey (F R O): **R** (to enable the pump to aspirate sample into reaction coil 1)

Insert

Device number: **8** (for the selection valve)

Enter time of event: **6**

Hotkey (P H): **P** (to enable the valve to move to the next port where the chromogenic reaction is situated)

Insert

Device number: **2** (for the Gilson pump)

Enter time of event: **8**

Hotkey (F R O): **R** (to enable the pump to aspirate chromogenic reagent into

reaction coil 1)

Insert

Device number: **8** (for the selection valve)

Enter time of event: **10**

Hotkey (P H): **P** (to enable the valve to move to the next port which connects the valve to the detector)

Insert

Device number: **2** (for the Gilson pump)

Enter time of event: **12**

Hotkey (F R O): **F** (to enable the pump to propel the reacted zone towards the detector)

Insert

Device number: **2** (for the Gilson pump)

Enter time of event: **60**

Hotkey (F R O): **O** (to stop the pump after the reacted zone is flushed from the manifold)

As soon as all the events of the method are entered the method is saved by entering **S** under the **File** option of the *method* menu. If an entry is found to be incorrect the entry can be rectified by deleting the specific event with the **Delete** function on the *method* menu. The experiment time

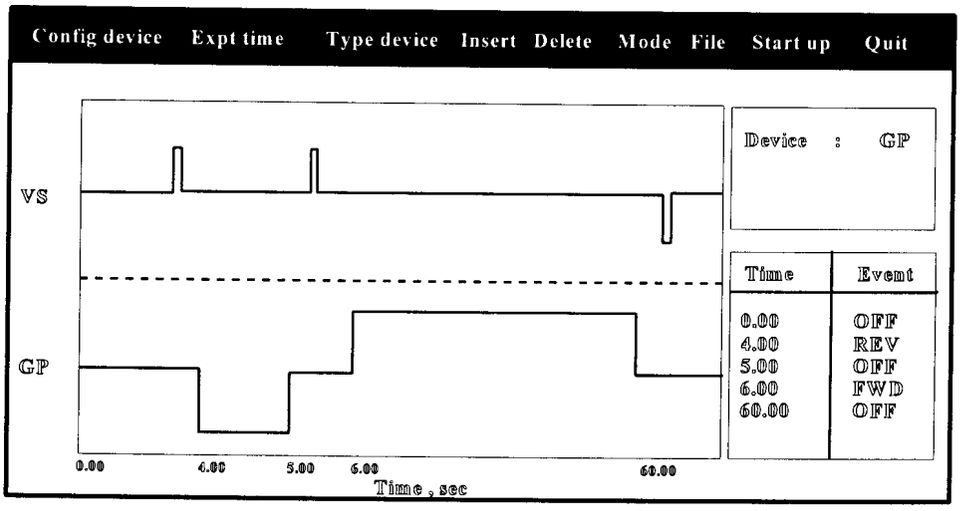

Fig 2 Method screen after the completion of a method.

can also be selected in order to acquire only the most important data. This is done by selecting **Expt time** on the *method* menu.

If it is necessary for the method to be repeated several times a procedure is written. The **Repeated** option in the *main* menu is selected. By selecting the **Build proc** option the following questions are asked:

Enter main procedure:	**C:\FLOWTEK\FIRST.PDR** (or whatever you would like to call the procedure, in this case FIRST.)
Enter method or procedure:	**FIRST.MET** (if you saved your method under the name FIRST)
Enter number of repetitions:	**5**

If more methods or procedures are to follow, the process is repeated until all the methods, together with their number of repetitions are listed. Otherwise **ESC** terminates the procedure definition. To use this main procedure file, the option **Main Proc** on the *method* menu must be chosen. The name of the main procedure file must then be typed in. The option **Red. Data file** on the *Repeated* menu selects a reduced data file for saving each experiment's peak parameter data and the relative experiment identification information. The experiment number counter is reset to 1 when the reduced data file name is changed or when the program is exited. Every time the program is restarted a new reduced data file must be created, otherwise the data of the previous run will be overwritten. The option **Profile file** on the *Repeated* menu selects the file root name for the storing of profile information. The file name extension gives the number of the experiment. If no profile root is chosen , profile files are not saved.

To execute the **Main procedure** the option **Go!** on the *Repeated* menu must be chosen. The **Once** option on the *Main* menu is chosen if only one run is needed. The *Main procedure* can be aborted at any time by pressing **ESC**.

References

1. **FlowTEK Reference Manual, Device Control and Data Acquisition software, ver 1.1**, Mintek, 1993.

Publications and Presentations

1. On-line monitoring of nitrite in fertilizer process streams, natural and waste waters with sequential injection analysis, J F van Staden, T A van der Merwe, **Mikrochimica Acta, 129** (1998) 33.

2. Spectrophotometric determination of nitrite in cured meat with sequential injection analysis, J F van Staden, T A van der Merwe, **S. Afr. J. Chem., 51** (1998) 109.

3. Determination of nitrite, nitrate and boron in liquid fertilizers with on-line sequential injection analysis, J F van Staden and T A van der Merwe, **ICFIA 98, Ninth International Conference on Flow Injection Analysis, Seattle, Washington, USA, 23 - 27 August 1998.**

4. Determination of nitrite, nitrate and boron in liquid fertilizers with on-line sequential injection analysis, J F van Staden and T A van der Merwe, **Euroanalysis X, Working Party on Analytical Chemistry of the Federation of European Chemical Societies and the New Swiss Chemical Society, Basel, Switzerland, 6 - 11 September 1998.**

5. Determination of nitrite, nitrate and boron in liquid fertilizers with on-line sequential injection analysis, J F van Staden and T A van der Merwe, **SCAR'98 XIVth National Conference on Analytical Chemistry, Division of Analytical Chemistry of the federation of European Chemical Societies and the Romanian Society of Analytical Chemistry, Piatra Neamt, Romania, 24 - 26 September 1998.**

6. Determination of nitrite, nitrate and boron in liquid fertilizers with on-line sequential injection analysis, J F van Staden and T A van der Merwe, **ANALYTICA '98, Third National Symposium on Analytical Science, S A Chemical Institute, Midrand, 12-14 October 1998.**